Laser Physics, Vol. 1, No. 4, 1991.

Review

Interaction of Ultrashort Powerful Laser Pulses with Matter

B. Luther-Davies[†], E. G. Gamaly[††], Y. Wang[†], A. Rode[†], and V. T. Tikhonchuk[††]

[†]*Laser Physics Center, Research School of Physical Sciences, the Australian National University, Canberra*
[††]*Lebedev Physics Institute, USSR Academy of Sciences, 53 Leninsky Prospect, Moscow 117927, USSR*

Manuscript received July 17, 1991

Abstract – The physical principles of generation of laser pulses with extremely high power (up to 10^{15} W) and extremely short duration (less than 1 ps) are considered as well as the basic properties of their interaction with matter. The qualitative differences in phenomena induced by high-power ultra-short pulses on transparent media and condensed targets is pointed out. Special emphasis is placed on qualitatively new nonlinear (including relativistic) effects in the electric fields of laser beams. Together with the theoretical analysis, recent experimental results and future research projects are surveyed.

Contents:

INTRODUCTION

In the past five years a new generation of lasers appeared with power exceeding one terawatt (1 TW = 10^{12} W), and facilities of the petawatt range (1 PW = 10^{15} W) are planned. Thus, new possibilities for studies of laser interaction with matter have appeared. In contrast to existing powerful (up to 200 TW) but huge installations for laser-driven fusion [1], the high power of new lasers is achieved by shortening their pulses down to the femtosecond range (1 fs = 10^{-15} s) and their total pulse energy is not very high (below 10 J). Several methods for pulse shortening have been demonstrated in different lasers using glass, crystals, and excimers as the active media. Lasers of the type in question are relatively compact and flexible instruments[1] which can work with repetition rates from several hertz to several kilohertz and with high contrast (more than 10^{10}). If short focal length optics are used, intensities greater than 10^{19} W/cm^2 can be achieved [2, 3]. In many laboratories, laser systems are under construction which would yield intensities up to 10^{23} W/cm^2 [4]. The majority of publications in this field (see, e.g., [1 - 9]) are devoted to the laser systems and their optimization, while their applications in studying laser-matter interaction is in the initial stage.

Generation of laser pulses with moderate intensity (up to 10^{14} W/cm^2) and related laser-matter interaction phenomena have been described in detail (see [10] and references therein). The purpose of this review is to present the physics of the generation of subpicosecond pulses with ultimately high power and the researches on laser-matter interaction using such pulses. In addition, new proposals and recent experimental results will be discussed. The issues which would be discussed herein have also been briefly surveyed in popular form in [11].

Let us consider the new possibilities for application of ultrashort powerful laser pulses in studies of laser-matter interaction. Firstly, the production of those states of a medium whose relaxation times are longer than the laser pulse, i.e., the fundamental properties of matter, can be revealed. Secondly, the possibility of generating pulsed electric fields whose amplitudes are of the order of or higher than those inside atoms is achieved. The magnitude of an intraatomic electric field is characterized by that of a field acting on an electron in the first Bohr orbit of a hydrogen atom, the orbiting radius being $a_b = \hbar/m_e e^2 = 5 \times 10^{-9}$cm,

$$E_a = e/a_b^2 = m_e^2 e^5 \hbar^{-4} = 5.1 \times 10^9 \quad \text{V/cm}. \quad (1)$$

This strength can be achieved in a linearly polarized laser beam with intensity

$$I_a = cE_a^2/8\pi = 3.4 \times 10^{16} \quad \text{W/cm}^2. \quad (2)$$

Laser radiation with such high intensity acting on a medium ionizes the matter and produces highly stripped ions. However, when using ultrashort (subpicosecond) pulses with much lower intensity (10^{12} - 10^{15} W/cm^2) for irradiating gases, a series of specific features of ionization were discovered, the most interesting of which is abovethreshold multiphoton ionization [12].

The parameter characterizing the process of ionization in a strong field is known as the Keldysh parameter [12]. Its value is the ratio of the ionization potential to the energy of electron oscillations in an oscillating electric field:

$$\Gamma^2 = J_i/2\varepsilon_{os}, \quad (3)$$

where J_i is the ionization potential (for example, for ionization of a K-shell electron from an atom with charge Z we have $J_i = Z^2 J_h$, $J_h = m_e e^4/2\hbar^2$), and ε_{os} is the energy of electron oscillations in the laser electric field E_0:

[1] In the literature they are referred to as T^3-lasers – Table-Top Terawatt Lasers [3].

$$\varepsilon_{os} = e^2 E_0^2 (1 + \alpha^2) / 4 m_e \omega_0^2. \quad (4)$$

Here, ω_0 is the laser radiation frequency, and α varies from zero to unity depending on the polarization of the light ($\alpha = 0$ for linear polarization, and $\alpha = 1$ for circular polarization).

In practice, it is convenient to represent Γ and ε_{os} as

$$\Gamma^2 = 0.73 Z^2 / I_{14} \lambda_{mkm}^2 (1 + \alpha^2),$$
$$\varepsilon_{os} = 9.3 (1 + \alpha^2) I_{14} \lambda_{mkm}^2 \text{ eV}, \quad (5)$$

where I_{14} is the laser intensity in units of 10^{14} W/cm^2, and λ_{mkm} is the laser wavelength in microns. It is seen from (5) that for lasers in the optical range $\lambda \leq 1$ μm and for intensity $I \leq 10^{14}$ W/cm^2, the parameter $\Gamma^2 > 1$ and, therefore, the limiting case of multiphoton ionization takes place. The most interesting results on multiphoton ionization were obtained only within this limit. When using a CO_2 laser ($\lambda = 10.6$ μm) the opposite limiting case of tunnel ionization was realized ($\Gamma^2 < 1$). At intensity $I \geq I_a$, tunnel ionization occurs with all known types of lasers. If the laser pulse duration is shorter than the times of electron-ion collisions and relaxation, then the state of ions produced is completely determined by the laser beam parameters. Hence, interactions of this type provide unique opportunities for the production and study of multiple ions.

It is of great interest to investigate nonlinear nonstationary processes in rarefied and dense gases (generation of supercontinua and higher harmonics, frequency upshifting and shortening of the pulse duration) at intensities below the ionization threshold, as well as during rapid ionization (over several periods of the field). Also, these studies are relevant to work on specific properties of plasmas produced by laser ionization. A possible application for such plasmas is the creation of media for X-ray lasers. Attention is also given to work on laser acceleration of particles to super-high energies.

When laser intensity is further increased ($I \gg I_a$), another physical threshold is reached when the energy of electron oscillations becomes equal to the electron rest energy $\varepsilon_{os} \approx m_e c^2$. The corresponding values of laser intensity and field amplitude (relativistic values) are

$$I_r = 4 n_c m_e c^3 = 1.14 \times 10^{19} \lambda_{mkm}^{-2} \text{ W/cm}^2,$$
$$E_r = 2 m_e c \omega_0 / e = 12.87 E_a / \lambda_{mkm}. \quad (6)$$

Here, $n_c = m_e \omega_0^2 / 4\pi e^2 = 10^{21} \lambda_{mkm}^{-2}$ cm^{-3} is the critical electron plasma density at the frequency ω_0. At intensities of the order of or above the relativistic value, plasmas with relativistic electrons and with density close to that of a solid may be produced. It should be mentioned that in very short pulses (shorter than 100 fs) electrons cannot transfer a significant fraction of their energy to ions, even if intensity $I > I_r$, hence no heating of the ions or plasma expansion occurs during the pulse. Such overdense plasmas are of practical interest in many fields, for example, as a source of ultrashort blasts of fast particles and hard X-rays, and as a medium for X-ray lasers, as a source of nuclear reactions induced by relativistic electrons and gamma quanta.

At the present time in several countries studies of the use of lasers with intensity $I > 10^{19}$ W/cm^2 ($E > 6.6 \times 10^{10}$ V/cm) in studies of nonlinear quantum electrodynamics, i.e. in physics of high energies, are in progress. The idea of such experiments is rather simple: to collide a beam of photons with low energies ($\varepsilon_{os} \sim 1$ eV) but with huge intensity and a beam of relativistic electrons ($\varepsilon_e = 30$ - 50 GeV). In an electric field of $(10 - 100)E_a$ the processes of scattering of photons by electrons are nonlinear and the energies of backscattered photons may amount to several tens of gigaelectronvolts. There is another way to consider the processes in question: in the rest reference frame of electrons, the laser field strength is γ times higher than in the laboratory frame ($\gamma = (1 - v_e^2/c^2)^{-1/2}$ is the relativistic factor of the electrons). This means that in collisions of electrons with energies of 50 GeV ($\gamma = 10^5$) and laser photons with intensity 10^{19} W/cm^2 ($E \approx 10^{11}$ V/cm) the electric field in the electron rest frame may reach 10^{16} V/cm, i.e. the limit for the stability of the field when the generation of electron-positron pairs and some other effects predicted by nonlinear quantum electrodynamics [13] become possible. Such projects mean that a multiterawatt subpicosecond laser and an electron accelerator will be combined into one installation equipped with proper instrumentation for measurements and data processing [14].

The plan of the present review is as follows.

Chapter 1 describes the most common ways of constructing petawatt lasers and the main problems related to shortening of pulses, improvement of contrast ratio, and increasing the intensity on targets.

Chapter 2 is devoted to the interaction of ultra-short laser pulses with gaseous media. The main issues considered are ionization in strong fields and specific features of plasmas produced thereby in contrast to plasmas produced by collisional ionization using longer (nanosecond) pulses. The greater part of the experimental results were obtained in the multiphoton limit (including abovethreshold ionization); however, the tunnel limit was also realized in experiments.

In addition, Chapter 2 includes a consideration of nonlinear phenomena in dense and rarefied gases at both moderate intensity (below the ionization limit) and at high intensity when ionization by the field is a source of nonlinearity.

Chapter 3 includes theoretical and experimental results on the interaction of ultra-short laser pulses with condensed targets. The specific feature of this interaction is connected with fast ionization (by the field and via collisions) and with a minor role of hydrodynamics during the pulse. The resulting plasmas differ greatly from those produced by longer laser pulses; first of all, their density and temperature are much higher. Heating of plasma by ultra-short laser

pulses and its X-ray radiation are discussed. Different applications of such plasmas are considered.

Chapter 4 is devoted to nuclear aspects of the interaction of ultrashort laser pulses with matter, namely, laser-induced nuclear reactions and nonlinear quantum electrodynamics effects. Such phenomena are expected to become observable at laser intensity $> 10^{20}$ W/cm^2 which will be achieved in the near future. In three sections of Chapter 4, possible effects of laser excitation of nuclei, nuclear reactions, and electron-photon interaction at high energies are considered, as well as the proposed projects for experiments in this field.

1. PETAWATT LASERS

1.1. Introduction

High energy lasers producing peak powers of several TW in pulses of nanosecond duration have been developed to support research on inertial confinement fusion (ICF) [15]. In general, these lasers can produce high coherence beams with a divergence of only a few times the diffraction limit and can be focused to produce intensities 10^{18} W/cm^2. For ICF research, however, such intensities are unnecessary and it is now common practice to artificially reduce beam coherence by increasing the laser bandwidth and by inserting random phase plates to reduce spatial coherence in an attempt to make the illumination of the ICF targets as uniform as possible. As a result, most fusion laser systems produce maximum intensities around 10^{15} W/cm^2.

Successful ICF experiments generally require the physics of the laser plasma interaction to be as near "classical" as possible, with as few as possible nonlinear processes included. In this "classical" regime, the laser pulse duration far exceeds characteristic collision or ionization times in the plasma; absorption is via collisional processes (inverse Bremsstrahlung); the laser intensity is carefully tailored to achieve isentropic compression of the core. A large number of important and often nonlinear physical phenomena of fundamental interest occur outside this "classical" regime.

A nonclassical situation arises even at moderate laser intensities if the duration of the pulse is reduced below that of: (a) hydrodynamic motion; (b) electron-ion collisions or (c) ionization occurring during the laser pulse. If ionization is avoided, for example, the optical electrons are driven into strongly anharmonic motion by the laser field and high order harmonics of the driving frequency can be emitted [16]. At intensities $I\lambda^2 \geq 10^{14}$ W·μm^2/cm^2 a host of nonlinear plasma phenomena arise, such as stimulated Raman (SRS) and Brillouin (SBS) scattering, self-focusing, various decay-type instabilities [17], such as the oscillating two-stream instability (OTS); and two-plasmon decay (TPD) instability. These processes occur when the ratio of the electron oscillation energy to the electron thermal energy of the plasma exceeds a certain threshold value, every instability occurring in to certain range of density. These instabilities have a finite growth rate and a reduction of the laser duration below the characteristic growth time can help to suppress them. Growth rates are in the range 10^{-12} - 10^{-13} s and the instability thresholds, therefore, will rise substantially using subpicosecond pulses.

At intensities above $I\lambda^2 \geq 10^{18}$ W·μm^2/cm^2, new physical phenomena, relativistic and nuclear, become important [18 - 21]. The processes involved are of fundamental interest particularly as a test of the predictions of quantum electrodynamics (QED).

The present limits on laser power and intensity allows access to the lower end of the relativistic physics range, although using when TW lasers the volume of space over which the intensity is high is exceedingly small (only few cubic microns). Clearly, for a useful study to be made of the "new" physics that is expected to occur at these extreme intensities, more powerful lasers are required.

The current goal is to produce petawatt ($\sim 10^{15}$ W) lasers since this peak power now appears within the grasp of current technology. In what follows, we will discuss the approaches and general problems associated with the construction of powerful lasers and the special experimental problems in their use in plasma physics and other experiments.

1.2. Laser Systems

For the foreseeable future, lasers generating powers of $\sim 10^{15}$ W will operate with subpicosecond duration pulses. Current laser technology makes single beam lasers producing about 1 kJ of energy quite conceivable (10^{15} W × 1 ps) while the cost of higher energy systems producing longer pulses with the same power (energy about 100 kJ) is generally considered prohibitive. At the fundamental level of physics there is also a distinct advantage of using sub-picosecond duration pulses as outlined above.

Designs for petawatt systems have, therefore, focused on producing sub-picosecond duration output pulses and there are a number of laboratories with programs to develop high power systems. Several types of lasers have potential in this regard, although probably only two of these are used for transition from the TW to PW level. Firstly, these are, chirped pulse amplification (CPA) systems based around Nd : glass [3, 10]. The chirped pulses are then compressed in special dispersion elements and their power is greatly augmented. Secondly, there are excimer lasers which possess a broad amplification spectrum and high inversion density [22]. Lasers with more limited scalability are dye and high pressure CO_2 [23].

All of these lasers face similar hurdles before they could be used in experiments with solid-targets at extreme intensity. Of major concern will be the production of pre-pulse radiation. The importance of pre-pulse emission is obvious when solid targets are irradiated at intensities around 10^{20} W/cm^2. In order to prevent

plasma formation before the main pulse arrives, the pre-pulse intensity should be less than the plasma production threshold, around 10^{10} W/cm^2. Hence, a power contrast ratio 10^{10} is required – a very difficult specification. If the pre-pulse levels exceed this value, the main pulse will no longer interact with a vacuum/solid interface, as is desirable for many experiments, but with a low density, pre-formed plasma instead. The physics in these two situations will differ markedly.

Sub-picosecond pulsed can only be amplified in lasing media with sufficiently large gain bandwidths. This precludes the use of common crystal materials such as Nd : YAG and Nd : YLF as well as many gas laser transitions. In the case of CO_2 laser, a large number of rotational-vibrational lines exist in the 9.6 - 11 μm region and pressure broadening can be used to overlap the individual lines to provide the required bandwidth [23]. Operating pressures of 10 - 20 atm are necessary and these poses substantial technical difficulties in constructing large volume devices required to produce PW powers. Excimer lasers, alternatively, have inherent wide gain bandwidths due to the dissociative nature of their ground state; several groups have demonstrated they can be used very effectively to amplify picosecond pulses [22, 24]. The width of the fluorescence line in Nd : glass is about 20 nm – more than an order of magnitude greater than that required for amplification of a 1 ps duration pulse. However, Nd : glass, being a solid material, suffers the disadvantage of large optical nonlinearity, making it unsuitable for amplification of very high intensity pulses [24, 25]. Fortunately, this problem can be overcome using the so-called chirped pulse amplification (CPA) technique.[1]

As a rule, Nd : glass lasers operate well when the mean intensity is about several gigawatts per square centimeter; hence, a petawatt system would need unreasonably large beam dimensions. But in the case of CPA, a long (nanosecond) pulse whose frequency changes linearly with time during the pulse is amplified by a conventional glass amplifier chain. Since the duration of the pulse is quite large, the glass amplifiers can be operated near to saturation and large energies can be extracted without exceeding the maximum intensity loading. The amplified pulse, however, retains the linear frequency chirp and it can be compressed in time, using a linearly dispersive delay, thereby generating a sub-picosecond, high power output pulse. An example of a suitable delay line is a parallel pair of diffraction gratings [26]. In typical conditions, pulses around 750 fs can be produced by compression of nanosecond output pulses from Nd : glass and power gains of nearly three orders of magnitude can be achieved. The CPA technique is one of the most commonly proposed for high power laser development since it builds on glass laser technology already highly developed for fusion research.

The final class of lasers use very wide bandwidth active materials such as dyes, alexandrite, or Ti : sapphire. These materials have sufficient gain-bandwidth to be able to generate and amplify pulses of 10 - 100 fs duration, although they are less well developed for high energy production than the other systems.

A major limitation in propagating femtosecond pulses is dispersion and self-phase modulation in transmission media. The CPA technique can again be used advantageously, however, by decompressing the pulse before amplification and recompressing it afterwards.

1.3. Chirped Pulse Amplification (CPA) Systems Based on Nd : Glass

1.3.1. Phase Modulation in Fibers. The typical components of a Nd : based CPA system are shown in Fig. 1. The output from a CW mode-locked Nd laser (usually Nd : YLF to provide a match to the peak fluorescence of Nd-doped phosphate glass amplifiers) producing a few watts of average power in pulses around 50-ps in duration is focused into a length (about 1 km) of single mode optical fiber. Within the fiber, the processes of phase modulation and group velocity dispersion act to broaden the spectrum and temporally disperse the pulse in the fiber.

To determine the output pulse profile (power and frequency) as a function of time, the following nonlinear Schrödinger equation is solved numerically:

$$\frac{\partial v}{\partial (z/z_0)} = -i\frac{\pi}{4}\left(\frac{\partial^2 v}{\partial \tau^2} - 2|v|^2 v\right) - \tilde{\gamma} v, \qquad (1.1)$$

where v is the complex pulse amplitude; $\xi = z / z_0$ is the dimensionless distance; $\tau = t' / \tau_0$ is the dimensionless time; $t' = t - z / u$ is the retarded time defined such that at any position along the fiber the center of the pulse lies at time $t' = 0$ and τ_0 is the normalized pulse duration; u is the pulse group velocity; $\tilde{\gamma}$ is the normalized loss coefficient; z_0 is a normalized distance expressed in terms of the fiber parameters as:

$$z_0 = 0.16\pi (1.76\tau_0)^2 / |k_0''|, \qquad (1.2)$$

where k_0 is the wave vector in the fiber; and its second derivative $k_0'' = (\partial^2 k_0 / \partial \omega^2)_{\omega_0}$ described group velocity dispersion.

Equation (1.1) was derived for slowly varying amplitudes [10] with due regard for temporal dispersion (the first term in the right-hand side), for cubic nonlinearity (the second term), and linear losses (the third term). Notice that the normalized fiber length z_0 is proportional to the square of the pulse duration indicating that short input pulses are favored.

A typical value for group velocity dispersion for a fused silica fiber is 30 ps/nm·km. Sample calculations for pulse with the following parameters are shown in

[1] Note that the intensity limitations are also valid for other laser systems, in particular, for gas lasers. Though their active media do not exhibit strong nonlinearity, the lasers unavoidably include optical elements (lenses, mirrors, etc.) which possess nonlinearity of the order of that of Nd : glass. Therefore, the same intensity limitations exist even for lasers with slightly nonlinear active media.

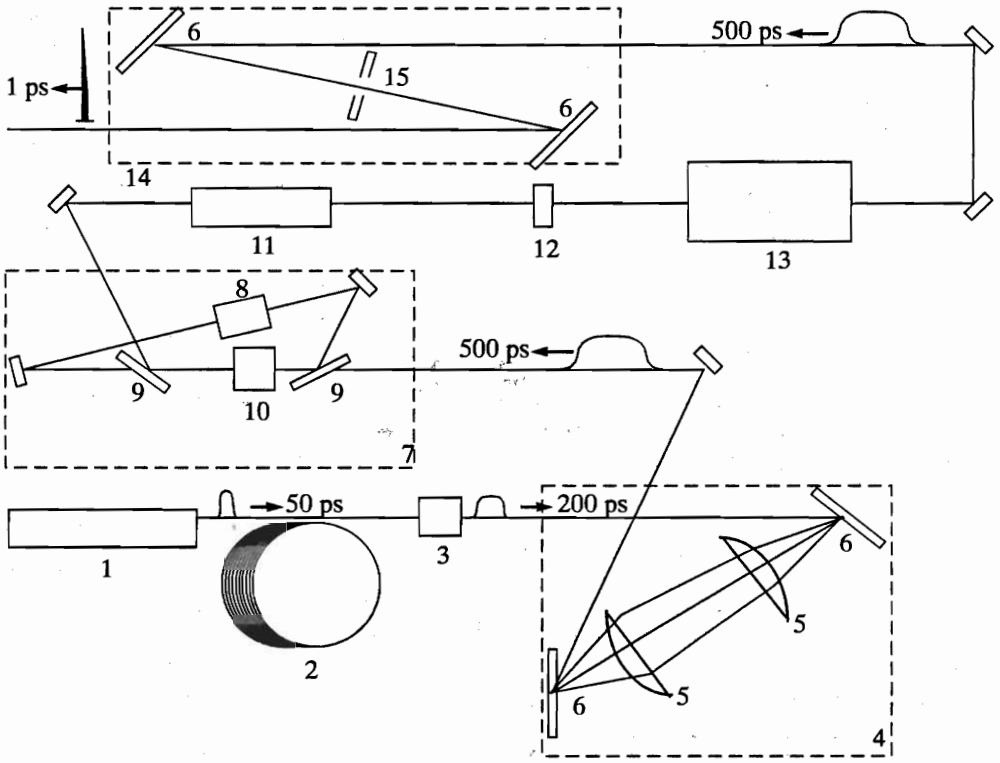

Fig. 1. *Typical lay-out of a CPA-laser: 1 – CW Nd : YLF laser; 2 – single-mode optical fiber as long as about 1 km; 3 – pulse shaper; 4 – pulse expander; 5 – lens; 6 – diffraction gratings; 7 – regenerating amplifier; 8 – active medium; 9 – polarizers; 10 – Pockels cell; 11 – preamplifier; 12 – dye cell; 13 – main amplifiers; 14 – compressor; 15 – spatial filter.*

Fig. 2. The input parameters for this calculation were, for pulse shape:

$$v(z = 0, t) = A \operatorname{sech}(t/\tau_0), \qquad (1.3)$$

τ_0 = 35 ps; peak power = 50 W; effective beam area = 4.5×10^{-7} cm^2. As is evident from Fig. 2, the output pulse, rectangular in time (region A in Fig. 2), develops some intensity modulation close to the leading and trailing edges (regions B and B'). In frequency space, the main part of the pulse (where the intensity is approximately uniform) has a linearly dependence of frequency on time. Near the edges, however, there are two regions where the frequency oscillates, one at the extremes of the frequency range (region B in Fig. 3), and the other around the central frequency of the pulse (region C and C'). Notice that these are a major source of pre-pulse emission after the pulse has been compressed.

There are several factors limiting the peak and average input powers that can be fed into the optical fiber. At high average powers, fibers are susceptible to thermal "fusing" which results in catastrophic damage. For kilometer length fibers this typically occurs at average powers of 1 - 5 W [27]. In addition to self-phase modulation, other non-linear processes can arise in the fiber such as stimulated Raman scattering (SRS). The threshold for this process depends on pulse duration but, for 60 ps pulses, is predicted to be about 80 W [28]. Since SRS results in a large fraction of the pulse energy being converted to the Stokes shifted sidebands, it makes the fiber very lossy and causes very strong spectral distortion.

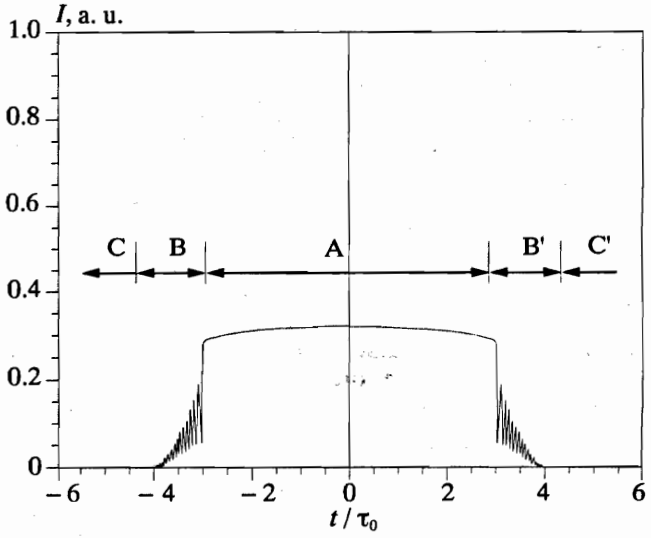

Fig. 2. *Temporal dependence of laser pulse power at the exit from a 1-km fiber, the input pulse duration and power being 35 ps and 50 W.*

In the particular example used above the 35 ps duration input pulse was transformed to a linearly chirped output pulse some 120 ps long, after transit through a 1 km length of fiber. The peak power was thus reduced from 50 to about 14 W, while the pulse bandwidth has increased from 0.044 to 3.5 nm. Calculations subsequently show that, after compression using an ideal linearly dispersive delay line (to which a grating pair is only a first approximation), compressed pulses ~1 ps duration can be obtained with a corresponding time-bandwidth product of about 2, indicating that the pulse is not bandwidth limited, since then $\Delta\nu\tau_0$ must be equal to 0.44 - 0.83 depending on the pulse shape. The result of an idealized linear compressor is shown in Fig. 4. Notice, here, that significant energy exists outside the main pulse, indicating the presence of pre-pulse radiation up to 50 - 100 ps before the main peak. Pre-pulse energy closest to the peak is caused by region B (Fig. 3) which undergoes imperfect compression in the linearly dispersive delay line. The pre-pulse component occurring about ± 60 ps from the peak corresponds to region C which has its frequency close to the central frequency of the pulse and is unaffected by the delay line.

1.3.2. Methods to Provide High Contrast Ratio. This example underlines the serious level of pre-pulse emission created by the optical fiber. In fact, the ratio of the energy in the main to pre-pulse is only 50 and, as early as 100 ps before the peak, the power contrast ratio is only around 300. These numbers fall far short of the required value of 10^{10}.

Fortunately, at least some of the pre-pulse energy can be removed quite simply by filtering out those frequency components furthest from the central frequency, that is, by removing region B. A number of methods can be adopted to achieve this. First, the output beam from the fiber can be dispersed using a diffraction grating and the extreme frequency components

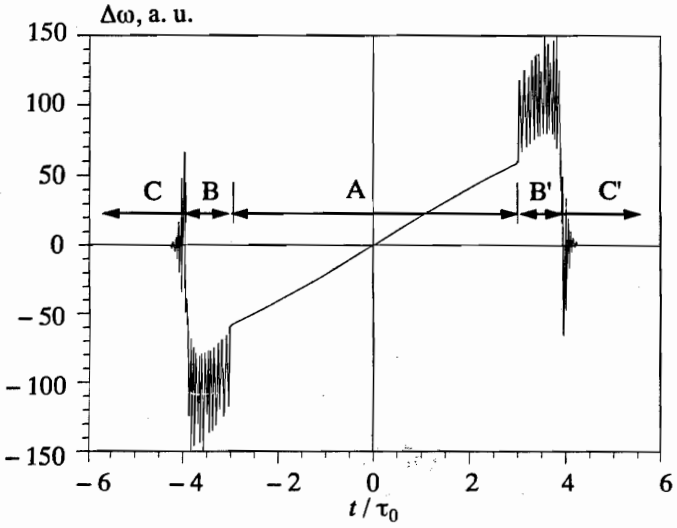

Fig. 3. *Frequency-versus-time dependence of a pulse at the exit from a 1-km fiber. Input parameters as in Fig. 2.*

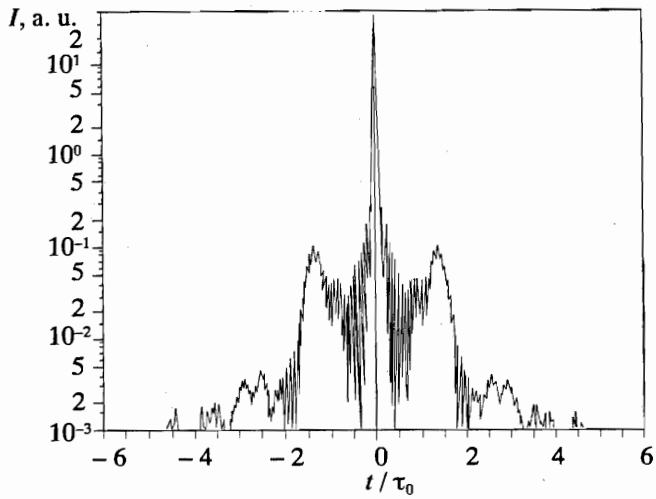

Fig. 4. *Pulse shape after compression with an ideal compressor consisting of two diffraction gratings at τ_0 = 20 ps.*

removed using an aperture as illustrated in Fig. 1. Additionally, since the output power from the fiber is very low, the pulse will be amplified in some medium with a finite gain bandwidth. Gain narrowing can, therefore, be used to effectively suppress region B. Both these processes have been demonstrated.

Perry *et al.* [25], used gain narrowing during amplification and showed that it produced a reduction of the spectral width from 3.5 nm to about 1.5 nm and made a substantial improvement in the contrast ratio of the compressed pulse. In spite of the spectral narrowing, it was found that the duration of the compressed pulse was in fact shorter than that before amplification. This was attributed to the change in the shape of the spectrum after amplification which approximated a Gaussian distribution, while before amplification it was rectangular. A linearly dispersed Gaussian frequency spectrum translates, after compression, into a Gaussian pulse in time. For Gaussian pulses, the time-bandwidth product has a small value equal to 0.44 in comparison with the value for a rectangular pulse which is 0.83. As a result the reduction in bandwidth simply altered the pulse shape without changing its FWHM duration.

Unfortunately, spectral filtering does nothing to remove the pre-pulse emission attributed to the central frequency components marked region C in Fig. 3. The main approach is to use a non-linear process to selectively pass the high intensity main pulse but block the low intensity prepulse. A simple example is a saturable absorber such as that used by Chuang and Meyerhofer [29]. A cell containing Kodak-9740 dye with an optical density of about 4 was inserted into the output beam of the laser after compression. The cell had a peak transmission of about 30% for the main pulse, which was shortened from 1 to 0.8 ps during passage through the cell, while the contrast ratio was improved to greater than 10^5 (the measurement limit) with some loss of beam quality (the divergence increased by a factor of two).

Alternative non-linear processes, such as polarization rotation (intensity dependent birefringence) have been suggested in the optical fiber [30], or harmonic generation [31, 32]. In the former case, the static (zero power) birefringence in the optical fiber is removed by using, for example, a Soleil-Babinet compensator at the fiber output to produce a linearly polarized output beam. At low powers, this beam is then rejected by a crossed polarizer. The high intensity pulse induces birefringence in the fiber and, hence, the high power part can undergo polarization rotation and pass through the polarizer. This scheme has a number of problems such as ensuring exactly 90 degrees of polarization rotation at the pulse peak and, secondly, mechanical or thermal fluctuations can change the static birefringence leading to poor rejection of the pre-pulse.

The process of frequency conversion provides another method of pre-pulse suppression. In the small signal limit the contrast ratio is improved by the factor $(I_m / I_p)^n$, where I_m is the peak intensity of the main pulse and I_p is the peak intensity of the pre-pulse and n is the order of the non-linear process. For this to be effective it is obvious that the ratio I_m / I_p should be initially quite large; clearly frequency tripling is a more effective process than doubling in this context. A difficulty with any non-linear process using a quadratic non-linearity and using short wide bandwidth pulses is phase – matching the interaction across the whole bandwidth. Additionally, group velocity dispersion can limit the effective interaction length and lower the conversion efficiency.

Some novel methods have been devised to overcome these problems. For example, it has been demonstrated that angularly dispersing the frequency components so that each enters the doubling crystal at its own phase matching angle is an effective means of improving the doubling efficiency for femtosecond pulses [32]. In the picosecond regime, a novel method of doubling frequencies with mismatching velocities, suggested by Wang and Dragila [31], provides a means for obtaining very high energy and power conversions. These two techniques are illustrated in Figs. 5 and 6. Group velocity mismatched frequency doubling relies on the fact that, for type II frequency doubling of 1 μm light in KDP, the group velocity of the second harmonic pulse falls midway between that of the o- and e-fundamental rays. As a result, by pre-delaying the e-relative to the o-ray by approximately half the total delay induced by group velocity dispersion in a complete pass of a crystal, a small time interval at the peak of the harmonic pulse is able to effectively interact with all parts in the fundamental pulse. The result is that the second harmonic pulse duration is much less than that of the fundamental and high conversion is predicted.

These non-linear conversion processes help to improve the contrast ratio although the maximum increase is less than that predicted in the small signal limit due to the effects of saturation (pump depletion). Nevertheless they will almost certainly need to be employed in obtaining the very high contrast ratios ultimately required.

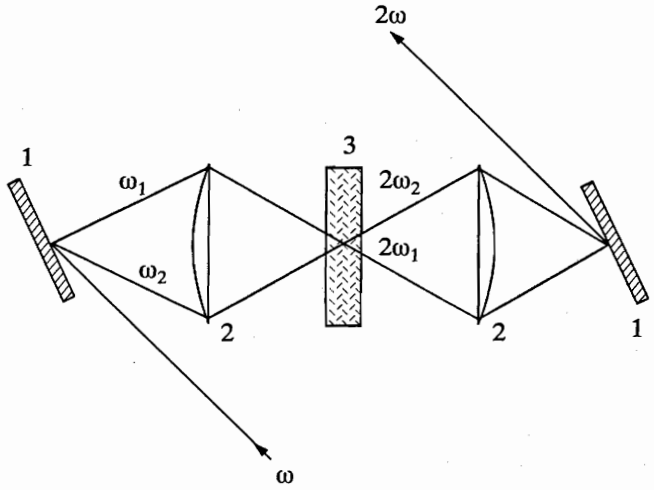

Fig. 5. *Scheme of generation of a harmonic of a ultra-short pulse with use of angular dispersion of frequency components to compensate the frequency dependence of phase matching angle [32]: 1 – diffraction grating; 2 – focusing lenses; 3 – nonlinear crystal.*

1.3.3. Amplification in Nd : Glass. The single pulse emerging from the optical fiber typically contains 1 nJ of energy and, hence, amplification to the 1 kJ level implies a large signal gain of 10^{12}. Typical Nd : glass amplifiers operate with small signal gain coefficients about 0.1 cm^{-1} and hence the total glass length will be between 2 or 3 m for amplification to the TW or PW levels respectively. In these conditions, gain narrowing will restrict the available bandwidth to values much less than the fluorescence linewidth of the lasing transition. The half gain points will occur at frequencies where the fluorescence yield is between 96.7% and 97.5% of the peak value. Assuming a Gaussian lineshape characteristic of the heterogeneously broadened line in Nd : glass, the available bandwidth is about 20% of the FWHM fluorescence linewidth, which is sufficient for amplification of a 1 ps duration pulse. These numbers also illustrate the impact of etalon effects in the amplifiers, since even a 1% modulation of the gain will lead to severe spectral distortion. Brewster angle and wedged elements, therefore, must be used to avoid undesirable reflection whenever possible.

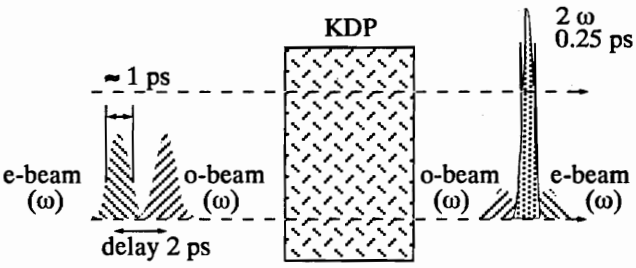

Fig. 6. *Frequency doubling in a type II KDP-crystal with use of detuning of group velocities [31].*

The general approach to obtaining the required gain is to amplify the output pulse from the fiber in a regenerative amplifier to the mJ level before injecting it into a fairly conventional Nd : glass amplifier chain. Both standing wave and ring regenerative amplifiers using Nd : glass have been used. In the case of the standing wave system, there is a special problem since depolarization of the circulating beam or imperfections in the optics will lead to a fraction of the amplified power being focused back onto the output of the optical fiber. Since the gain in the regenerative amplifier is very high, a fraction of a percent of the final power is sufficient to damage the fiber. As a result, in early systems, is was necessary to add a lossy mirror between the regenerative amplifier and the fiber (Maine *et al.* [25]). The ring system overcomes that problem and is the preferred geometry.

So far, we have mentioned only the problem of pre-pulse generation due to the fiber grating compressor. There is an additional source of pre-pulse, namely, amplified spontaneous emission (ASE) from the laser amplifiers. As is the case for any multi-stage amplifier, the major contribution to such noise comes from the laser "front end", since it is signals from this source that experience the full system gain (this assumes that the same spectral and solid-angle widths are maintained throughout the whole amplifier chain). It is easy to estimate the spontaneous emission power relative to the injected power, assuming that only spontaneous emission within the beam divergence of the pulse injected into the regenerative amplifier is of importance. This ratio, about 10^{-6}, and although the ASE is less than the pre-pulse power created by the fiber-grating system, is nevertheless high enough by itself to prevent the required contrast ratio being obtained. Additionally, the duration of the ASE pulse can be 10 - 100 times that of the injected pulse, leading to very poor energy contrast. One important point to be noted about ASE, in comparison with pre-pulse from region B in Fig. 2, is that power is unaffected by compression since the emission frequency is not chirped. As a result, compression improves the power contrast ratio by the ratio of the uncompressed to compressed pulse duration which can exceed a factor of 100.

Clearly, the amount of ASE is affected by the design of the amplifier chain and it is not always possible to restrict the solid angle in the high power stages to the diffraction limit. In general, the design of glass laser amplifier chains is dictated by compromises between the efficient use of the available cross-sections of the amplifiers and the need to restrict the growth of beam non-uniformities due to filamentation. Usually, for efficient use of the amplifiers, the beam should have as near to a uniform intensity distribution as possible – a "top-hat" profile is required, as well as operation near the saturation flux limit (about 1 J/cm^2 for sub-nanosecond Nd : glass). The problem with such a beam profile is that it rapidly develops strong modulation due to diffraction effects because of the steep intensity gradients near the edges and close to the saturated flux the average beam intensities will be very high leading. These diffraction ripples form the seed for filamentation instability originating due to the refractive index non-linearity of the laser glass.

It is well established that the susceptibility to filamentation is determined by the bean break-up integral, B, where

$$B = (2\pi/\lambda) \int (4\pi\eta_2 I/c)\, ds. \qquad (1.4)$$

Notice that B is proportional to the product of the average intensity $< I >$ in the amplifier chain multiplied by the length L. Obviously, minimizing the average intensity helps reduce B and this can be simply achieved by making the gain coefficient, Γ, as high as possible since $< I > L$ is proportional to the ratio system gain / gain coefficient, i.e. $\exp(\Gamma L) / \Gamma$. In a word, short high gain amplifiers should be used.

Filamentation is the growth of high spatial frequency modulation on the otherwise uniform laser beam because of the refractive index non-linearity associated with the laser glass. The optimum growth rate occurs for spatial frequencies given by

$$k_m = (2\pi/\lambda)\, (2\eta_2 I/\eta_0)^{1/2}. \qquad (1.5)$$

Because this optimum frequency is rather high (about 100 cm^{-1}), spatial filters can be used effectively to attenuate the growth of the high spatial frequency filaments. The laser design will, therefore, include successive stages of amplification interspersed with spatial filters. The maximum accumulated B integral between spatial filters should typically not exceed 2 (the relative growth of the filament $\Delta I / I \alpha \exp(B)$) whereas the total B integral for the whole amplifier chain can approach 10 without a serious increase in wavefront distortion.

In order to maintain the "top-hat" intensity distribution in every amplifier, relay-imaging can be employed [33]. Here, the output beam from the pre-amplifier stages is filtered, expanded and then truncated using an aperture to provide an almost uniform input to the amplifier chain. Since such a beam would rapidly create diffraction rings, the imaging property of the spatial filters (telescopes) is then used to successively relay the smooth flat-topped intensity distribution into each amplifier in turn. In the regions between the amplifiers, the beam develops intensity modulations due to diffraction, however, since these fall outside the laser glass and hence they do not grow in intensity due to filamentation. Notice, however, that such a relay imaging system can only maintain the flat-topped distribution if the spatial filtering is not too severe, i.e. the spatial filters must pass frequencies much higher than those corresponding to the lowest time frequency component of the beam. As a result, the angular acceptance of the amplifiers-spatial filters is typically an order of magnitude larger than given by the diffraction limit for the beam, a fact that proportionally increases the amount of ASE from these stages.

1.3.4. The Compression Stage. Although several types of compressors could be used, in general a pair of parallel diffraction gratings best matches the dispersion characteristics in the output pulse from a CPA glass laser. The first grating angularly disperses the different frequency components in the beam and causes them to travel different distances to a second identical grating which then removes the angular dispersion. The grating separation for correct cancellation of the linear frequency chirps is given by:

$$D_g = 6.4\pi c^3 d^2 \tau_0^2 \cos^2\psi / A\lambda^3, \qquad (1.6)$$

where ψ is the angle between the normal to the input grating and the diffracted beam; d is the groove spacing; λ is the central wavelength of the pulse; $1.76\tau_0$ is the FWHM intensity duration of the pulse; $A = (P/P_1)^{1/2}$ is the normalized input pulse amplitude which is related to the pulse and fiber parameters by [28]: $P_1 = 10^{-7}\eta_0 c\lambda a_{\text{eff}} / 16\pi z_0 \eta_2$ is the characteristic power in Watts, z_0 is defined in (1.3); η_2 is the nonlinear coefficient of the core material (in esu); η_0 is the refractive index of the core; and a_{eff} is the effective area of the core. Notice that the diffraction grating pair operates as an ideal compressor to the first order only and that second order terms, in fact, introduce significant distortion of the pulse shape. Fortunately the second order term leads to the formation of a post pulse at the output which is a far less serious problem than the pre-pulses formed other sources.

Note that the grating separation is reduced by increasing the grating dispersion and this can be achieved by either increasing the grating constant or the angle of incidence. The major problem with the single pass geometry illustrated in Fig. 7a is that, at the output, the different frequency components appear at different positions across the beam. Obviously, accidental truncation of the beam can remove some components and increase the pulse duration. The double pass geometry in Fig. 7b eliminates this problem although larger area gratings are then required to spatially separate the input and output beams at the beam splitter. To obtain high efficiency, blazed gratings are generally used in the near-Littrow configuration and using *s*-polarized light. The reflectivity for a grating blazed at 750 nm and operated using *s*-polarized light at 1053 nm can exceed 90% when an aluminum coating is used. This can be improved further by replacing the aluminum with gold.

For replicated gratings, the damage threshold for picosecond duration pulses has been found to be about 100 mJ/cm^2, which restricts the usable level to about 25 mJ/cm^2 or 25 GW/cm^2. The grating size for a petawatt laser would then be around 2 m × 3 m – a prohibitively large size. Petawatt laser will, therefore, almost certainly require improvements in grating technology to permit higher operating intensities.

The Littrow configuration does not lead to the shortest pulse durations. The rapidly increasing dispersion leads to a smaller time-bandwidth product for the compressed pulse at larger angles of incidence. The slight loss of reflectivity induced by this angular change is more than compensated by the reduction in pulse duration.

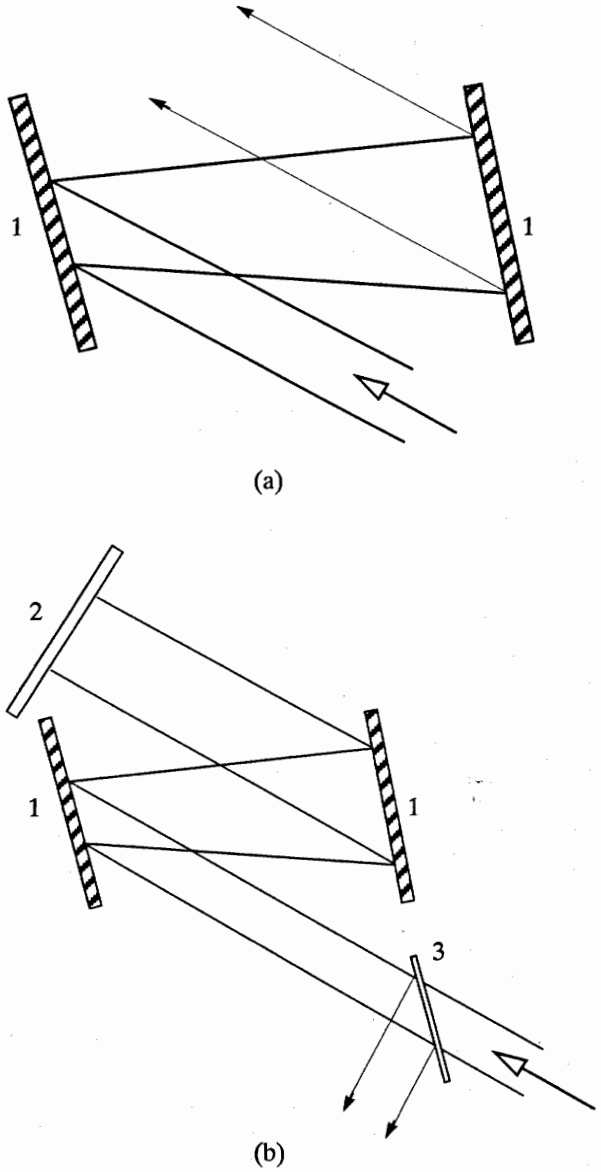

Fig. 7. *One-pass grating compressor with spatial separation of components of the output beam (a) and two-pass compressor compensating this separation (b). 1 – diffraction grating; 2 – 100% mirror; 3 – beam splitter.*

Therefore, CPA systems based around Nd : glass have the potential to produce PW powers using technology already highly developed for fusion research. Currently, systems exist which produce peak powers of about 10 TW although the problem of pre-pulse suppression still requires further work. Improvements in diffraction grating technology appear to be essential before a practical PW laser could be constructed. A large amount of work remains on optimization of frequency doubling or tripling techniques for short pulses since that could provide a method of pre-pulse elimina-

tion as well as permitting experiments at a variety of wavelengths. Wavelength versatility has proved to be particularly important in fusion research and will also be so in studying the non-classical physics to which PW lasers will be applied.

1.4. Excimer Lasers

Excimer lasers are the main alternative to the CPA glass system for petawatt generation. Although they are not as well developed as high power glass lasers, their short wavelength, high efficiency, and gaseous lasing medium make them the most promising of the possible driver lasers for ICF reactors and, hence, rapid development of their technology can be anticipated. The highest energy system reported using KrF is the AURORA laser at the Los Alamos National Laboratory in the USA which has produced 10 kJ pulses in 500 ns from a 1 m^2 area beam.

Both KrF and XeCl, for example, have an inherently large bandwidth (3 - 4 nm) which makes them ideal for amplification of subpicosecond duration pulses; they possess a low saturation intensity I_s = 2 MW/cm^2, which means that excimer amplifiers will always be operated in the strongly saturated regime; they have a low energy storage lifetime (about 5 ns) which means they are power converting rather than a power multiplying media; they also have a high small gain (about 10%/cm) and large non-saturable losses. These characteristics dominate excimer laser technology and in particular the very short storage lifetime means that they can only be efficiently excited using electron beam or fast discharge pumping. If the pump pulse duration exceeds the storage lifetime, high extraction efficiency will only be obtained for long output pulses or by multiplexing the amplifier. Hence the large duration of the output pulses from AURORA. The development of high power pumping systems itself is a considerable technical challenge.

The large small-signal gain combined with saturated operation means that ASE is a major problem in the design of high power excimer lasers. ASE can lead to a depopulation of the lasing transition and create large pre-pulse levels at the target surface. Depopulation limits the small signal gain of the amplifiers. The optimization of these systems is a complex matter and recent design data from the Rutherford-Appleton Laboratory (RAL) suggest typical operating parameters after the effects of ASE, gain saturation and extraction efficiency [34, 35] are taken into account should be: output intensity (3 - 4)I_s, gain-length product ΓL = 8 - 12, transverse gain-length product $\Gamma D \geq 3$ [34]. This implies that the amplifiers must have a high aspect ratio, i.e. $L / D \geq 3$.

The short storage lifetime makes the construction of high coherence oscillators using the excimers almost impossible. As a result, high power excimer lasers are driven by oscillator pulses generated by some other laser. For example, a system developed at the University of Tokyo by Watanabe *et al.* ([22], Fig. 8), uses a synchronously pumped Rh590 dye laser operating at 616 nm to provide output pulses for frequency doubling to 308 nm in β barium borate and subsequent amplification in XeCl. The dye laser was pumped by a frequency doubled CW Nd : YAG laser fitted with a fiber-grating compressor to provide 3.5 ps duration pump pulses for the dye laser. The 616 nm pulse was measured to be ~ 320 fs in duration. It was amplified in a four stage dye amplifier chain using Kiton-Red-620 and Sulphorhodamine dyes pumped by a XeCl laser. Approximately 130 μJ of energy was obtained at the output and this frequency was doubled to provide about 20 μJ of UV power. This pulse then underwent preamplification in two discharge pumped XeCl amplifiers with careful spatial filtering between amplifier stages to eliminate ASE. The typical output pulse energy was 3 mJ with "no" ASE background.

A system developed at the Rutherford-Appleton Laboratory in the United Kingdom for use with KrF (248 nm wavelength) is quite similar [22]. Again, a frequency-doubled mode-locked CW Nd : YAG laser synchronously pumped a mode-locked laser, this time tuned to operate at 746 nm. Output pulses of ~ 3 ps duration were then amplified using a three stage excimer-pumped dye laser amplifier before being frequency tripled in a pair of KDP crystals. The tripling process effectively eliminated any ASE from the dye amplifiers, and the output pulse was then amplified to 100 μJ in a discharge pumped KrF laser. This whole system could be operated at repetition frequencies of about 10 Hz. The long oscillator wavelength required when frequency tripling is employed permits some of the dye laser amplifiers to be replaced by Ti : sapphire. Ti : sapphire has an intermediate upper lasing level life-

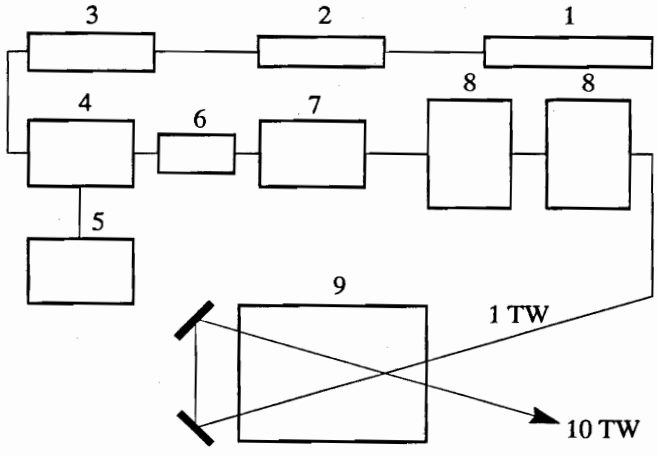

Fig. 8. *Powerful sub-picosecond excimer laser [22]: 1 – CW Nd : YAG mode-locked laser; 2 – compressor; 3 – synchronously pumped Rh590 dye mode-locked laser; 4 – four-stage dye-laser amplifier; 5 – XeCl pumping laser; 6 – frequency doubling crystal; 7 – electric-discharge excimer amplifier with high repetition rate; 8 – two stages of excimer amplifier; 9 – electron-beam-pumped excimer laser.*

time (about 1 μs) and, hence, an improved storage time and lower gain than dyes. It is expected to be used to construct large area pre-amplifiers to boost the laser power prior to frequency tripling to provide large signal levels for the main amplifier chain.

The Tokyo group amplified the seed pulses into two XeCl discharge pumped amplifiers to obtain a final output power of 1 TW in 310 fs. The addition of an e-beam pumped amplifier and conversion of the system to operate on KrF is expected to boost the output power to 10 TW in 0.5 ps [22].

A similar system is proposed for construction at RAL and is to provide up to 50 TW single pulse, single beam power in a 0.3 ps duration output pulse [38]. Multiplexing this system so that six beams passed through each amplifier sequentially to enable energy extraction over 150 ns pump duration has been estimated to boost the total output power to 0.25 PW and a four channel system would then be required to obtain 1 PW. Such a system would not necessarily achieve the same brightness as a single beam PW laser since the energy would be delivered in 24 independent beams to the target.

As is the case with the CPA systems, pre-pulse suppression is a major difficulty with the excimer lasers although in their case the pre-pulse originates solely from ASE. The problem is exacerbated by the fact that the amplifiers are operated in the saturated regime which makes the gain for the ASE (which experiences the small signal gain) much larger than the gain for the main pulse. A number of strategies can be adopted to reduce the ASE level. First, the input pulse to the main amplifiers from the dye laser front end should be as large as possible to provide a good signal-to-noise ratio. Since this pulse is delivered through frequency doubling or tripling the output from the dye oscillator-amplifier chain, the non-linear conversion process effectively eliminates ASE at the input. Subsequently, care must be taken to limit the small signal gain between of the main amplifiers; spatial filtering can be used to restrict the solid angle over which amplification occurs thus restricting the ASE; spectra and polarization filtering can result in useful improvements; and, finally, saturable absorbers can be inserted between the amplifiers to attenuate the pre-pulse emission.

In this last case it has recently been demonstrated that acridene, in either methanol or ethanol, can act as an effective saturable absorber for KrF radiation [37]. The typical saturation energy is 1.2 - 1.4 mJ/cm^2. Work with the ASHURA laser in Tokyo demonstrated contrast ratio improvement from about 10 up to 10^5 with some loss (about 2) in output energy. A recent system analysis performed at RAL [38] suggests that with all these ASE reduction techniques employed intensity contrast ratios 5×10^{11} and energy contrast ratios of 5×10^7 are obtainable using 1 ps duration output pulses. This level would be sufficient for experiments at intensities around 10^{20} W/cm^2.

Obviously CPA techniques can also be applied to the KrF system, in this case the picosecond pulse being first stretched in time using a grating decompressor thereby generating a pulse up to 1 ns duration for amplification. After amplification, the pulse can then be recompressed using a similar pair of gratings. This scheme does not suffer from the pre-pulse problems of the fiber-grating CPA systems developed for Nd : glass since it does not use an optical fiber to generate the frequency chirp.

1.5. Raman Lasers

In addition to production of high powers from the excimer system directly, Raman lasers have been developed that are pumped by excimer systems as an effective means of transferring the energy from a long pulse or series of multiplexed excimer laser pulses into a single high quality output pulse [35]. The method has been used extensively at RAL where it has been demonstrated that very high brightness can be produced in the Raman beams even when low coherence KrF pumps are available.

The Raman active medium normally employed with KrF systems is methane which produces in a first Stokes output at 268 nm. Methane is chosen because of its short dephasing time (T_2 = 30 ps) which makes it suitable for amplification of pulses in the several picosecond range. At RAL, the high quality seed beam, subsequent amplification on large aperture Raman amplifiers was generated in the following manner: The short pulse output from the frequency tripled dye laser at 248 nm was first double-passed through a discharge pumped KrF amplifier which boosted the pulse energy to about 10 mJ. A small part (about 30 μJ) of this pulse was focused into a 2.7 m long cell containing 3 atm of methane. The output contained emission at several Stokes and anti-Stokes wavelengths and the first Stokes line was selected by a dispersive prism. After spatial filtering to obtain a diffraction-limited beam the first Stokes pulse was amplified to an energy of about 1 mJ in a 3 m long Raman amplifier containing 5 atm of methane with the remaining KrF output being used as the pump beam. The Raman and KrF beams were slightly non-collinear in the cell enabling any beam non-uniformities in the pump to be spatially averaged over the Raman beam, thus maintaining the latter beams high uniformity.

Further amplification of the Raman pulse is possible, and a number of novel geometries are under investigation for high power stages. Cells with reflecting walls offer the possibility that the KrF pump beam can be multiply reflected in a waveguide fashion down the cell. This ensures that the any intensity non-uniformities are spatially averaged to help maintain high coherence for the Raman beam. In addition, multiple reflections essentially reduce the velocity of the pump wave relative to the axially directed Raman pulse. This means that the Raman pulse can pass through the whole pump pulse in a single transit of the cell and, hence, the energy contained in a long pump pulse can be effi-

ciently transferred to a shorter Raman pulse to achieve a degree of pulse compression. A possible disadvantage with this scheme is, however, that the path length for the pump beam in the cell is greater than that of the Raman beam which means that the gain for self-generated Raman emission in the amplifier considerably exceeds that for the main Raman pulse, especially when the Raman pulse is only a few picoseconds in duration. As a result the amplifier can become unstable to the amplifier spontaneous Raman emission. In addition to this essentially forward Raman geometry, backward Raman pulse shortening can be used to effectively transfer energy from long pump pulses to a short Raman pulse. Backward Raman processes, however, are not preferred since they can lead to pulse shape instabilities and large conversion to second Stokes radiation.

Raman amplifiers suffer from a number of other problems when required to operate with ultra-short pulses. For example, anomalous dispersion is induced in the cell associated with changes in the population of the Raman transition, which itself depends on the local beam intensity. Self-focusing of non-uniform beams can result in not only pulse chirping (self-phase modulation), but also in the leading and trailing edges of the pulse. Furthermore, the duration of pulses that can effectively be amplified in Raman media depends on the spectral bandwidth of the pump pulse and the width of the Raman resonance. This, in practice, limits Raman pulse durations to greater than a few picoseconds.

1.6. Conclusion

Currently, rapid progress is being made towards the development of PW laser systems suitable for the study of laser-matter interactions at extreme intensities. Most efforts are currently being directed to CPA glass lasers and excimer systems. The major limitation on the operation of both these systems is the emission of pre-pulse radiation. Several approaches are being pursued towards the elimination of this pre-pulse, whose power must be around ten orders of magnitude lower than that of the main output pulse to prevent plasma production in experiments with solid-targets by exposure to the pre-pulse.

High-power sub-picosecond laser systems are being successfully operated or built in many laboratories. Table 1 illustrates the present-day status of those facilities. Note that we classify an installation to be operational if the parameters have been achieved. However listed, not all the facilities are being used for research since new methods of detection of transient processes are to be developed. The related issues will be partially covered in the following sections.

2. INTERACTION OF ULTRA-SHORT LASER PULSES WITH TRANSPARENT MEDIA

Ultrashort laser pulses allow us to study the effects induced by strong fields in their "pure form", i.e. during so short a time that neither relaxation nor slower processes can exhibit themselves. First of all, these effects include ionization by the field, i. e., multiphoton ionization by optical quanta whose energies are smaller than the ionization potential ($\hbar\omega_0 \ll J_i$). This effect is of importance for understanding different issues to be considered below. Though multiphoton ionization (MPI) was discovered rather long ago [12, 39], experiments done recently with ultrashort pulses have revealed the new unexpected effect of abovethreshold multiphoton ionization. It was found that strong nonlinear effects appear at field values $E \ll E_a$ (and related intensities) which are much lower than was expected. Also, the intensity thresholds of ionization were seen to increase as the duration of pulses is shortened. Therefore, the optical nonlinearities could be studied at much higher field amplitudes. Moreover, the optical nonlinearities below and above the ionization threshold (nonlinear polarization and nonlinear polarization plus nonlinearities related to nonlinear current, respectively), which were considered earlier as phenomena with different

Table 1. Parameters of powerful sub-picosecond lasers

Laser type	Wave length, nm	Pulse duration, fs	Energy, J	Power, TW	Power contrast	Intensity, W/cm^2		Laboratory
						Achieved	Planned	
KrF [9]	248	280	0.41	1.5	10%	$\leq 10^{18}$		Inst. Solid State Phys., Univ. Tokyo
KrF [36]	268	12000	5		$< 10^{-10}$	$> 5 \times 10^{17}$		Rutherford Appleton Lab., U.K
Sub. Sprite	268	10000		30				
Nd [5]	1064	1000	30	30	$< 10^{7}$	$> 10^{18}$		Inst. Laser Eng., Osaka Univ.
Nd [7]	1064	1200	24	20		5×10^{17}	$> 10^{19}$	Centre d'Etudes Limeil, France
dye [6]	500	10 22	0.5×10^{-6}					Lawrence Berkley Lab., Univ. Calif.
XeCl [2]	308	335	0.25			4.6×10^{18}	6.4×10^{19}	Los Alamos Nat. Lab., USA

physical origin, were observed to exhibit certain similarities (such as time-dependent resonances) and result in similar effects (e.g., phase self-modulation of laser pulses). That is why it seems to be reasonable to consider together the effects of ultrashort pulses for intensities below the ionization threshold (these effects are related to optical nonlinearities), and ionization by fields, and effects related to nonlinear ionization in order to follow the conceptual connection between these phenomena if such a connection does exist.

2.1. Ionization of Matter in Strong Electric Fields

The review [12] is available that covers a series of experimental and theoretical works on multiphoton ionization. Here we consider ionization by the fields of ultrashort laser pulses (thresholds of ionization, and their dependence on pulse duration, intensity and ionization potentials) as well as the characteristics of plasmas produced by ionization. For studying the process of multiphoton ionization, the experiments were done with gases at low pressure (10^{-4} - 10^{-6} torr). Laser radiation was focused into region with linear dimensions l_{foc} = 10 - 100 μm. For sufficiently short laser pulses the time needed for an electron to leave the focal volume $t = l_{foc} / v_e$ exceeds the pulse duration. Due to the low concentration of ions the plasma produced is transparent for incident radiation ($\omega_0 \gg \omega_{pe}$, where $\omega_{pe} = (4\pi e^2 n_e / m_e)^{1/2}$ is the plasma frequency) and the time between consequent collisions of an electron $1/\nu_e$ is larger than the pulse duration (here ν_e is the electron collision frequency). If the above mentioned conditions are fulfilled, then the state of the plasma produced is completely determined by the interaction of the laser field with individual atoms of the medium.

2.1.1. Abovethreshold Multiphoton Ionization. The photoionization thresholds for laser pulses with durations about one picosecond and shorter and with wavelengths in the visible and ultraviolet are about 10^{12} - 10^{14} W/cm^2. In the case of ionization near the threshold, the electron produced leaves the atom with kinetic energy $\varepsilon_0 = s\hbar\omega_0 - J_i \leq \hbar\omega_0$ (where $\hbar\omega_0$ is the energy of the incident photon, J_i is the ionization potential, s is the number of absorbed photons, and $J_i \leq s\hbar\omega_0$). The probability of MPI decreases rapidly as the number of absorbed quanta s increases. That is why photoionization was said to produce "cold" free electrons with mean energies smaller than the energy of one laser quantum $\langle \varepsilon_e \rangle = T_e \leq \hbar\omega_0$. However, the spectrum of photoelectrons obtained from rarefied gases under the conditions formulated above and at intensities above the ionization threshold proves to be discrete $\varepsilon_s = \varepsilon_0 + s\hbar\omega_0$ (s = 1, 2, 3, ...), the number of electron peaks seen in some experiments being more than ten. As the intensity increases up to a certain value I_{cr} the amplitudes of electron peaks with high energies ($s > 1$; $\varepsilon_s > \varepsilon_0$) start to exceed those with low energies. The ionization (the yield of ions with a given value of charge) saturates at $w\tau_0 \geq 1$ (where w is the probability of ionization and τ_0 is the laser pulse duration) and at the corresponding value of the intensity I_{sat}. It was discovered in experiments that with a slight excess of I_{sat} over the threshold (about 10 to 20%) the maximum amplitude corresponds to the maximum electron energy in the spectrum [49].

That is, it proved to be "advantageous" for an electron to absorb more quanta than it needs to become free, this being in contradiction with the probability of absorption of s photons by an atomic electron (see [39]) calculated using perturbation theory. It follows from theory that in the limit of MPI ($\Gamma^2 \gg 1$) and at small laser intensity I ($E \ll E_a$) the probability of absorption of s photons is $w_s \cong I^s \cong \Gamma^{-2s} \cong (\varepsilon_{os} / 2J_i)^s$. Therefore, $w_{s+1} \ll w_s$. However, the experiments showed that the probabilities to absorb more photons than necessary for ionization are comparable. So perturbation theory failed in this case, though the amplitude of the laser wave ($I \cong 10^{14}$ W/cm^2) is well below the intra-atomic value.

The number of electron peaks and their amplitudes depend on the laser intensity, wavelength, polarization, and pulse duration. In particular, if the intensity of linearly polarized radiation with duration 100 ps (λ = 1064 nm, $\hbar\omega_0$ = 1.16 eV) acting on low-pressure xenon ($P \approx 10^{-7}$ torr) increases up to 6.4×10^{13} W/cm^2, then the number of peaks increases to 9 [44]. Fig. 9 shows typical spectra of photoelectrons. At shorter wavelength (λ = 532 nm, all other parameters being kept the same) the number of peaks increase only to 4 [44]. Also, if the laser pulse is shortened, the number of electron peaks decreases until they disappear completely at a certain value of duration below one picosecond [46]. The role of polarization is also very important. In the case of circular polarization (λ = 1064 nm, $I = 9.6 \times 10^{13}$ W/cm^2, τ_0 = 100 ps) the maximum energy of the electrons reaches 15 eV [44]. Since a free electron cannot absorb a photon, the absorption process seems to occur whilst the electrons are in a bound state. In this case the laser field affects the positions of the energy levels, thus inducing a Stark shift in an oscillating field, and hence new resonances can appear whose positions depend on time. That is why many researchers consider the two effects, the dynamic Stark effect and time-dependent resonances, to determine the difference between experimentally observed probabilities of ionization and those given by the Keldysh theory. It should be noted that the phenomenon of abovethreshold ionization is rather complicated and its exhaustive theory is now far from being completed. Because multiphoton ionization is a strongly nonlinear process, the influence of experimental conditions (e.g., spatial and temporal dependencies of intensity and distributions of spatial charge within the focal volume) strongly affect the electron spectra, hence their interpretation proves to be rather difficult. We think, however, that the experimental and theoretical data available allow us to presume the effect to be predominantly determined by the interaction of a laser field with an individual atom.

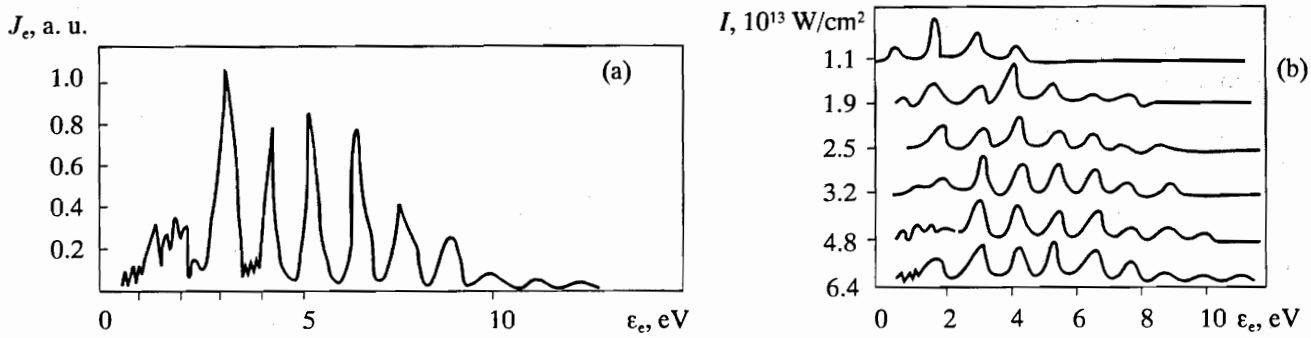

Fig. 9. *Spectra of photoelectrons from Xe under irradiation by a laser with λ = 1064 nm, τ_0 = 100 ps and pulse energy 11 mJ at intensities higher than 10^{13} W/cm^2 (linear polarization): spectrum at $I = 2 \times 10^{13}$ W/cm^2 (a), dependence of the number of electron peaks on intensity [44] (b).*

This suggestion was first formulated and shown, at least qualitatively, in [47]. In that work, the non-stationary Schrödinger equation was solved for a one-electron atom in a strong rapidly oscillating field $E_0 \sin\omega_0 t$, the shape of the potential being given by a certain model that was introduced by the same authors in [48]. Under the assumption that 10 photons are needed for ionization, the spectra of ionized electrons were calculated for which the maximum electron energy corresponded to absorption of 17 photons. This theory simulated the increase of the number of peaks in relation to increasing field amplitude, as well as the Stark shift, i.e., the growth of the ionization threshold under the effect of the ponderomotive potential $U = e^2E_0^2/4m_e\omega_0^2$.

2.1.2. Thresholds for Multiphoton Ionization. The most exhaustive data on MPI were obtained for noble gases (He, Ne, Kr, Ar, Xe). Their ionization thresholds lie within the range of intensity 10^{13} - 10^{14} W/cm^2 for picosecond pulses and have a tendency to increase as the pulse shortens. According to [44], at τ_0 = 100 ps (λ = 1064 nm) the ionization threshold of Xe^{+1} lies near 10^{13} W/cm^2. As the pulse is shortened toward a picosecond (τ_0 = 1.2 ps and τ_0 = 40 ps), the threshold remains the same [50] but the intensity corresponding to saturation of the number of ionized atoms is higher by a factor of 1.4 for the case of the shorter pulse. This tendency stays valid if the pulse is further shortened. In particular, at τ_0 = 500 fs, λ = 616 nm, the saturation of Xe^{+1} occurs at 3.1×10^{13} W/cm^2 [46], while at τ_0 = 100 fs (λ = 670 nm) it occurs at 1.7×10^{14} W/cm^2 [45]. Finally, at τ_0 = 22 fs, i.e., when pulse duration is about 7 light periods (λ = 625 nm), the ionization threshold of xenon goes up to $(3 - 4) \times 10^{13}$ W/cm^2 [51, 52]. Fig. 10 shows the dependence of the yields of xenon ions of different charge on the intensity and duration of the laser pulses. Note that shortening of the pulses affects the thresholds much more than the wavelength does. The experimental thresholds and ion yields above the MPI threshold agree rather well with the Keldysh theory corrected for the Stark shift in an oscillating field and for resonances [39, 41 - 43, 52]. It should be noted that for very short pulses (τ_0 = 22 fs and 90 fs) [52] good agreement with the classical work by Keldysh [39] was obtained without regard for resonances. According to [52], for pulses as short as several light periods there is no time to establish a new quasi-stationary state for the elec-

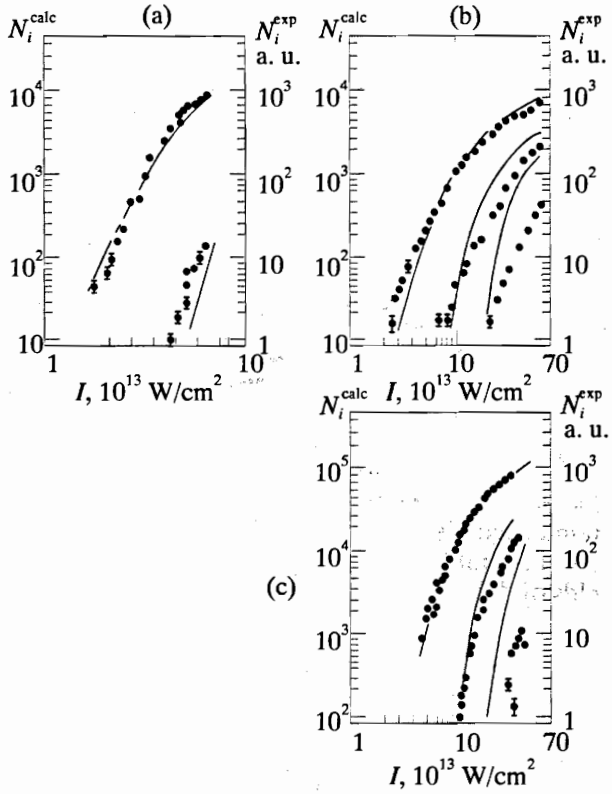

Fig. 10. *Yield of xenon ions with different charges (up to Xe^{+3}) as a function of intensity for different pulse durations: τ_0 = 900 fs, λ = 616 nm (a); τ_0 = 90 fs, λ = 625 fs (b); τ_0 = 22 fs, λ = 625 nm (c) [52]. Solid lines are the results of calculations using the theory of [80]. Calculations give the absolute number of ions N_i^{calc} (left-hand scale) corresponding to the actual geometry and gas density of the experiments. The experimental number of ions N_i^{exp} is given in arbitrary units in the right-hand scale. The experimental and theoretical curves are shifted so that an impression of their agreement could be obtained. The standard deviation of the experimental values are shown.*

trons under the ponderomotive force of the laser field. The time for establishing such resonances may be estimated from the following qualitative consideration. Suppose that all high states are displaced by the ponderomotive potential $\hbar\Delta\omega(t) \approx U(t)$ whose maximum rate of variation [52] is:

$$\dot{U} = (dU/dt)_{\max} \approx U_0/\tau_0, \qquad (2.1)$$

where $U_0 = e^2E_0^2/4m_e\omega_0^2 \equiv \varepsilon_{os}$ is the maximum value of ponderomotive displacement during a laser pulse with duration τ_0. Let us consider a two-level system with the transition frequency ω_{ab}. Resonance between this frequency and the adjacent harmonic of the laser field $k\omega_0$ can appear during a time interval in which the phase of the electron wave function changes by 2π

$$\delta\varphi = \Delta\omega t = (t^2/\hbar)(dU/dt)_{\max} \leq 2\pi. \qquad (2.2)$$

Then we find the time for a resonance to be established

$$t_p \approx [\hbar(dU/dt)^{-1}_{\max}]^{1/2} \propto (\hbar\tau_0/I\lambda^2)^{1/2}. \qquad (2.3)$$

For the intensity $I = 10^{14}$ W/cm^2 and $\lambda = 616$ nm we get $t_p \approx 13$ fs for $\tau_0 = 90$ fs and $t_p \approx 6.3$ fs for $\tau_0 = 22$ fs. It was mentioned in [52] that resonances existing during only a few optical cycles (in the given case the cycle lasts about 2 fs) can hardly affect the ionization rate. This explains why the experimental curve for the yield of xenon ions versus laser intensity agrees with the Keldysh theory. If the pulses are longer and the intensity is lower, the effect of resonances becomes significant, which is in agreement with experiments.

2.1.3. Multiple Ionization. To date, uranium ions with a maximum charge of +10 [54] and xenon ions with a charge of +9 [56] have been produced by field ionization, i.e. without collisions. The most extensive experimental information is available for noble gases. Just as in the case of single ionization, the threshold intensity of double and triple ionization of xenon increases as the pulse is shortened from picoseconds to femtoseconds; in particular, at $\tau_0 = 22$ fs, $\lambda = 625$ nm the threshold is 1.5 to 2 times higher [52], the thresholds of double and triple ionizations lying in the ranges 5×10^{13} - 10^{14} W/cm^2 and $(2 - 3) \times 10^{14}$ W/cm^2, respectively. In [53] the dependencies of the threshold intensities for the ionization of argon, krypton, and xenon were measured in the range 10^{13} - 4×10^{14} W/cm^2 in the field of a dye laser ($\lambda = 586$ nm, $\hbar\omega_0 = 2.17$ eV), and the experimental dependence of the threshold intensity on the ionization potential was plotted in the range $J_i = 10$ - 80 eV.

Ionization by laser fields for a series of atoms (He, Ne, Ar, Kr, I, Xe, Eu, Yb, and U) was studied using a laser with pulse duration $\tau_0 = 5$ ps and $\lambda = 193$ nm ($\hbar\omega_0 = 6.59$ eV) in the intensity range from 10^{15} to 10^{17} W/cm^2 [54]. The yields of xenon ions with different charges were measured as functions of intensity. It was found that increasing intensity from 10^{15} to 10^{16} W/cm^2 results in an increase of the maximum charge of ions from +6 to +8. If the intensity further increases, then the maximum charge stays the same while the absolute yields of ions with smaller charges grow. The comparison of the results of [54] and [55, 58] enables us to define the dependences of the ion yield on the laser wavelength under fixed intensity. In the case of krypton, the comparison of the results for $\lambda = 1064$ nm [55] and $\lambda = 193$ nm [54] shows that the maximum charges are the same ($Z = +4$) though the ion yield is one order of magnitude greater for the short-wavelength laser. A similar comparison done for xenon with $\lambda = 193$ nm [54] and $\lambda = 532$ nm [57] demonstrates that shortening the wavelength augments the maximum charge of the ion up to +6.

When analyzing the experimental results on multiple ionization it is of great importance to establish the ionization mechanism, i.e., whether it is of cascade-type (consequent) or direct-type (simultaneous decoupling of several electrons). In [58, 59] it was supposed that electrons from the inner shells can be excited under the influence of coherent motion of outer-shell electrons induced by the strong external field. In [54], where many different atoms from helium to uranium were studied, the shell effects were said to be seen and the direct mechanism of multiple ionization was considered to be possible. However, no convincing experimental data exist till now which would confirm the direct mechanism of ionization. On the contrary, the majority of researchers think the cascade mechanism to be more probable.

Let us present here some experimental data to support the latter interpretation. In [60] the effect of a laser with $I = 3 \times 10^{17}$ W/cm^2 ($\tau_0 = 0.7$ ps, $\lambda = 248$ nm) on low-density xenon was studied. The idea from the experiment was to measure the "fast" X-ray response with high temporal resolution. If electrons of inner shells are excited by the laser radiation, then fluorescence arising from relaxation of those excitations should be detected. For xenon, the X-ray radiation in the range 90 to 140 eV or 500 to 1,000 eV must correspond to the transitions between N ($n = 4$) and O ($n = 5$) or M ($n = 3$) and N levels, respectively. However, in 52,000 laser pulses no X-ray event was detected.

The cascade character of ionization was also confirmed when studying ionization by the second harmonic of a neodymium laser ($\lambda = 532$ nm, $\tau_0 = 0.6$ ps, $I_{\max} = 3 \times 10^{15}$ W/cm^2) of HI molecules which have the same number of electrons as xenon atoms [61]. From studying the ionization mechanism of such molecules and xenon under similar conditions one could draw conclusions about the ionization mechanism. When subjected to ultrashort laser pulses, HI molecules give rise to photoionized atoms of hydrogen and iodine and the positive ions recoil. The molecule decomposes in a very short time (about 10 femtoseconds); in fact, it explodes. This phenomenon of explosive dissociation of molecules experiencing ultrashort laser pulses is called Coulomb

explosion. The energy of hydrogen ions and multiple iodine ions (up to +6) were measured by the time of flight method. If multiple ionization would occur directly, then the recoil force and the resulting energy of the ions would be much higher than in the cascade process. However, the experiments of [61] convincingly indicate that the cascade process is the true mechanism.

Practically all of the results mentioned above are related to ionization in the multiphoton limit ($\Gamma^2 \gg 1$). As the laser intensity increases to $I > 10^{17}$ W/cm^2, field ionization over the entire range of laser wavelengths (λ = 0.2 - 10.6 μm) must occur in the tunnel limit ($\Gamma^2 \ll 1$). Since there is a tendency to use higher intensities in experiments, the latter mechanism will be the most important for studying interactions with superstrong fields. Until now there are only a few laser experiments on tunnel limit ionization. The earlist work was reported in [157] using 20 ps duration Nd laser pulses to ionize helium and argon. In [54] the tunnel ionization of xenon at $\approx 10^{17}$ W/cm^2 (λ = 193 nm) was investigated with $\Gamma^2 \approx 10^{-2}$. In [62, 63] ionization of xenon by CO_2 laser radiation (λ = 10.6 μm) with intensity 10^{13} - 10^{14} W/cm^2 ($\Gamma^2 < 10^{-2}$) was studied. And, finally, in [63] ionization of noble gases by a neodymium laser (λ = 1.06 μm) at 10^{16} W/cm^2 was investigated. The results obtained agree well with the theory taking into account the dynamic Stark effect and the multielectron structure of atoms (see [12, 64, 68]). They do not contradict the cascade mechanism of ionization. The experiments with high intensity are of great interest since they could reveal the ionization mechanism, the maximum ion charge, and its dependence on the laser parameters.

2.1.4. Distribution of Electrons in Collisionless Plasmas Produced by Fast Ionization in Strong Fields. The parameters of collisionless plasmas produced during fast nonlinear ionization by strong picosecond fields differ significantly from those of collisionally ionized plasmas. The differences include the distribution of the ions among the several degrees of ionization (the ions exist in various excited states and are practically immobile) and the distribution of energies of the ejected electrons. The experiments and calculations of [65, 66] demonstrated that the mean energies of electrons produced by powerful ultrashort laser pulses in collisionless plasmas are strongly influenced by the polarization of the pumping field. Let us estimate, as it was done in [65, 66], the distribution function and the mean energy of electrons produced during nonlinear ionization of rarefied gas by laser radiation with different polarizations. Let us represent the field of a laser wave propagating along the z-axis as

$$\mathbf{E} = \{E_x, E_y\} = \{E_0 \cos\omega_0 t, \alpha E_0 \sin\omega_0 t\}, \quad (2.4)$$

where the amplitude $E_0(t)$ varies smoothly during the pulse $\tau_0 \gg 1/\omega_0$ and α is the degree of polarization ($\alpha = 0$ corresponds to linear and $\alpha = 1$ to circular polarization). Let us assume that E_0 is high and that ionization occurs in the tunnel limit, i.e. in a quasistatic electric field ($\omega_0 \ll \omega_a^4$, here $\omega_a = m_e e^4/\hbar^3 = 4.1 \times 10^{16}$ s^{-1} is the atomic unit of frequency). Using the static formulae of [67] and averaging them over the complete optical cycle [68] we obtain the formula for the probability of ionization of a hydrogen-like ion:

$$w(t) = A|\mathbf{E}|^{-1/2} \exp(-b/|\mathbf{E}|), \quad (2.5)$$

where

$$A = 4\sqrt{3/\pi}\omega_a (J_i/J_h)^{7/4} E_a^{1/2}$$

and

$$b = (2/3) E_a (J_i/J_h)^{3/2}.$$

Here J_i and J_h are the ionization potentials of the given ion and hydrogen, respectively, and $E_a = e/a_b^2$ is the atomic unit of electric field. In a strong field, the energy retained by the electron after the laser pulse depends only on the field phase when the electron leaves the atom, provided the conditions $\varepsilon_{os} \gg J_i \gg \hbar\omega_0$ are fulfilled and no electron collisions occur. The energy of free oscillations of electrons in field (2.4) are known to be

$$\begin{aligned} \varepsilon_e(t) &= m_e (v_x^2 + v_y^2)/2 \\ &= (e^2 E_0^2 / 2 m_e \omega_0^2)\ (\sin^2\omega_0 t + \alpha^2 \cos^2\omega_0 t) \end{aligned} \quad (2.6)$$

and for circular polarization ($\alpha = 1$) it does not depend on the field phase. The distribution function of electrons produced by ionization is

$$dn_e/d\varepsilon_e = N_0 w\{t(\varepsilon_e)\}\, dt(\varepsilon_e)/d\varepsilon_e.$$

Then we can easily determine the average energy an electron keeps after the field is switched off:

$$<\varepsilon> = \frac{\int_0^\theta \varepsilon_e(t)\, w(t)\, dt}{\int_0^\theta w(t)\, dt} = \frac{\int_0^\pi \varepsilon(\varphi)\, w(\varphi)\, d\varphi}{\int_0^\pi w(\varphi)\, d\varphi}. \quad (2.7)$$

Here $\varphi = \omega_0 t$ and $\theta = 2\pi/\omega_0$.

It follows from (2.7) that for circular polarization ($\alpha = 1$) $<\varepsilon> = 2\varepsilon_{os}$, where $\varepsilon_{os} = e^2 E_0^2 / 4 m_e \omega_0^2$ is the energy of electron oscillations in the linearly polarized electromagnetic wave averaged over the light wave period. At $\alpha = 0$, we obtain from (2.6) and (2.7) that

$$<\varepsilon_e> = 2\varepsilon_{os} \int_0^\pi \sin^2\varphi\, w(\varphi)\, d\varphi \Big/ \int_0^\pi w(\varphi)\, d\varphi. \quad (2.8)$$

Analyzing (2.8) we find that in the case of linear polarization the mean energy is much lower than in the case of circular polarization. Qualitatively, this is

connected with the fact that the probability $w(t)$ is maximum at the field peak, while the oscillation velocity is phase-shifted by $\pi / 2$ and therefore has a minimum at the same moment in time. This effect was detected in experiments on the interaction of a CO_2 laser with duration 2.5 ps (λ = 9.3 μm) with rarefied xenon ($P \approx 10^{-6}$ torr). In the case of linear polarization ($I \approx 5 \times 10^{13}$ W/cm^2, ε_{os} = 402 eV) the drift energy of electrons in the direction of the laser field was 50 eV. For circular polarization ($I = 10^{14}$ W/cm^2, ε_{os} = 804 eV) the energy of the electrons was 1.2 keV [65]. The measured and calculated spectra proved to agree well.

Therefore, by properly choosing the polarization of laser radiation one can control the energy of the electrons in the plasmas produced. In particular, one can use linearly polarized light to prepare a "cold" plasma as a medium for an X-ray recombination laser. In this case the mean electron energy ("temperature") must not exceed the potential of ionization from a certain state. On the other hand, using circularly polarized light one can obtain blasts of fast electrons as short in time as the laser pulse. In particular, at $I \approx 10^{19}$ W/cm^2 and λ = 10 μm, the electron energy must exceed 100 MeV [65].

2.1.5. Laser Acceleration of Particles. There is one most promising application of strong electric fields, namely, the acceleration of particles (usually, electrons) up to high energies using ultra-short laser pulses. Conventional vacuum accelerators cannot provide accelerating fields higher than 100 to 200 kV/cm, hence an increase in the energies of particles requires growth in the dimensions and costs of machines which have already reached their critical scale. In laser-based accelerators, much higher accelerating fields can be obtained; they use plasma as the accelerating medium and can provide a much higher rate of acceleration. Hence their dimensions are smaller. Several new approaches to acceleration of particles are surveyed in the literature [95]. Here we will briefly touch upon the ideas that make use of ultra-short laser pulses.

The electromagnetic field of light waves is transverse and therefore cannot be directly utilized for the acceleration of particles. This field must be transformed into a longitudinal electric field which can interact with a particle over a long time. Tajima and Dawson [96] proposed the use of longitudinal Langmuir waves for the acceleration of electrons. These waves are excited in a plasma by the beating of two light waves with slightly different frequencies ω_0 and ω_1 which are propagating in the same direction. In this case, the condition of resonance of the beat frequency with the plasma frequency must be fulfilled: $\omega_0 - \omega_1 = \omega_{pe} = (4\pi e^2 n_e / m_e)^{1/2}$. The plasma must be prepared in advance from an independent source, e.g. by using multiphoton ionization. Since the frequency resonance condition must be met over the entire acceleration path, there are very strict requirements for the plasma homogeneity.

In order to estimate the maximum achievable field strength E_p in a Langmuir wave E_{max}, let us suppose that all plasma electrons are shifted with respect to the ions by a certain distance $1 / k_p$, where $k_p = (\omega_{pe} / c)(1 - \omega_{pe}^2 / \omega_0^2)^{1/2}$ is the wave vector of the plasma wave. Then the Poisson equation div $E_p = 4\pi e(n_e - n_i)$ gives:

$$E_{max} = 4\pi e n_e / k_p \cong m_e \omega_{pe} c / e.$$

This field is very strong, e.g. for plasma density $n_e = 10^{16}$ cm^{-3} it is 170 GV/cm. In fact, the perturbation of electron density in a Langmuir wave does not achieve its maximum value, because at higher values of E_p, the motion of electrons becomes relativistic, their dynamic mass increases, the plasma frequency decreases, the resonance between the beats of light waves detunes, and the plasma wave amplitude ceases to grow. According to [97], E_p saturates at

$$E_s \cong E_{max} (16 I_0 I_1 / 3 I_r^2)^{1/3},$$

that is, for achieving high amplitudes of an accelerating field, laser pulses must be used with intensities of relativistic orders. Calculations done in [95, 96] demonstrated that the electron energy in the beat wave grows in the optimal way, provided that the initial electron energy is $m_e c^2 \gamma_0$, where $n_c = m_e \omega_0^2 / 4\pi e^2$ is the critical density and $\gamma_0 = n_c / n_e$ is the relativistic factor. Then an electron may augment its energy by a factor of $2\gamma_0$ in the path as long as $2\gamma_0^2 c / \omega_{pe}$. It is clear that for relativistic acceleration, low density plasmas $n_e \ll n_c$ and/or short wavelength laser radiation must be used. However, at lower n_e the values of the accelerating field and the accelerating path increase. This is not desirable, since it requires laser pulses with longer durations and higher energies.

A beat wave accelerator is the most developed scheme for laser acceleration. In experiments with nanosecond CO_2 laser pulses, longitudinal electric fields as strong as 10 MV/cm were achieved in beat waves [102]. A scheme was proposed that allows a higher rate of acceleration to be obtained in the beat wave due to stabilization of electrons in the accelerating phase of an electric field by a weak transverse magnetic field [98]. However, excitation of a phased wave over the entire acceleration path requires the plasma density to be kept constant over a long distance (about several tens of centimeters); this is a difficult technical problem.

In this connection, other schemes for exciting Langmuir waves with high amplitudes by short bunches of charged particles moving though a plasma [99] or by an electromagnetic field [100, 101] (so-called wake field acceleration) were proposed. A laser pulse propagating through a plasma produces a perturbation of polarization that accompanies the pulse as a plasma wave. In contrast to the method of beat waves the latter method does not require high homogeneity of the plasma, but the laser pulse duration must be extremely small, about the reciprocal plasma frequency $\tau_0 \cong \omega_{pe}^{-1}$. For plasma with density $n_e \cong$

10^{16} cm^{-3}, this amounts to about 200 fs. Electric field strength in a wake wave may be as high as E_{max}, provided the intensity I is of the order of I_r. It should be mentioned that such a laser pulse does not require a preliminary plasma to be produced, since the plasma will appear due to photoionization. The main problem of the wake field acceleration is to overcome diffraction effects and to provide high intensity of laser radiation over an accelerating path as long as about ten centimeters.

In general, the problems related to laser acceleration of particles are now in the phase of preliminary theoretical consideration. The experimental basis for those works will appear with development of powerful subpicosecond lasers.

2.2. Nonlinear Phenomena Which Appear When Powerful Ultra-Short Laser Pulses Pass Through Transparent Media

These phenomena are superbroadening of the laser pulse spectrum (generation of supercontinuum) in gases; induced scattering and self-focusing of laser beams; Cherenkov radiation of ultrashort tightly focused pulses in transparent dielectrics; and generation of higher harmonics of the laser frequency. These have been known for a rather long time and are properly described in the literature [10]. However, when femtosecond pulses with sufficiently high intensities ($\geq 10^{13}$ W/cm^2) were obtained, new experimental results became available which allowed us to understand better the related processes and to establish the conceptual relationship between the phenomena at low and high intensities in atomic and plasma media [52].

2.2.1. Supercontinuum Generation Under the Action of Ultra-Short Laser Pulse. This effect, known more than 20 years in a nonlinear medium, is a threshold phenomenon that arises in a step-wise manner as the intensity exceeds a certain threshold value [10]. This effect can be observed in all transparent media (solid, liquid, and gaseous). Also, the resulting spectrum is of universal character, its short-wavelength region being similar for gases with different compositions and pressures [52], while the long-wavelength region differs. The step-wise increase of the spectral width is very large, in particular, the width of a superbroadened spectrum in xenon ($\lambda_0 = 625$ nm, $\tau_0 = 70$ fs) was measured to be $\Delta\lambda \geq 300$ nm in the intensity level of 0.01, while that below the threshold was only $\Delta\lambda \approx 20$ nm. Fig. 11 shows typical spectra of supercontinua. At different values of pumping power below the threshold, the spectral width agrees well with the theory that takes the self phase modulation of the light into account [10]. Though it is clear from the physical point of view that generation of a supercontinuum occurs due to laser-induced nonlinearities of the medium, no exhaustive interpretation of the effect exists until now. Different effects were supposed to contribute: self phase

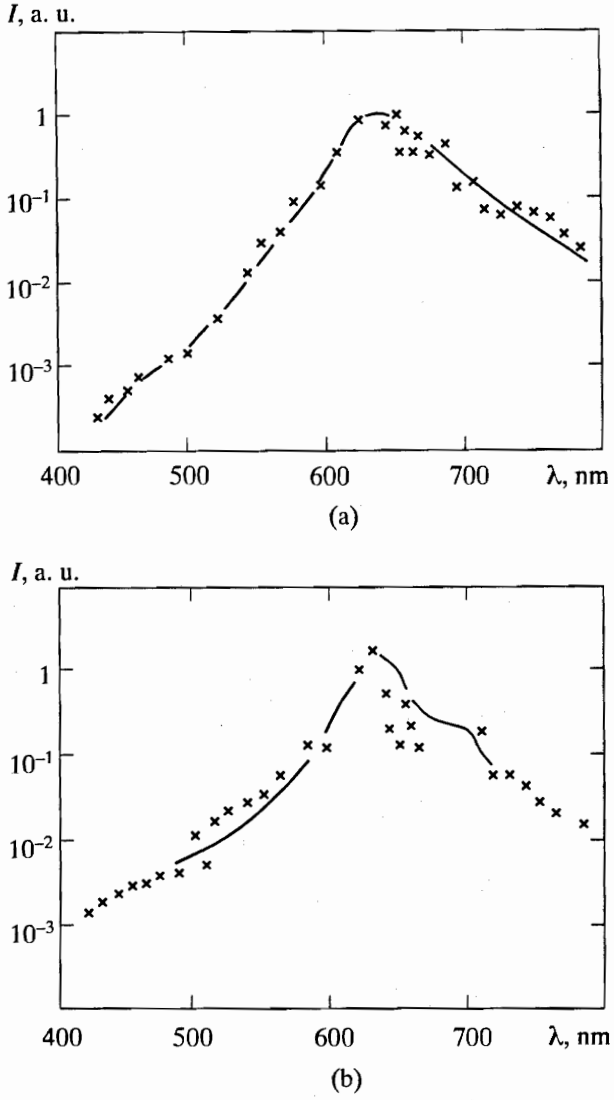

Fig. 11. *Superbroadened spectra (generation of supercontinuum): in xenon at P = 30 atm (a) and in hydrogen at P = 38 atm (b) under a pulse with λ = 625 nm and τ_0 = 70 fs above the self-focusing threshold I ≥ 10^{13} W/cm^2 [52].*

modulation; self-focusing; nonlinearity due to partial ionization; motion of foci; etc. [10]. The issue was understood better after a series of works on supercontinuum generation and related effects in gases appeared [52]. Gases are a convenient medium for studying nonlinear phenomena: first, the degree of nonlinearity may be controlled by pressure, i.e. by the number of active atoms, and, second, the nonlinear properties of an individual atom are determined by its outer-shell electrons whose state, in turn, depends on the external field strength (or intensity). By varying the pressure and intensity, different effects may "switched" on and off.

Experiments of [52] with rarefied xenon ($P \approx 10^{-6}$ torr) helped in establishing that the intensity thresholds for ionization are $(2 - 3) \times 10^{13}$ W/cm^2. It is clear that in such low pressure gas collective nonlinear effects are of no importance. At pressures or about 5 to

20 atmospheres, the main contribution comes from the cubic nonlinearity ($\chi^{(3)}$ in susceptibility and η_2 in refractive index), hence the mechanism of broadening is mainly related to self phase modulation of the laser beam. At higher pressures (15 to 30 atm) and intensities about 10^{13} W/cm^2 superbroadened spectra of xenon were detected with pulse durations of 2 ps and 70 fs at λ = 0.625 μm). Note that the thresholds for superbroadening and self-focusing practically coincide. According to the measurements, the ionization level was very low and could not affect the nonlinear properties of the gas. This is confirmed in particular by the low absorption coefficient (< 3%) and by the symmetric shape of the spectrum due to self phase modulation at intensities slightly below the threshold. Hence, ionization is not the effect to be considered as the cause of superbroadening. The work reported in [52] indicates that in this case the nonlinear properties of atoms are determined by time-dependent resonances. Seemingly, the nonlinearity in the given case is so strong that polarization cannot be represented as an expansion in the powers of the field, just as the perturbation theory fails to explain abovethreshold multiphoton ionization.

2.2.2. Ĉherenkov Radiation from Ultra-Short Pulses. Ĉherenkov radiation of moving bunches of nonlinear polarization [71] was recently observed with the use of tightly focused femtosecond pulses, as was predicted by G.A. Askar'yan almost 30 years ago in [70].

In the case of sharp focusing of the laser beam, there appears a spatial zone of nonlinear polarization with dimensions of several microns, and this zone moves through the medium with the group velocity of the laser pulse. This motion may be considered as the motion of a dipole moment emitting in a wide range of frequencies from radiowaves to far infrared with velocities in excess of the speed of light. Since the phase velocity of emitted waves v_{ph} is smaller than the group velocity of the pulse v_g, the radiation produces in a cone with angle $\cos\theta = v_{ph} / v_g$, just like a shock wave which appears in supersonic hydrodynamic motion of a body. The properties of such radiation are very similar to those of Ĉherenkov radiation from a charged particle moving faster than light in the given medium. However, certain differences exist: first, it is a dipole rather than a charge that emits, and, second, its dimensions are much larger than those of a particle and are comparable with the radiation wavelength. These features determine the temporal, spectral, and spatial properties of radiation emitted by the moving bunch of nonlinear polarization. The duration of a Ĉherenkov radiation pulse and the initial pulse are comparable, but that of Ĉherenkov radiation is longer and increases with the radius of the initial beam [10].

Experiments on the excitation of Ĉherenkov radiation by femtosecond pulses were reported and interpreted in [71]. Radiation from a dye laser with wavelength λ = 625 nm and duration 50 fs was focused into a uniform lithium tantalate crystal ($LiTaO_3$), the minimum beam diameter being 1.5 μm and the intensity 100 GW/cm^2 (10^{11} W/cm^2). Ĉherenkov radiation proved to be coherent with a maximum intensity at about 4.2 THz (4.2×10^{12} c^{-1}). Also, using copper vapor amplifiers, the same effect was observed at a much higher intensity of the optical pulse (up to 20 TW/cm^2 ≡ 2×10^{13} W/cm^2)). It is of interest to mention that the intensity of the emitted field increase as the minus fifth power of the duration of the pumping pulse ($I \propto \tau_0^{-5}$). On this basis, it was concluded that for reliable detection of Ĉherenkov radiation one must use sufficiently transparent media with small attenuation and laser pulses with durations shorter than 100 fs.

A theory explaining many features of the effects involved is based on the model of anharmonic electrons and ion oscillators coupled by the nonlinear interaction. This model results naturally in the predominance of the quadratic contribution to the nonlinear polarization $P_i(t) = \chi_{ijk} E_j(t) E_k(t)$. Interaction of a magnetic field with transverse optical phonons results in resonances in the linear and nonlinear susceptibilities. When the duration of the pumping optical pulse is shorter than the period of the lowest infrared lattice resonance, strong dispersion effects appear that influence the radiation and the shape of the optical pulse. Since the optical properties of lithium tantalate are first of all related to the ionic nonlinear polarization, then the lattice resonances are of importance, in particular, they restrict the generation of shorter pulses of Ĉherenkov radiation in this material. The model with one ionic resonance describes emission in agreement with experimental data. However, it cannot explain the dispersion and absorption of an optical polariton in this material. At the present time, Ĉherenkov radiation of ultrashort pulses in nonlinear media is considered as a method to generate femtosecond pulses of coherent radiation in a specific range of frequencies (up to 5 THz), as well as a means to study electro-optical properties of nonlinear media.

2.2.3. Nonlinear Optical Phenomena Related to Fast Ionization in Gases. When the incident laser power exceeds the ionization threshold ($I > 3 \times 10^{13}$ W/cm^2) the nonlinearity starts being determined by plasma effects. For sufficiently short pulses (τ_0 < 100 fs) which are shorter than the recombination time and the time of electron flight through the focal region, one of the most important mechanism is the non-stationary refraction index that is due to the rapid growth of electron density because of field ionization. The ionization rate varying in time intervals comparable with the laser field period determines the nonlinear current and, therefore, the spatial-temporal and spectral parameters of the pulse in the medium involved. In particular, this mechanism can shift the laser frequency and change the laser pulse shape.

The complete problem of characterizing an ionizing pulse propagating through the plasma it produces involves the Maxwell equations, the ionization equations, and the equations of motion for electrons:

$$\text{rot rot } \mathbf{E} = -(4\pi/c^2)\,\partial\mathbf{j}/\partial t - c^2\partial^2\mathbf{D}/\partial t^2,$$
$$\mathbf{j} = e\mathbf{v}_e n_e, \qquad d\mathbf{v}_e/dt = e\mathbf{E}/m, \tag{2.9}$$
$$dn_e/dt = N_0 w\{\mathbf{E}(\mathbf{r}, t)\}.$$

Here N_0 is the initial density of the particles in a gas, n_e is the electron density, $w\{\mathbf{E}(\mathbf{r}, t)\}$ is the probability of ionization depending on the laser electric field strength $\mathbf{E}(\mathbf{r}, t)$ (see, e.g., (2.5)), the rest of notation being standard. In the case of multiple ionization the last equation in (2.9) must be substituted by a chain of coupled equations taking into account the consequent stages of ionization. The important property of (2.9) is that the ionization probability depends on the instantaneous laser field strength, rather than on the laser intensity. Hence, the concentration of free electrons includes, in addition to the slow component, a component rapidly oscillating with the frequency of the laser field. That is why the laser pulse is frequency shifted and compressed.

The blue frequency shift that occurs during the rapid growth of electron density can be estimated on the basis of simple physical principles [73, 79]. It follows from the dispersion relation for electromagnetic waves in homogeneous plasmas $\omega^2 = k_0^2 c^2 + \omega_{pe}^2$, that as the plasma electron frequency ω_{pe} changes, the laser pulse frequency also changes. Taking into account that the pulse travels through the medium with group velocity v_g we find

$$v_g d\omega^2/dx \approx d\omega_{pe}^2/dt. \tag{2.10}$$

Neglecting the effect of the medium on the pulse velocity we estimate $\Delta\omega$ and take $v_g \approx c$. The frequency shifts in the path L is

$$\Delta\omega = \frac{L}{2\omega_0 c}\frac{4\pi e^2}{m_e}\frac{dn_e}{dt} \tag{2.11}$$

or, for the wavelength

$$\Delta\lambda = -\frac{e^2\lambda^3 L}{2\pi m_e c^3}\frac{dn_e}{dt}. \tag{2.12}$$

Thus, the frequency is displaced to the blue side when electron density increases $dn_e/dt > 0$. Rigorously speaking, (2.11) and (2.12) are only valid for slow variations of density $dn_e/dt \ll \omega_0 n_e$, though they describe qualitatively the case of rapid variation of $n_e(t)$. It is clear from (2.11) and (2.12) that the frequency can only grow in small distances, provided that the growth rate of electron density is very high, as in photoionization of a gas by subpicosecond pulses with intensity higher than 10^{14} W/cm^2. This effect was observed in experiments [72, 74, 78]. In [72] the propagation of pulses of a dye laser ($\lambda = 0.625$ μm, $\tau_0 \approx 100$ fs, $I_{max} \approx 10^{16}$ W/cm^2) which was focused into a 2-micron spot in air at atmospheric pressure was studied. First, it was determined that neither the central wavelength nor the spectral width ($\Delta\lambda = 18$ nm) change until intensity reaches the breakdown threshold ($I^{(1)} = 10^{14}$ W/cm^2 for $\tau_1 = 0.9$ ps and $I^{(2)} = 5 \times 10^{14}$ W/cm^2 for $\tau_2 = 0.1$ ps). Hence, it was experimentally demonstrated that nonlinearities with nonplasma origin (for example, cubic nonlinearity in polarization $\chi^{(3)}$) do not contribute noticeably to the frequency shift. When increasing the intensity above the breakdown threshold and up to $I = 2 \times 10^{15}$ W/cm^2, the blue shift increases to $\Delta\lambda_b = 10$ nm but then, up to $I = 10^{16}$ W/cm^2, it remains the same. This value of displacement agrees well with (2.12) if we suppose that air is strongly ionized ($n_e = 2.7\times10^{19}$ cm^{-3}) and the length $L = 100$ μm corresponds to the experimental conditions.

Experimental results on the propagation of laser radiation with the parameters given above through argon and neon at 5 atm ($N_0 = 1.5 \times 10^{20}$ cm^{-3}) has been published [78]. The blue shift of the central line is about 14 nm for both gases, while the shape of the spectrum for neon calculated by solving (2.12) numerically with the probability of single ionization taken from the paper by Keldysh [39] coincides well with the experimental data (see Fig. 12). The spectral width in neon nearly coincides with that of the initial optical pulse. On the other hand, the spectrum in argon is noticeably (by a factor of three or more) wider than in neon; this is not yet explained theoretically.

Hence, the effect of fast ionization on the propagation of ultrashort pulses through the plasma they produce is much more complicated than could be expected from simple qualitative arguments. This is confirmed by the theoretical analysis done in [75 - 77]. In particular, in [76] the solutions of (2.9) were investigated analytically, the temporal dependence of electron density being approximately taken into account retaining only up to the second harmonic of the frequency of the initial pulse. It was predicted that the frequency doubles in the length of about 1 cm (in qualitative agreement with (2.11)), and the spectrum narrows $\Delta\omega \propto 1/\omega_0$.

The effect of self phase modulation of a laser pulse in the plasma which it produces could be used to create a pulse with a specified temporal dependence of its frequency, for example, (see Chapter 1 and [10]), to suppress undesirable nonlinear effects in amplification of ultra-short pulses. There is a well-known phenomenon of self phase modulation in a nonlinear medium (say, in a fiber) [10] in which the frequency within a wave pack depends linearly on time. In [77] it was supposed that a similar role can be played by rapid ionization of the medium, since the frequency increases proportionally to the growth rate of electron density. However, in order to obtain the required temporal dependence of frequency one must properly choose the shape of the initial pulse depending on the temporal dependence of ionization. In addition, the regime must be chosen so that the change in the wave pack group velocity be determined mainly by the increase of frequency, which may be considerable if the path in the medium is long.

The effect of nonstationary ionization may also result in shortening of the laser pulse because the growth of the electron concentration reduces the group velocity of light and, therefore, the trailing edge of the pulse runs faster and overtakes the front. Authors of [77] predicted that pulses of a neodymium laser (λ = 1064 nm, $I = 10^{14}$ W/cm^2) with duration 0.5 ps to be shortened by a factor of 15 in atomic gas at 100 atm in a path shorter than 1 cm.

2.2.4. Short Wavelength Radiation from Media Under Ultra-Short Laser Pulses (Low Intensities). It follows from experimental data on multiphoton ionization [12, 54 - 63], that the ions produced at or above the ionization threshold can be excited. Therefore, there are several reasons to study radiation at wavelengths much shorter than the incident one. Thus the following can occur: (a) the generation of harmonics of laser radiation due to nonlinearity and non-stationarity of atomic polarization; (b) the generation of harmonics in induced plasmas due to nonlinearity of current produced by fast ionization; (c) radiation from transitions between excited states and, probably, from recombination; and (d) parametric processes.

In many experiments on multiphoton ionization such radiation could not be detected because of the low gas pressures involved. In experiments [8 - 83, 86] the generation of harmonics for gas densities in the focal spot of about 10^{17} - 10^{18} cm^{-3} were studied in conditions when the expected intensities were sufficient for detection. At the present time, the experimental results on generation of harmonics are available for different pulse durations, wavelengths and laser intensities. Here we discuss the results of experiments in which the related mechanisms can identified.

In [81], radiation from a Nd-glass laser (λ = 1064 nm, $I_{max} = 10^{13}$ - 10^{14} W/cm^2, τ_0 = 30 ps, repetition rate 10 Hz) was focused on a jet of krypton, argon, or xenon, the pressure in the focal spot being about 10 torr (particle density up to 10^{18} cm^{-3}).

In each gas, more than twenty harmonics $\omega_k = k\omega_0$: Ar ($k \leq 33$), Kr ($k \leq 29$), Xe ($k \leq 21$) were detected. The intensities of harmonics with $k > 5$ were almost the same, until a sharp decrease occurred after the maximum; the direction of their emission was along the laser beam axis. Since the generation of harmonics was observed initially at a laser intensity 3×10^{13} W/cm^2, we can expect that the threshold from single ionization was exceeded. No conclusion can be made about the degree of ionization, because the ion yields and charges were not measured. Simultaneously with the generation of harmonics, fluorescence from excited states was observed as well as the resonance lines of transitions in neutral atoms.

It is of interest to compare the above mentioned results with data on generation of harmonics using a krypton-fluorine laser (λ = 248 nm) with pulse duration

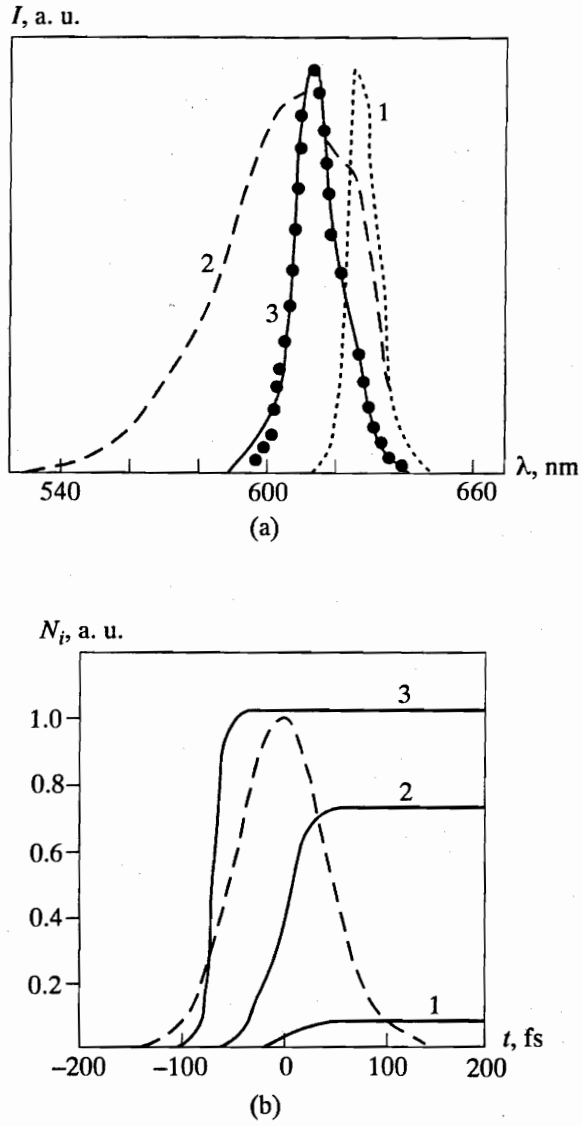

Fig. 12. *Displacement of the spectrum under laser pulses with duration 90 fs at maximum intensity 10^{16} W/cm^2 acting on argon and neon at a pressure of 5 atm [78]. (a) Initial spectrum of the pumping pulse (1), and spectra in argon (2) and neon (3). Points at curve (3) are the results of calculations done using Keldysh theory to evaluate the ionization rate. (b) Fraction of singly-ionized neon atoms (J_0 = 21.6 eV, $\hbar\omega_0$ = 2 eV) calculated from Keldysh theory as functions of intensity and time at $I = 10^{15}$ W/cm^2 (1), 2×10^{15} W/cm^2 (2) and 10^{16} W/cm^2 (3). Comparison with a Gaussian pulse (dashed curve) shows that ionization occurs predominantly in the pulse front.*

τ_0 = 350 fs and intensity $I = 10^{15}$ - 10^{16} W/cm^2 [83]. As in the work referred to above, the gases involved (He, Ne, Ar, Kr, Xe) were introduced into the experimental chamber as gas jets. According to estimations, the gas density in the focal region was about 10^{18} cm^{-3}, as in [81]. Two types of short wavelength radiation ($\lambda' \ll \lambda$): were observed: Generation of harmonics and fluorescence from transitions between excited states. The authors of those

experiments mention an anticorrelation between the two types of radiation. The experimental results are summarized in Table 2.

Table 2. Experimental results on generation of harmonics

Gas	Maximum harmonics number	Wave length, nm	Maximum ion charge	Binding energy in the given charge state, eV
He	13	19.1	2	79
Ne	17	14.6	4	224
Ar	7	35.5	8	627
Kr	7	35.5	8	544
Xe	9	27.6	9	630

The fluorescence lines of ions of argon (4^+, 5^+, 6^+, 7^+), krypton (6^+, 7^+, 8^+) and xenon (6^+, 7^+, 8^+) lie within the spectral range from 9.8 to 48.1 nm and some of them could be identified with known transitions. According to the estimates in [81], the recombination times under the experimental conditions are rather long (about 600 ps) and collisions must play no role in the plasma radiation. Comparing the results of the two experiments, we can conclude that in the second case the harmonics are generated in the plasma produced by fast ionization by ultrashort pulses. In this case, the maximum number of harmonics for heavy gases is low (for xenon it is 9 rather than 33 in [81], the same as for argon and krypton). However, in the same condition the higher numbers of harmonics were obtained using the light noble gases (for helium it is 13, for neon it is 17). Comparing the results on the generation of harmonics in helium [83] with those of [82], where the seventh harmonics was observed under irradiation by a krypton-fluorine laser (λ = 248 nm, τ = 15 ps, $I \cong 10^{15}$ W/cm^2), we see that the situation differs strongly from that of heavy gases, namely, long pulses generate fewer harmonics than short ones. In addition, in [82] higher harmonics were seen to have smaller intensity.

In relatively weak fields (at intensity not much higher than 10^{13} W/cm^2) the degree of ionization is not high and the predominant mechanisms for generating harmonics is seemingly the nonlinear polarization of the atoms. In this case, rapid variations of the induced dipole moment result in the generation of high-frequency radiation. In nonlinear optics such effects are considered in terms of an expansion of the susceptibility in powers of the field, the order of nonlinearity required in this case being rather high [83]. In addition, the nonlinear response of the system is not quasi-stationary (as it is often taken in optics) and proves to be the case in experiments with ultrashort pulses.

The approach proposed in [84, 85, 87] seems to be more adequate. It is based on ab initio numerical solution of the Schrödinger equation for an atom of a noble gas placed into strong oscillating electric field, the solution being carried out to the single-electron approximation with the effective potential of the ion residual. It was demonstrated [84] that under conditions close to those of [81, 83] the radiation spectrum includes more than twenty harmonics. It must be emphasized that an experimental spectrum is, in principle, determined not only by the response of an individual atom, but also by the distribution of the individual emitters in phases along the radiation path. This is so because the emitting atoms are not independent since they are excited by the coherent pumping wave that sets up certain phase relationships between excited atoms lying on its trajectory.

In [85], the nonstationary Schrödinger equation was solved for a xenon atom, the self-consistent potential being taken in a rather simple model form. In this work, the spectrum of 17 harmonics with an abrupt drop after the last one was obtained; this agrees qualitatively with experiments. Also, certain specific features of the experimental spectra were reproduced, namely, approximately equal amplitudes of harmonics starting from the fifth one; a continuous pedestal near the base of the harmonics; an abrupt drop of the spectra, and an increase in the number of harmonics with increasing intensity. No collective effects were needed to fit the calculations to the experimental data. In the same work, the discrete spectrum of electrons produced in abovethreshold multiphoton ionization were calculated and the number of electron peaks coincided with the number of harmonics. Hence, the relationship between the generation of harmonics and abovethreshold ionization seems to be established.

At laser intensities much higher than the ionization threshold, generation of harmonics can be explained by the presence of plasma nonlinearities [88]. If the ionization of atoms occurs in the tunneling regime, then the rate of ionization has maxima coinciding with the maxima of the electric field in the laser wave. As a result, the electron concentration contains components oscillating at the frequencies of the laser field and its harmonics $\omega_k = k\omega_0$. Usually, the second harmonic has the greatest amplitude (because the ionization rate depends on the field modulus). Also, there are even high-frequency components ($k = 2n$, $n > 1$) due to the exponential dependence of the ionization rate on the field. The nonlinear current, determining the reemission from the plasma so-produced, is the product of electron density and velocity. The electron velocity is the sum of the oscillatory and drift velocities, the latter being determined by the field phase at the moment when the electron decouples from the atom.

Hence, the nonlinear current includes only odd harmonics. The spectrum of harmonics can be determined by solving Maxwell equations numerically with due regard for the nonlinear current (2.9); this spectrum also includes only odd harmonics coherent to the laser wave. We think that this mechanism of generation is close to that taking place under the experimental conditions of [83].

In [94], the generation of harmonics in noble gases (helium, argon, neon) at the maximum intensity of a

KrF laser (λ = 248 nm) in the range 10^{15} - 10^{18} W/cm^2 was observed. A laser pulse with duration 280 ± 35 fs was focused onto a gas jet with density 7×10^{17} cm^{-3} and area 4.5 × 6.5 μm^2. The following maximum numbers of harmonics were detected: neon – 27, helium – 23, and argon – 15. The spectrum of the harmonics had no plateau. However, though the intensities of harmonics with higher numbers were lower, a certain inversion effect was observed for the first time, namely, the intensities of some high harmonics were greater than those of the lower ones, in particular, for neon $I_{19} > I_{17}$, for helium $I_{21} > I_{19}$ and for argon $I_{13} > I_{11}$. In addition, the dependence of the harmonics intensities on the intensity of the pumping radiation was measured. It was found that harmonics with the numbers 7, 13, and 19 saturate at $I \cong 10^{17}$ W/cm^2.

Thus, we now understand qualitatively a series of experimental effects of the generation of harmonics; however, in some cases no quantitative agreement could be reached. Note that generation of harmonics by pulsed lasers in noble gases produces coherent radiation in the range from 14 to 130 nm with much higher spectral brightness than by other sources, hence it may compete with X-ray lasers.

2.2.5. Generation of Harmonics by Laser Radiation with Ultrarelativistic Intensity. These intensities have not yet been achieved ($I_r \approx 10^{19}$ W/cm^2 for λ = 1064 nm), but some laboratories plan to build laser systems in the near future which would produce intensities of the order of 10^{21} - 10^{23} W/cm^2 [1 - 5]. Below, we present the results of some theoretical work which predict the effects to be expected under such strong radiation. For the sake of simplicity we consider the interaction with so rarefied a gas media that electron collisions may be neglected during subpicosecond pulses. Under a pulse with 10^{21} - 10^{23} W/cm^2, the gas medium becomes a plasma in a time comparable with a laser wave period, the plasma containing electrons and highly stripped ions. Since we assume that $\omega_0 > \omega_{pe}$ and $\omega_0 > \nu_e$, then the interaction of radiation with the medium reduces, in fact, to the interaction of electrons and ions separately (below we will briefly touch upon the collective effects). At $I \gg I_r$ (recall that when $I = I_r$ $\varepsilon_{os} = m_e c^2$) the interaction of radiation with an individual electron has the character of nonlinear (multiphoton) Thomson scattering, since $\hbar\omega_0 \ll m_e c^2$. Therefore, the scattered radiation has a spectrum consisting of a set of harmonics of the incident frequency $n\omega_0$ whose maximum is shifted towards higher frequencies, while the amplitudes of harmonics are functions of the laser intensity. The problem of the interaction of an elliptically polarized wave with an initially resting electron was considered in [90] within the classical approximation (i.e. with reaction of radiation neglected). The characteristic parameter of radiation is the value $q = eE_0 / m_e\omega_0 c$ which in the nonrelativistic case has the sense of the ratio of the electron velocity to the speed of light. This value can be expressed from the laser intensity and wavelength as

$$q^2 = 7.44 \times 10^{-5} I_{14} \lambda^2_{mkm}.$$

In the case of $q^2 \gg 1$ and circularly polarized radiation, harmonics with approximately constant amplitude (proportional to the incident power) are generated with the numbers of harmonics $n \le n_c$ (where $n_c \approx q^3$ is the number of the maximum harmonic). For $n > n_c$ the amplitudes of harmonics decrease exponentially. The radiation from all harmonics with $n \le n_c$ is concentrated within a cone with the angle $\theta_0 = \sqrt{8/q}$ with respect to the laser beam axis and the power of harmonics per unit solid angle increases proportionally to q^5. At $I = 10^{21}$ W/cm^2 and $\lambda = 10^3$ nm we have $q = 27$ and $n_c \approx 2 \times 10^4$, i.e. $\lambda_c \approx 5 \times 10^{-2}$ nm.

Numerical calculations of nonstationary interactions of laser radiation at 10^{19} - 10^{22} W/cm^2 with atoms demonstrated [91] that the radiation spectrum of atoms consists of the harmonics of the incident radiation until $I = 10^{19}$ W/cm^2 and then changes qualitatively to a complicated structure with a predominance of the atomic frequencies.

In [92, 93] the authors have considered the collective effects (influence of a self-consistent field in a plasma) on the motion of electrons at 3×10^{20} W/cm^2 and $\omega_{pe} = 0.28\omega_0$. It was demonstrated that the energy distribution of electrons becomes less regular than was predicted in [90]; however, the maximum energies of electrons may be higher.

Summarizing these papers, which are few till now, we can expect that at ultrarelativistic intensity the laser radiation would experience conversion into short-wavelength harmonics of the incident frequency $n\omega_0$ ($n > 10^4$) with an efficiency higher than 10^{-5}.

3. ACTION OF POWERFUL ULTRA-SHORT LASER PULSES ON CONDENSED TARGETS

Development of lasers with pulse durations less than one picosecond, with high contrast and with power higher that one terawatt opens new possibilities for studying the properties of matter in strong electric fields. When such radiation hits a condensed target, the matter rapidly ionizes with the production of thin layers of surface plasma (as thin as about one micron), the plasma possessing a series of unusual properties of great interest for research and practical applications.

One of the main features of such plasmas is their high density, close to that of solids. This is due to the rapid ionization by the laser field and by the inertia of ions which remain stationary during the laser pulse. In experiments with terawatt lasers which were carried out till now, the electron temperature in the surface layer rises up to several hundreds of eV. It is possible that at higher laser power, electrons could be heated up to relativistic temperatures and this would yield a unique laboratory plasma whose parameters are close to those of stars. Obviously, it is of great scientific interest to study such plasmas.

It is possible to point out practical applications of such plasmas. First, the unique combination of high density, high temperature and short lifetime yields a promising source of pulsed X-ray radiation which could be used for studying transient chemical processes; for microscopy of biological objects; for diagnostics of laser-produced plasmas, for microlithography, etc. Second, such plasmas may prove to be useful as active media for X-ray lasers with wavelengths <10 nm; the efficiency of transformating thermal energy into coherent radiation may be rather high due to the high laser intensity. Such plasmas may also be used as a source of highly stripped ions, as particle accelerators, and for a series of other application, e.g. to study substances at extremely high pressures.

In this connection, it is of interest to consider the properties of plasmas produced by ultra-short laser pulses and their ultimate parameters and to determine the conditions for optimizing the yield of X-ray radiation. In this section we concentrate on three basic issues of laser-plasma interaction: (1) absorption of laser radiation and production of plasmas; (2) transport of energy absorbed at the surface into the bulk matter by electron thermal conductivity; (3) expansion of the plasma into vacuum towards the laser beam. These issues are clearly correlated, however, when analyzing them we specify the main factor governing the process. Also, this scheme is convenient for discussing the experimental results.

3.1. Theory of the Interaction of Ultra-Short Laser Pulses with Condensed Matter

3.1.1. Ionization of the Targets. By the term "ultrashort laser pulse" we mean a pulse with duration less than one picosecond and with high contrast such that no plasma appears before the main pulse comes to the target. Usually the time of expansion of the laser-heated substance is much longer than a picosecond laser pulse, hence the target ions remain immovable and cold. The effect of laser radiation on a target depends on the intensity and on the target material. Transparent dielectric targets retain their state up to intensity about 10^{14} W/cm^2. The linear character of the interaction of radiation with metal target breaks down much earlier. At intensity $\geq 10^{12}$ W/cm^2, additional ionization and heating of the electrons significantly affect the process of absorption of the laser power, which becomes quite nonlinear. Above the ionization (breakdown) threshold there is no difference between metal and dielectric targets, since the number of free electrons within in the interaction range and their energies are self-consistently determined by the parameters of the laser pulses.

Two additional ionization mechanisms are possible: Ionization by inelastic collisions of atoms with electrons heated by the laser field; and photoionization due to bound-free transitions of atomic electrons under the electric field of the laser radiation. The relationship between the two mechanisms depends on the electron collision frequency; on the frequency and strength of the laser electric field; and on the target material [103]. Collisional ionization results in an exponential growth of the number of free electrons, i.e. in an avalanche breakdown, but it requires the electron collision frequency and initial electron density to be relatively high. Those conditions are well met in metals, hence their breakdown thresholds are low. Photoionization is more characteristic of rarefied gases and dielectrics. Since the energy of a laser quantum $\hbar\omega_0$ ranging from 1 to 4 eV is smaller than the ionization potentials of atoms J_i, the photoeffect involves many photons and, hence, is a strongly nonlinear process. The ionization rate (probability of ionization of one atom per unit time) in the multiphoton limit $\Gamma^2 \gg 1$, i.e., at moderate laser intensities [12, 103] is

$$w_n \cong \omega_0 n^{3/2} (\varepsilon_{os}/J_i)^n. \tag{3.1}$$

It is determined by the number of absorbed quanta $n = J_i/\hbar\omega_0$ and by the laser intensity ($\varepsilon_{os} = e^2|E_0|^2 / m_e\omega_0^2$, i.e. the energy of oscillations of a free electron in the laser field is proportional to the intensity of laser radiation $I = c|E_0|^2 / 4\pi$). In (3.1) it was assumed that $\varepsilon_{os} \ll J_i$; that is why the multiphoton photoeffect is the most important for short wavelength lasers. The physics of multiphoton photoionization under the conditions of applicability of (3.1) was considered in detail in the previous section and in the surveys of [12, 89]. Here we only mention that multiphoton photoionization can compete with collisional ionization only in rarefied gases. In condensed media, the latter mechanism is dominant, since its probability is

$$w_c \cong \nu_{ein} \varepsilon_{os}/J_i, \tag{3.2}$$

where ν_{ein} is the frequency of inelastic collisions between the electrons. This probability does not depend strongly on laser intensity.

Here we will be mainly interested in the case of high laser intensities for which $\varepsilon_{os} \gg J_i$. (For $J_i = 10$ eV and $\lambda_0 = 1$ μm, the condition $\varepsilon_{os} = J_i$ is fulfilled at $I = 10^{14}$ W/cm^2). Ionization of the target is then due to the tunnel effect whose probability [12, 103]

$$w_t \cong (J_i/\hbar)\ \exp[-(4/3)\ (J_i/\hbar\omega_0)\ \sqrt{J_i/2\varepsilon_{os}}\ ] \tag{3.3}$$

becomes greater than or of the order of w_c (3.2). At $I \approx 3 \times 10^{16}$ W/cm^2, the laser field strength E_0 becomes equal to the atomic strength $E_a = e/a_b^2$ and the exponential index in the formula for w_t becomes unity. Therefore, atoms become ionized during less than one period of the laser field, i.e. almost immediately. We can state that at intensities higher than 10^{15} W/cm^2 there is no difference between metals and dielectrics, and the interaction of laser radiation with condensed targets acquires a universal character [104]. Namely, when laser radiation with high contrast ratio hits the target surface, then a plasma layer with electron concentration $n_e \geq 10^{24}$ cm^{-3} and high conductivity forms in a few

femtoseconds, and this layer reflects back the main part of the laser radiation and screens the target, i.e. the electron concentration is much higher than the critical value $n_c = m\omega_0^2 / 4\pi e^2$. Thus, a near-surface plasma layer appears which is as thick as the skin-layer (the depth of penetration of laser radiation into the matter). The layer then expands into the target due to collisional ionization, the rate of expansion being determined by the efficiency of absorption of laser power as described in the next section.

Here we only mention two important facts. Firstly, because of the high conductivity of the surface plasma, the electric field strength of the laser wave in the plasma proves to be much lower than in vacuum. Thus, the coefficient of absorption of laser radiation is rather low and the nonlinear effects related to the laser field are weak. Secondly, in contrast to gases, collisional ionization occurs specifically in condensed targets and the degree of ionization depends mainly on average electron energy (temperature) rather than on the laser intensity. Because of this, much higher electron temperatures and degrees of ionization may be achieved on condensed targets.

3.1.2. Absorption of Laser Radiation in Near-Surface Plasmas (Low Intensities). Subpicosecond laser pulses provide new possibilities for the production of plasmas with very steep gradients of density from vacuum to solid, the power being directly coupled into the region of abovecritical density. This is one of the main differences from the well known case of nanosecond laser pulses acting on solid targets. In that case a plasma corona appears on the surface with a gradually decreasing density (the scale of the inhomogeneity being of the order of the wavelength or greater), energy is deposited in regions with densities smaller than or of the order of the critical value, and heat transport into regions of higher density is provided by electron thermal conductivity. In addition, the temperature is high in the absorption region, while the regions of high density remain relatively cold.

Under the conditions we now consider, the plasma temperature and density, the skin-layer thickness and the absorption coefficient are correlated and time-dependent. However, the rates of their variation are determined by the rate of absorption of the laser radiation and usually they are slow compared with the laser frequency. This allows us to consider the absorption process assuming the plasma parameters to be known. Then the absorption coefficient determined in this way will self-consistently control the dynamics of the plasma parameters.

Absorption of electromagnetic radiation in overcritical plasmas ($n_e \gg n_c$) may occur in regimes of either the normal or anomalous skin-effect depending on the relationship between the electron mean-free-path l_e and the skin-layer thickness l_s. In the case of relatively low intensities and, therefore, low electron temperatures $l_e < l_s$, the normal skin-effect takes place. Then the relationship between the electric field of the laser radiation and the conductivity current is almost local and the solution of Maxwell's equations results in the Fresnel formula [105] for the reflection coefficient:

$$R_s = \left| \frac{\sin(\theta_0 - \theta_t)}{\sin(\theta_0 + \theta_t)} \right|^2, \qquad R_p = \left| \frac{\tan(\theta_0 - \theta_t)}{\tan(\theta_0 + \theta_t)} \right|^2, \tag{3.4}$$

where θ_0 is the angle of incidence of the electromagnetic wave on the plane target surface, $\theta_t = \arcsin(\sin\theta_0 / \sqrt{\varepsilon})$ is the complex refraction angle, $\varepsilon = 1 + 4\pi i\sigma / \omega_0$ is the plasma dielectric constant, and σ is the plasma conductivity. Note that in the case involved ($n_e \gg n_c$) the plasma is opaque for the incident radiation, i.e. $\mathrm{Re}\varepsilon < 0$. Reflection occurs as from a mirror, the indices s and p determine the type of the incident wave, i.e., whether the polarization vector lies in the incidence plane (p) or is perpendicular to this plane (s).

Absorption of the laser energy is determined by the work of the electric field acting on charges, the absorption coefficient being $A = 1 - R$. The normal skin-effect corresponds to the case of $\mathrm{Re}\sigma \gg \mathrm{Im}\sigma$, the skin-layer thickness being given by the following formula

$$l_s = (c/\omega_p)\sqrt{\mathrm{Re}\sigma/\mathrm{Im}\sigma}\cos\theta \ . \tag{3.5}$$

In many cases, it is convenient to take the plasma dielectric function as in the model by Drude [106]:

$$\varepsilon = 1 - \omega_{pe}^2/\omega_0(\omega_0 + i\nu_{ef}), \tag{3.6}$$

where $\omega_{pe} = (4\pi e^2 n_e / m_e)^{1/2}$ is the electron plasma frequency and the value ν characterizes the effective frequency of electron collisions. In this case

$$l_s = (c/\omega_{pe})\sqrt{\nu/\omega_0}\cos\theta \ .$$

Note that in the case of normal skin-effect $\nu > \omega_0$.

Fig. 13 shows the angular dependence of the reflection coefficient for several characteristic values of ν / ω_0 and $n_e / n_c = 30$. In the case of s-polarization, the reflection coefficient monotonically grows due to ejection of field from the medium. The behavior of $R_p(\theta_0)$ is more complicated; it achieves its minimum at a certain value of the angle θ_0. This additional absorption is due to the field of separation of charges that is excited at the plasma-vacuum boundary by the normal component of the electric field of the wave. This effect is similar to resonance absorption of p-polarized electromagnetic radiation in the vicinity of the critical density in slightly heterogeneous plasmas [106]. As for semi-infinite plasma with abovecritical density, the absorption due to the normal component of the electric field was considered in [107, 108] and has the following qualitative interpretation using the

example of a plasma with infinite conductivity ($\mathrm{Im}\sigma \to \infty$). In this case, the electric field does not penetrate into the plasma and produces work only on those electrons leaving the plasma. The ambipolar electric field drives the electrons back, and with the additional energy they are thermalized via collisions. Thus, energy can be absorbed even in the case when the electromagnetic field does not penetrate into the plasma.

At the laser intensity 10^{12} - 10^{14} W/cm^2, the thermal energy of free electrons is relatively low (from one electronvolt to several tens of electronvolts). That is why the number of electrons in a Debye sphere is small and, therefore, the plasma proves to be non-ideal ($\nu \cong \omega_{pe}$). The calculations of the plasma dielectric permeability is a complicated problem [109]; however, the Drude model (3.6) describes the experimental data with reasonable accuracy (see Section 3.2 below). As the laser intensity grows the plasma electron temperature increases and the collision frequency decreases. Hence, the absorption coefficient decreases, the electron thermal conductivity coefficient increases, and the growth of plasma temperature slows down. At the present time, electron temperatures of 300 to 400 eV at the intensities $\cong 10^{14}$ - 10^{15} W/cm^2 for pulses with duration ≤ 0.4 ps have been obtained.

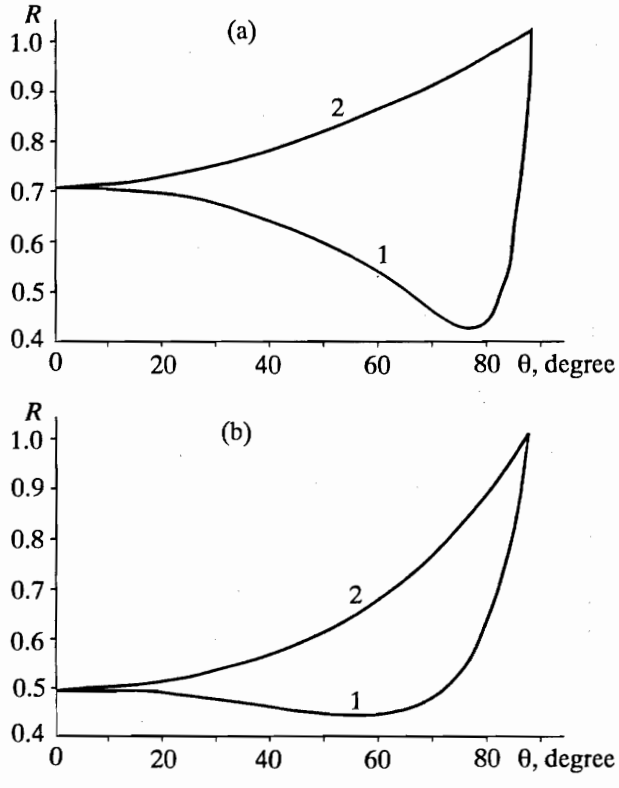

Fig. 13. *Angular dependence of the reflection coefficient of a plane electromagnetic wave from a semi-infinite over-critical plasma in the cases of p- and s-polarizations (curves (1) and (2), respectively) for $\nu_{ef}/\omega_0 = 1$ (a) and 10 (b) at $n_e/n_c = 30$.*

These parameters may be of interest for development of X-ray sources (see Section 3.1.7 below), but for some other applications higher electron temperatures are required. However, in the regime of the normal skin-effect it seems to be impossible and higher laser intensities are needed.

3.1.3. Absorption of Laser Radiation by Condensed Targets (High Intensities). We can expect the physics of absorption to change qualitatively at intensities $\geq 10^{16}$ W/cm^2, when plasma temperatures exceeds 1 keV. The reasons are the following: First, as was pointed out above, the rate of ionization augments due to the tunnel effect (3.3) and the charge of ions increases because of the higher temperature. Second, the electron mean-free-path proves to be higher than the skin-layer thickness (depth of penetration of the field). Therefore, the local approximation for plasma conductivity ceases to be valid and absorption becomes collisionless, i.e. the anomalous skin-effect begins to take place. The skin-layer thickness

$$l_s = (c^2 v_t/\omega_0\omega_{pe}^2)^{1/3}$$

is a function of the increasing temperature [110, 111]. Also, together with l_s, the absorption coefficient increases

$$A_s = A_0\cos\theta_0,$$
$$A_p = \frac{A_0\cos\theta_0}{(\cos\theta_0 + A_0/4)^2 + 3A_0^2/16}. \qquad (3.7)$$

Here $A_0 = (8/3\sqrt{3})\,(\omega_0 l_s/c)$ is the absorption coefficient for normal incidence ($\theta_0 = 0$) of an electromagnetic wave in the regime of the anomalous skin-effect (we assume that $A_0 \ll 1$). For an obliquely incident s-polarized wave, the absorption coefficient A_s decreases as the incidence angle θ_0 increases. For a p-polarized wave the absorption coefficient A_p grows and reaches its maximum ($\max A_p = 2/3$) at a grazing angle $\theta_{0\max} \approx \pi/2 - A_0/2$.

The third reason for the different physics of the laser-plasma interaction at $I > 10^{16}$ W/cm^2 is the possibility of additional absorption due to the excitation of plasma instabilities within the skin-layer and to other nonlinear effects in the strong laser fields [147, 148]. It is known that parametric instabilities are of importance for nanosecond pulses, these instabilities being related to transformation of laser energy into plasma waves in the regions where plasma density is lower than or of the order of its critical value [112]. For subpicosecond pulses, parametric instabilities can hardly be excited since the plasma density is far abovecritical. However, ion instabilities can be expected to appear, provided that $\omega_0 \cong \omega_{pi}$ (ω_{pi} is the ion plasma frequency), as well as electromagnetic instabilities [144] related to the anisotropy of electron distribution functions within the skin-layer. Such anisotropy will necessarily appear because absorption

of laser energy in the regime of the anomalous skin-effect is collisionless.

Additional absorption related to instabilities may be characterized by effective collision frequency $\nu_{ef} \geq \omega_0$ (for ion instabilities $\nu_{ef} \cong \omega_{pi} \cong \omega_0$, and for anisotropic instabilities $\nu_{ef} \cong \omega_{pe}(T_e / mc^2)^{1/2} \cong \omega_0$) and by the additional absorption coefficient $A_{ef} = \sqrt{\nu_{ef}\omega_0} / \omega_{pe}$ which can prove to be greater than A_0 (3.7).

The fourth reason for interest in the range of high intensities $I > 10^{16}$ W/cm^2 is the possibility of significantly superheating the absorption region due to limitations of the thermal flux. As will be demonstrated below, the estimations done using classical theory of heat transport yield values of the thermal flux close to those for free molecular flow. In this case, an instability is known to appear that limits the thermal flux and causes a rapid growth of temperature in the absorption region. This issue is considered in detail in the next section.

And, finally, essentially nonlinear effects in absorption of laser radiation could be expected at $I > 10^{19}$ - 10^{20} W/cm^2, when the motion of target electrons in the laser radiation field becomes relativistic.

3.1.4. Thermal Balance within Skin-Layer. Electron Thermal Conductivity. Temperature is an important parameter that determines the character of the laser-plasma interaction. The thermal balance within the skin-layer in the absence of hydrodynamic motion is determined by absorption of laser energy and energy losses due to electron thermal conductivity and thermal radiation. According to estimations, the radiation losses play a minor role in the energy balance, since thermal conductivity is very high due to the high plasma density. The effect of expansion will be discussed in the next section; here we should only mention that it may be neglected for sufficiently short laser pulses due to the inertia of the ions.

Let us consider, first of all, the case when pulses with relatively low intensity $I \leq 10^{15}$ - 10^{16} W/cm^2 hit a target such that the plasma is heated in the regime of the normal skin-effect. Since the skin-layer thickness is usually small ($l_s \cong 10$ nm) it is natural to suppose that the penetration depth of a thermal wave (heating depth) is $l_t \gg l_s$, while thermal conductivity follows the classical diffusion model.

Thus, we obtain the problem of propagation of a thermal wave in semi-infinite plasma with a given thermal flux at the boundary. This problem is described by the ordinary equation of thermal conductivity:

$$\begin{gathered}(3/2)\, n_e \partial T_e / \partial t = -\partial q / \partial z \\ q = -\chi \partial T_e / \partial z; \qquad (3.8) \\ q(0, t) = AI; \qquad q(\infty, t) \to 0.\end{gathered}$$

In contrast to the classical problem of [113], the thermal flux at the boundary AI varies in time, since the absorption coefficient A depends on the electron temperature T_e. Using the classical expressions for the collision frequency

$$\nu_{ef} = \pi^{3/2} Z e^4 \Lambda / 4\sqrt{2} m_e^2 v_t^3,$$

absorption coefficient $A = 2\omega_0 l_s / c$, skin-layer depth (3.5) $l_s = (c/\omega_p)\sqrt{2\nu_{ef}/\omega_0}$, and coefficient of thermal conductivity $\chi \cong 4 n_0 v_t^2 / \nu_{ef}$ we can obtain a self-similar solution to (3.8). Fig. 14a [111] shows the shape of the thermal wave. The temperature at the plasma boundary (within the skin-layer) grows in time as $T(0, t) \propto t^{1/6}$, the absorption coefficient decreases as $A \propto t^{-1/8}$, and the thickness of the heated region increases as $l_t \propto t^{17/24}$.

The estimations done on the basis of the above formulae are in reasonable agreement with experiments [114 - 116]. This theory is limited at low intensities and at short pulses by the condition $l_t \cong l_s$, i.e. by the condition that the thermal wave must have time to leave the skin-layer. At low laser intensity $I \leq 10^{14}$ W/cm^2 and, correspondingly, at low temperatures $T_e \leq 50$ eV, the flow of heat from the absorption region may be neglected and the equation for temperature in the skin-layer becomes simply:

$$(3/2)\, n_e \partial T_e / \partial t = AI / l_s \cong I\omega_0 / c\,. \qquad (3.9)$$

Thus, the temperature grows linearly in time $T_e \propto t$. We should keep in mind, however, that under the conditions involved the plasma is non-classical [117] and evaluations done using (3.9) overestimate the temperature because the energy spent in ionization is not taken into account, though it is rather large in this case.

Therefore, in the case of absorption of laser radiation within the framework of the normal skin-effect and classical thermal conductivity, temperatures higher than several hundreds of electronvolts can hardly be achieved. Much higher temperatures can be expected in experiments with ultrathin foils ($l \leq l_t \cong$ 100 nm) or with higher laser intensities $I > 10^{16}$ W/cm^2 when additional absorption becomes possible and, this being more important, electron thermal conductivity proves to be limited. In order to illustrate the two effects separately, let us first consider the case of absorption in the regime of the anomalous skin-effect and classical thermal conductivity. If we take into account the appearance of nonlinear absorption and the limitation of thermal conductivity, then (3.8) with the absorption coefficient taken from (3.7) yields the minimum (pessimistic) value for the temperature in the absorption region.

The self-similar solution of (3.7) and (3.8) for the case of normal incidence ($\theta_0 = 0$) determines the shape of the thermal wave (see Fig. 14b) and results in the following temporal dependencies of the basic plasma parameters:

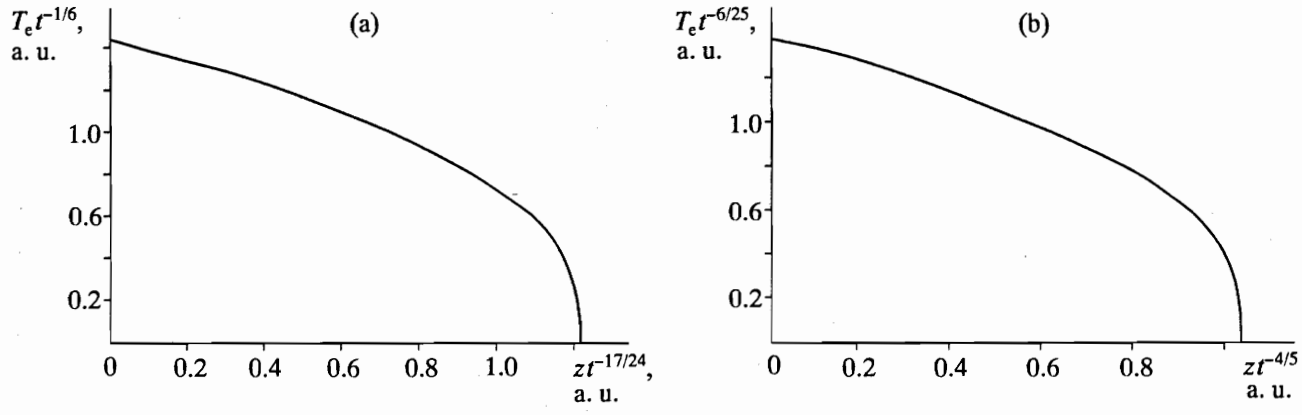

Fig. 14. *The profile of a self-similar self-consistent thermal wave in the cases of normal (a) and anomalous (2) skin-effects for classical thermal conductivity [111].*

$$T_e(0,t) \propto t^{6/25}, \qquad A_0 \propto t^{1/25},$$
$$l_t \propto t^{4/5}.$$

Thus, these parameters now grow faster than in the case of the normal skin-effect. Nevertheless, the predicted values of $T(0, t)$ are not higher than 1 to 2 keV even at $I \cong 10^{18}$ W/cm^2. Note that numerical simulation of thermal transport at $I \cong 10^{16}$ W/cm^2 done in [118] using of LASNEX code proved to be in good agreement with this self-similar solution.

Also, at $I > 10^{17}$ W/cm^2 the estimations of $T_e(0, t)$ obtained within the framework of classical thermal conductivity indicate that the electron mean-free-path is comparable with or greater than the heating depth. Thus, we must expect that the real thermal conductivity is less than in the classical case. In order to estimate the maximum rate of heating in the case of the anomalous skin-effect, let us consider, as was done in [104, 119], the case of extreme limitating the thermal transport by assuming that all absorbed energy remains within the skin-layer. Then according to (3.9), the temperature must grow linearly in time $T_e \propto t$, the heating rate being about 1 MeV/ps for the laser intensity $\cong 10^{18}$ W/cm^2 see [104]. For a pulse with duration $\cong 0.1$ ps, this estimation yields temperature two orders of magnitude higher than was predicted in the model of classical thermal conductivity. Note also, that according to [119], this high rate of heating is accompanied by distortions of the distribution function. The distribution function obtained in [119] is as follows

$$f_e(v,t) \propto vt^{-4/3} \exp(-\delta v^3/t), \qquad (3.10)$$

where δ is a certain constant. This distribution function depends self-similarly on the parameters v^3/t and is characterized by a small number of particles in the region of $v < v_t$ and $v > v_t$ as compared to the Maxwellian distribution function. This accumulation of heated electrons in the region of $v \cong v_t$ can be explained by the low electron-electron collision frequency. Note that self-similar distributions as in (3.10) can be obtained in experiments on irradiation of thin foils ($l \cong l_s \leq 0.1$ μm) by laser radiation.

Therefore, when irradiating targets by laser pulses with 10^{18} - 10^{20} W/cm^2, electron temperatures in the range of several hundreds of kiloelectronvolts can be in principle obtained. Several interesting consequences follow: First, highly stripped ions, up to hydrogen-like uranium ions, can be produced. Second, ions with energies of several hundreds of kiloelectronvolts can appear in the expansion of the plasmas. Third, pressures of several thousands of megabars can be obtained in the expansion of plasmas. Fourth, nuclear transitions can be excited by high-energy electrons. Hence, we conclude that the regime of high intensity of laser pulses is very attractive for study.

3.1.5. Quasistatic Magnetic Fields and Surface Electromagnetic Waves in Overdense Plasmas Produced by Ultra-Short Laser Pulses. The action of powerful laser radiation on condensed targets must be accompanied by the generation of strong quasistatic magnetic fields which can significantly affect absorption of the laser radiation; the dynamics of electrons; thermal transport, and the expansion of the plasma. There are several mechanisms for generating quasistatic magnetic fields in laser produced plasmas. The first is excitation of a thermo-electric current in the plasma due to non-collinearity of gradients of temperature and density. The growth rate of the magnetic field is given by the following formula from [143]:

$$\partial \mathbf{B}/\partial t = -(c/e)\,[\nabla \ln n_e, \nabla \mathbf{T}_e].$$

For nanosecond pulses, this mechanism results in the generation of megagauss magnetic fields. In this case the temperature gradient is normal to the target surface, while the density gradient connected with inhomogeneity of the laser power over the focal spot is directed along the beam radius. The magnetic field is toroidal and its value $B \cong c\tau_0 T_e / edl_t$ (here d is the focal spot diameter and l_t is the heating depth on the target) may amount to up to hundreds of megagauss at

$\tau_0 \cong 100$ fs, $T_e \cong 1$ keV, $d \cong 10$ μm, and $l_t \cong 100$ nm. The electron cyclotron frequency $\Omega = eB / m_e c$ in this magnetic field is comparable with the laser frequency, i.e., the plasma becomes magnetized.

The second mechanism for generating quasistatic magnetic fields is connected with an instability of the electron distribution functions in the case of the anomalous skin-effect. Anisotropy of the distribution function results in excitation of the Weibel instability [144] which corresponds to the generation of small-scale magnetic fields with toroidal configurations. The characteristic spatial scale of the magnetic field is about c / ω_{pe}, i.e. it is comparable with the skin-layer thickness. The value of the magnetic field, in the condition that the instability saturates, follows from the requirement that the radius of electron gyrations in the magnetic field v_t / Ω equals the inhomogeneity scale c / ω_{pe}. Then $\Omega \cong \omega_{pe} v_t / c$ [145], this also resulting in values of several hundreds of megagauss.

There is one more mechanism for generating quasistatic magnetic fields which can only take place for circular polarized radiation and is connected with the inverse Faraday effect [146]. In contrast to the mechanisms considered above, the magnetic field in this case is perpendicular to the target surface and is due to circular motion of electrons in the laser field. Each electron is like a circular current with a radius $\rho_E = v_E / \omega_0$, where v_E is the velocity of an electron in the laser radiation field, and thus it produces magnetic momentum. However, the currents produced by adjacent electrons compensate each other and the resulting magnetization appears only because of inhomogeneities of laser radiation. In order to estimate the magnetic field strength, let us assume the laser beam to have a circular cross section with diameter $d \gg l_s$ and homogeneous distribution of intensity. Then non-compensated current with density $j_E = e n_e v_E$ runs on the periphery of the laser beam in a layer as thick as about ρ_E and, according to the Ampere law, produces magnetic field $B \cong 4\pi j_E \rho_E l_s / cd$ in the beams center. Expressing v_E from the intensity of the laser beam in vacuum we find the following expression for magnetic field inductance:

$$B_z \cong (\omega_0 m_e c/e)\,(I/I_r)\,(\omega_{pe} l_s/c)^2\,(l_s/d)\,.$$

At $I \cong I_r$, using the theory of the anomalous skin-effect for l_s we obtain the estimation $\Omega \cong (\omega_0 \omega_{pe}^2)^{1/3}(v_t / c)^{2/3}$ which yields a magnetic field of the same order as the two above mechanisms.

The production of superdense plasmas with sharp boundaries and non-local characteristics in the skin-layer would allow surface electromagnetic waves propagating along the boundary [120, 121] to be excited. Two applications of such surface waves were proposed for increasing the laser absorption coefficient and as diagnostics of the plasma. It is known [122] that at a certain angle of incidence for an electromagnetic wave on the interface of a plasma, a surface wave running over the interface can be excited, which is then completely absorbed by the plasma. A similar situation takes place in the case of oblique incidence of an ultra short *p*-polarized laser pulse. Such a pulse produces plasma and simultaneously excites a surface wave which may be completely absorbed when the field achieves its peak value, provided that the plasma parameters and the incidence angle are properly chosen. In principle, this effect can noticeably increase the absorption coefficient.

If a superdense plasma produced by an ultrashort pulse is illuminated with a *p*-polarized wave with low intensity so as not to perturb the plasma, then the properties of the laser-produced plasma can be revealed from the reflection of this probe wave. That is, the surface wave may be a useful diagnostic of laser-produced plasmas.

3.1.6. Hydrodynamics of Plasmas in Subpicosecond Laser Fields. The regime of a thermal wave considered above is strongly limited by expansion of the target plasma into vacuum. Expansion is due to motion of the ions which is much slower than motion of electrons because of the big difference in masses. The velocity of the thermal wave is of the order of the electron thermal velocity, i.e. much faster than ions. That is why in short time scales the thermal conductivity is dominant over the ion motion. However, in the course of time, the ions at the plasma-vacuum boundary are accelerated by the ambipolar electric field and a rarefaction wave starts moving into the plasma. The laser radiation is then screened by the region of critical density $n_c \ll n_e$ and cannot reach the dense plasma. Thus, the hydrodynamic regime of interaction is established, which is characterized by deposition of energy in the rarefied plasma and by screening of the dense plasma by the absorption region. The regions of energy deposition and evaporation are connected by virtue of electron thermal conductivity. This regime was considered in detail in papers on controlled thermonuclear fusion (see, e.g., [123, 124]).

In experiments of [125 - 127], the plasma density profile was studied in its dependence on the laser pulse shape and intensity. For pulse durations τ_0, about several tens of picoseconds [125], a density profile is set up, the characteristic scale of the density inhomogeneity $L = (d \ln n_e / dz)^{-1}$ being of the order of several wavelengths ($L \cong \lambda_0 \cong 1$ μm). As τ_0 decreases, the scale L reduces down to $L / \lambda_0 \cong 0.1$ - 0.2 [126, 127]. A further decrease of L depends significantly on the laser pulse shape. In order to create steep profiles with $L \leq l_s \cong 10$ nm it is necessary to provide a steep front on the laser pulse with a duration not longer than several tenths of a picosecond and with high contrast ratio so that the intensity on the target remains below the plasma production threshold ($\cong 10^{10}$ - 10^{12} W/cm^2) until the main pulse arrives. The requirements of the steep front and high contrast are specific to the interaction of laser radiation with a condensed target and they are rather difficult to achieve in practice.

Calculations of absorption [116, 128, 129] demonstrate the absorption coefficient to change non-monotonically when the inhomogeneity scale increases, i.e., it slowly decreases at $L/\lambda \leq 0.1$ and then again increases at $L/\lambda \geq 1$. However, the temperature maximum is displaced toward the absorption region when L increases. That is why the hydrodynamic regime corresponds to cooling of dense plasma layers.

Let us determine the condition of the expansion regime, i.e. let us estimate the minimum time needed for ions to receive significant energy from the electrons. Before doing that, let us estimate (with no regard for losses) the maximum energy of electrons and the related pressure assuming that energy is absorbed under the conditions of the normal skin-effect. Then we find

$$\dot{\varepsilon}_e = d\varepsilon_e / dt = \omega_0 I / cn_e = 2\pi I / \lambda n_e.$$

Then the material pressure within the skin-layer is

$$P \approx n_e \varepsilon_e \approx 2\pi I t / \lambda.$$

At $\lambda = 1$ μm, $I = 10^{19}$ W/cm^2, $t = 10^{-13}$ s, this pressure is $P \approx 6 \times 10^5$ Mbar ($\varepsilon_e \approx 370$ keV), this being comparable with pressures to be achieved inside compressed targets for laser-driven fusion to provide ignition ($\rho_{DT} \approx 100$ g/cm^3; $T_{DT} \approx 10$ keV; $P_{DT} \approx 3 \times 10^5$ Mbar). In addition, the target experiences light pressure during the pulse

$$P_0 = I/c = 3.3 \times 10^{-2} I_{14} \text{ Mbar}$$

that hinders expansion though this pressure is much smaller than the material pressure. Heating of ions by collisions may be estimated from

$$\dot{\varepsilon}_i \approx (m_e/m_i) Z \dot{\varepsilon}_e .$$

That is, this heating is weak.

The strongest effect that terminates the stage of target heating is the expansion of heated electrons and the acceleration of ions by the ambipolar field. The maximum energy of the ions is $\varepsilon_i \approx Z\varepsilon_e$, and their velocity $v_i = (2Z\varepsilon_e / m_i)^{1/2}$ is approximately equal to the velocity of sound in the plasma c_s.

The thermal regime changes to a hydrodynamic one when the characteristic scale of inhomogeneities becomes equal to the dimensions of the absorption region. Since the laser spot diameter on the target is much larger than the heating depth, the hydrodynamic motion looks like a one-dimensional isothermal rarefaction wave. Equalizing the inhomogeneity scale $L \cong c_s t$ and the skin-layer thickness l_s we find the time of existence of the thermal regime to be

$$t_h \cong l_s / c_s. \qquad (3.11)$$

Substituting the expressions for the anomalous skin-layer thickness and for ε_e into (3.11) we obtain the formulae for the onset of the hydrodynamic regime in the form of a scaling

$$t_h \approx \omega_0^{-1} (n_c m_e c^3 / I)^{1/4} (m_i / Z m_e)^{3/8},$$

and a similar expression for the maximum energy of electrons at the target

$$\varepsilon \approx \omega_0 I t_h / c n_e$$
$$\approx m_e c^2 (n_c/n_e) (I/I_r)^{3/4} (m_i / Z m_e)^{3/8}.$$

This expression may be considered as the maximum possible electron energy for heating of a condensed target (optimistic estimation). Heat losses reduce the value of ε_e. Fig. 15 shows the boundaries of different regimes of absorption calculated under the assumption of classical thermal conductivity for laser radiation with the wavelength $\lambda = 0.25$ μm. It is seen that to enter the regime of the anomalous skin-effect and, therefore, for the production of hot electron plasmas, laser pulses shorter than 100 fs, with intensities greater than 10^{17} W/cm^2 and with contrast ratio of about $\cong 10^{-7}$ - 10^{-8} are needed.

3.1.7. X-Ray Radiation from Dense Plasmas. There are three different physical mechanisms of X-ray radiation of dense plasmas: (1) bremsstrahlung radiation having continuous spectra with mean energy of about the electron temperature $\hbar\omega_x \cong T_e$; (2) line radiation due to electron transitions in atoms and ions (to be used in X-ray lasers); and (3) generation of higher harmonics of the laser frequency $\omega_k \approx k\omega_0$ ($k \cong 20$ - 30). Let us consider these three mechanisms.

Using the above mentioned estimates of the parameters of laser-produced plasmas and the expression for thermal bremsstrahlung radiation per unit volume [104] (with no regard for self-absorption):

$$P_x \cong (e^2/\hbar c)\, \nu_{ef} n_e T_e^2 / m_e c^2 \qquad (3.12)$$

we can calculate the intensity of broadened X-ray radi-

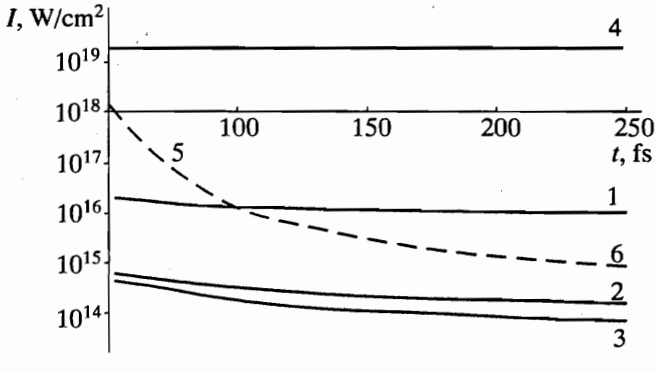

Fig. 15. *Boundaries of different regimes of the interaction of laser radiation (wavelength 0.25 μm) with a condensed gold target A = 200, Z = 10. Curve 1 separates regions of normal (below) and anomalous (above) skin-effects. Below curve 3 a thermal wave has no time to penetrate into the absorption region. Above curve 4 the oscillation energy of electrons inside plasma exceeds their thermal energy. Curves 5 and 6 separate the regions where the hydrodynamic motion becomes dominant and the plasma density in the interaction region decreases.*

ation. Multiplying (3.12) by the thickness of the heated region l_t we find the brightness of X-ray radiation $J_x = P_x l_t$. The ratio $K_x = J_x / I$ determines the efficiency of conversion of laser energy into X-ray radiation. In particular, in the case of the normal skin-effect and for laser pulses with the optimum duration (3.11), we find

$$K_x \cong 2 \times 10^{-7} A^{1/3} Z^2,$$

where A and Z are, respectively, the atomic mass and average charge of the target material. The fact that $K_x \ll 1$ points out that radiation losses play a minor role in the plasma energy balance nevertheless the brightness of X-ray radiation may be rather high. In particular, at $A \cong 100$, $Z \cong 10$ and $I \cong 10^{16}$ W/cm^2, the brightness of an X-ray source is $J_x \cong 10^{12}$ W/cm^2. It is of importance, in addition, that the real intensity of X-ray radiation may be higher than $K_x I$, since the duration of the X-ray pulse may be longer than that of the laser. This effect was obtained in [118] from numerical simulations using the LASNEX code; it is explained by the slow cooling of plasma after the end of the laser pulse. Also, this effect was observed in experiments of [115]. It was mentioned in [130] that X-ray pulses may be shortened by the proper choice of the target. In order to increase the cooling rate of the plasma, the target must be made of a light material with an admixture of a heavy material. In addition to broadband bremsstrahlung radiation, laser-produced plasmas may emit line radiation. By choosing the plasma parameters properly one can, in principle, obtain a population inversion on certain transitions and obtain monochromatic radiation at specific wavelengths. Of practical importance would be X-ray lasers in the range from 1 to 5 nm where no absorption transitions of water molecula lies. This radiation could be used for microradiography of biological objects with high temporal and spatial resolution.

At present, laser generation in the soft X-ray range was obtained from plasmas produced by very large and expensive nanosecond lasers [131 - 133]. The efficiency of such lasers is very low (about 10^{-6}), e.g., a kilojoule laser pulse induced an X-ray pulse with an energy of several millijoules. X-ray lasers would be very practical, if they could be made more compact and effective. That is why it seems to be desirable to use subpicosecond lasers for pumping, since they are rather compact and provide very high concentration of intensity (T^3-laser – Table-Top Terawatt Lasers). However, the existing lasers supply only 1 J per 1 ps, hence, the inversion scheme and the emitting transition must be looked for more carefully.

One of the most popular schemes for an X-ray laser involves generation in the $n = 3 \rightarrow n = 2$ transition of hydrogen-like ions. To realize this scheme with carbon ions C^{+6} (wavelength 18 nm), a plasma temperature of about 200 eV was estimated to be necessary. That is, about 3 keV per atom must be put into the target (with energy of ionization taking into account). Such energy deposition seem to be possible, provided a laser energy of 1 J is focused into a strip 10 μm wide [134]. However, the optimum concentration of C^{+6} ions is then about $\cong 10^{20}$ cm^{-3}, i.e. laser generation can only occur during plasma expansion. It is more interesting to consider the same transition in hydrogen-like aluminum Al^{+13} with a wavelength of about 4 nm. According to [134] this scheme requires about 400 J to be deposited in a volume of 1 cm × 10 μm × 1 μm. In this scheme effective generation does not require expansion of the plasma, while the expected yield of X-ray radiation is about one millijoule. It is worth noting that to obtain effective inversion, the plasma must be ionized very rapidly, i.e. the pulse duration must be less than 1 ps and the contrast must be so high that no cold and underdense plasma will appear on the target surface due to the prepulse.

Since the parameters of plasmas produced by subpicosecond laser pulses can be controlled, a recombination scheme is now of interest which uses the transition $2 \rightarrow 1$ of the hydrogen-like aluminium ion [134, 135]. However, in order to provide inversion in this transition, recombination into the level $n = 2$ must be fast, this being only possible in sufficiently cold and dense plasmas. The possibility for creating such plasmas was demonstrated in [136], where the mean electron energy in the case of linearly polarized laser radiation was demonstrated to be much smaller than in the case of circular polarization (see Section 2.2 for more detail).

One more mechanism for generating coherent X-ray radiation in the range $\hbar\omega_x \leq 100$ eV is connected with the generation of higher harmonics of the laser frequency. As was mentioned above in Section 2, the process of generation of harmonics is of universal character, namely, it can be observed both below and above the ionization threshold and both in gaseous and condensed media. The specific feature of condensed targets is that the efficiency of generation may be much higher due to the sharp boundary between the plasma and vacuum. In [137, 138] one described the mechanism for generating harmonics at the electron density jump due to the p-component in the laser electric field. This was done in connection with experiments on the observation of high harmonics $\omega_k = k\omega_0$ (up to $k = 47$) of the frequency of a nanosecond CO_2 laser [139, 140]. In those experiments the density jump was produced by the ponderomotive force. According to [138], electrons oscillate near the plasma-vacuum boundary under the electric field normal to the target surface. Oscillations of particles crossing the boundary is strongly anharmonic, hence they efficiently emit at both ω_0 and its harmonics. The intensities of the harmonics I_k decreases gradually with k until $k \approx k_{max} \approx \omega_{pe} / \omega_0$.

The effect of generation of higher harmonics in interactions of subpicosecond laser pulses with condensed targets has not yet been observed because, seemingly, the laser intensities were too low. The following conditions must be met for detection of higher harmonics: (1) p-polarized laser radiation must be obliquely incident on a target; (2) laser intensities

$\geq 10^{16}$ W/cm^2 must be achieved so that electrons could perform collisionless oscillations to a depth of the order of the skin-layer thickness (i.e., the case of the anomalous skin-effect must be realized); (3) electron density must vary abruptly on a scale L smaller than that of electron oscillation. According to [137 - 140], the efficiency of conversion of laser radiation into higher harmonics may be sufficiently high ($\cong 10^{-5}$), hence under certain condition the mechanism in question may prove to be competitive with bremsstrahlung and line radiation.

3.2. Experiments on Interaction of Ultra-Short Pulses with Overdense Plasmas

Experiments on the interaction of ultra short laser pulses with condensed targets were aimed at studying the parameters of reflected signals and at revealing the parameters of laser-produced plasmas by this basis. One of the first works in the field was that by Milchberg and Freeman [141] (see also [117]) who used 400 fs pulses with wavelength 308 nm and energy 5 mJ. They used XeCl excimer output amplifiers with a repetition rate of 10 Hz. After each shot the aluminum target was shifted so that each pulse hit fresh surface. In these experiments the incidence angle was fixed at $\theta_0 = 45°$, but both polarizations (s and p) were used and a wide range of intensities from 10^{11} to 10^{14} W/cm^2 was spanned.

Fig. 16 shows the dependence of the absorption coefficient on polarization and intensity obtained in those experiments. There are three regions seen in the figure: low intensity below 10^{12} W/cm^2, when the absorption coefficient is practically constant, an intermediate region of $10^{12} - 10^{14}$ W/cm^2, when absorption increases; and the region of $I > 10^{14}$ W/cm^2 when absorption saturates and reflection slightly increases. Note that absorption of p-polarized radiation is higher than that of s-polarized radiation.

Data on reflection [141] were used to calculate the dc conductivity of a target for different values of laser intensity corresponding to different temperatures. The conductivity was calculated using the Drude model: $\sigma = \omega_{pe} / 4\pi\nu$, i.e. the effective electron collision frequency was defined. The average temperature was determined by the Doppler shift of the reflected radiation. Note that the reflected radiation propagated exactly in the specular direction. This shows that the plasma surface was plane and the expansion was one-dimensional.

The dependence of the resistivity on laser intensity is given in Fig. 17. It must be mentioned that the dependencies $\rho = \sigma^{-1}$ obtained from reflection of p- and s-polarized radiation are similar, which confirms the correctness of the measurements. The range of low intensities corresponds to the constant collision frequency $\nu / \omega_{pe} \leq 0.06$, which seems to be due to electron-phonon collisions. Then the resistivity increases by about two orders, and at $I \cong 10^{14}$ W/cm^2 the

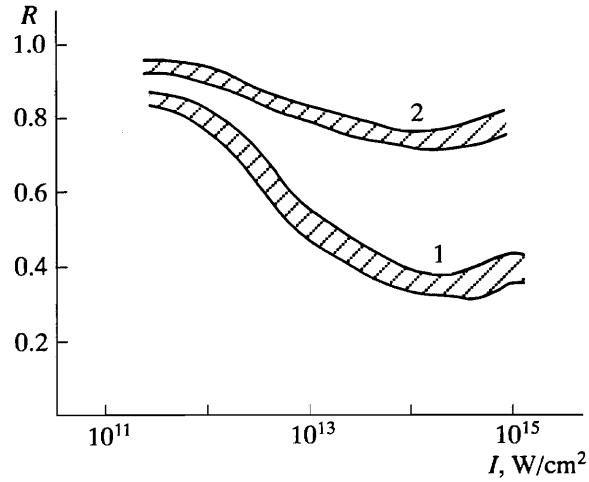

Fig. 16. *Dependence of the reflection coefficient of laser radiation on the intensity on the surface of an aluminum target for p- and s-polarized radiation (curves (1) and (2), respectively) [117]. The laser wavelength is 308 nm, pulse duration 0.4 ps.*

value ν / ω_{pe} is comparable with unity. This shows that the plasma is non-ideal. A further decrease of resistivity corresponds to a decrease of ν / ω_{pe}, i.e. to reduction of the non-ideality. Note, that calculations of the effective collision frequency with due regard for long range correlations performed in [109] agree qualitatively with the experiments of Milchberg.

An even greater range of laser intensities was spanned in [116]: $I \cong 10^{10} - 10^{16}$ W/cm^2. The basic difference from [117, 141] is that a wavelength of $\lambda \approx 1$ μm and longer pulses were used. The absorption was observed to start growing from a lower value of intensity $\cong 10^{11}$ W/cm^2, while at $I \geq 10^{13}$ W/cm^2 absorption saturates at the level of 40 to 50%. This difference seems to be due to longer pulses and, therefore, to longer times of expansion. In particular, the inhomogeneity scale at the pulse end was estimated in [117] to be $L \cong c_s\tau_0 = 20$ nm, while in experiments [116] it was necessary to take $L \cong 200$ nm to fit the absorption curves. Note also, that at $I > 10^{15}$ W/cm^2 the experimental data of [116] contradict the Drude model. This indicates that nonlinear processes arise in the region of critical plasma density.

In [114, 129], the angular dependencies of absorption coefficients of s- and p-polarized radiation were systematically studied for different targets made of aluminum, copper and gold. These experiments are characterized by the use of laser radiation high contrast ratio, namely, the prepulse intensity was $10^{-7} - 10^{-8}$ of the pulse intensity, i.e., below the threshold of plasma production ($\cong 10^8$ W/cm^2). Amplifiers with KrF mixture were used, the wavelength was 248 nm, and the pulse duration on the target was 250 fs. The electron density and collision frequency in the plasma were determined on the basis of measurements of the angular dependence of the reflection coefficient and its comparison with the Drude model. At 10^{14} W/cm^2 the

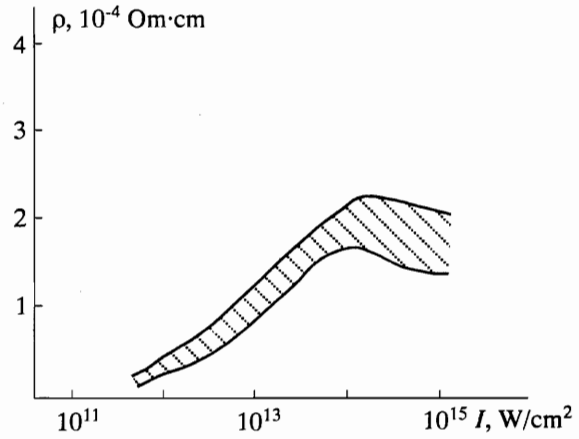

Fig. 17. *Dependence of specific resistivity of aluminum on temperature (according to experiments of [117]).*

electron density was 30 times above the critical value $n_c \approx 1.8 \times 10^{22}$ cm^{-3}, the electron temperature was about 60 eV, the depth of penetration of the thermal wave was $l_t \cong 20$ nm, i.e., comparable with the skin-layer thickness $l_s = 10$ nm, and the scale of density inhomogeneities $L \approx 4$ - 8 nm was negligible. This points out that smearing of the target boundary was not significant, while the plasma was strongly non-ideal, namely, only 2 to 3 particles resided in a Debye sphere. At intensity 2.5×10^{15} W/cm^2, the electron plasma temperature grows up to 200 - 300 eV and the heating depth increases up to 40 - 60 nm, but the inhomogeneity scale increases up to 10 - 30 nm and affects the absorption of laser radiation. Actually, the comparison of experimental parameters with the data of Fig. 15 and with (3.11) shows that the thermal regime of interaction terminates at $t_h \cong 100$ fs and then the plasma expansion starts to be the dominant factor. The value of temperature obtained in experiments [114, 129] $T_e = 300$ eV agrees well with calculations of plasma heating in the regime of the normal skin-effect done in [111] (see Section 3.1). This agreement indicates that nonclassical effects in thermal transport are not significant in this case.

In [115] experiments with the shortest laser pulses $\tau_0 = 160$ fs were carried out. A dye laser with $\lambda = 616$ nm, and pulse energy up to 5 mJ and repetition rate of 10 Hz was used. The intensity on the target was up to 10^{16} W/cm^2. The absorption coefficient of silicon and tantalum targets was from 20 to 60% and decreased as the laser intensity changed from 10^{12} to 10^{16} W/cm^2. Maximum plasma temperature was 230 eV, this value being evaluated by two methods: from measurements of the reflection coefficient and from the ratio of intensities of lines of Al^{+4} ions. Special attention in [115] was paid to the measurements of plasma X-ray radiation and its dependence on prepulse energy. It was demonstrated that prepulses with energies less than 4 μJ (contrast better than 10^{-3}) do not affect plasma radiation. The X-ray pulses have duration less than 2 ps, this being the ultimate resolution of the present-day instrumentation. However, the duration and energy of X-ray pulses increase with the prepulse energy. In particular, for the contrast value ≅ 10%, the duration of X-ray pulses increases up to 70 to 100 ps, while its energy increases by a factor of 3. By the end of the pulse, the average energy of the X-ray quanta decreases from 300 - 500 eV down to less than 50 eV. In [115], this long-lived radiation was interpreted to be related to slow cooling of rarefied plasma loosing contact with the target.

Precise measurements of the heating depth by ultrashort laser pulses were done in [142]. They used KrF excimer amplifiers, laser pulses had the wavelength 248 nm, duration 1 ps, energies 25 mJ, and intensity on the target was 10^{16} W/cm^2 due to tight focusing, (the focal laser spot was only 16 μm in diameter). In comparing these parameters with the data of Fig. 15 we see that the experiments were done, mainly, in the hydrodynamic regime, since the inhomogeneity scale was about ≅ 50 - 150 nm. In order to measure the heating depth, special laminated targets were used: bulk aluminum targets covered with a thin layer of iron (as thick as 15 nm). At low prepulse energies (less than 0.3%), the spectrum of plasma radiation contained lines of iron. At prepulse energies about 3% (i.e. about 1 mJ) no lines of iron were seen. This means that the prepulses completely evaporate the iron layer, this being natural since the prepulse intensity (≅ 10^{11} - 10^{12} W/cm^2) was above the threshold of plasma production. It should be mentioned that the heating depth without prepulses (≅ 15 nm) in this experiment was much less than in [134] and that it follows from the scalings of [111]. We think two factors to be of importance: long pulse duration and low contrast in experiments of [142] so that the interaction regime was far from being thermal and more close to the hydrodynamic regime. This is also confirmed by the estimation of the electron density carried out in [142] from line spectra of the plasma radiation, i.e., by the end of the pulse the electron density proves to be one order lower than that of the solid. This confirms once more that the role of expansion of plasma is important in the conditions of [142].

Therefore, the theoretical analyses and experiments demonstrate that interaction of subpicosecond laser pulses with condensed targets may have a specific thermal character determined by the absence of hydrodynamic motion and propagation of thermal waves. The depth of heating may prove to be greater than in the hydrodynamic regime due to high values of heat flux. The time of existence of the thermal regime is rather short, about 100 fs, and it is reduced as the laser energy decreases. Further on, the thermal regime changes into the hydrodynamic one in which the scale of inhomogeneities exceeds the skin depth and the heating depth. In this case, the energy deposition occurs in the region of critical density and the thermal coupling between the regions of absorption and evaporation weakens.

Dense plasmas produced by subpicosecond laser pulses are a promising source of pulsed broadband X-ray radiation and media for X-ray lasers. The temperatures of laser-produced plasmas are now rather low, about 200 to 300 eV. They are limited by electron thermal conductivity and by adiabatic cooling due to expansion into vacuum. Higher temperatures may be achieved by decreasing the laser pulse duration down to 100 fs with a corresponding increase of intensity up to 10^{17} - 10^{18} W/cm^2. According to theoretical estimations, the absorbed energy density may reach $\geq 10^4$ J/cm^2. This regime will be characterized by nonlinear effects in absorption and thermal transport which would result in electron temperatures up to several tens (or even hundreds) of kiloelectronvolts. Hence, the domain of applications of such plasmas will be greatly extended.

4. NUCLEAR AND NONLINEAR QUANTUM ELECTRODYNAMICS EFFECTS IN STRONG LASER FIELDS

4.1. Nuclear Reactions in Laser Focus

Since nuclear forces are too large, direct effects of laser fields on the states of nuclei is hardly possible. However, there are some methods of indirect action on the basis of secondary processes induced by laser radiation in matter. In particular, the possibility to produce relativistic electrons in target plasmas by lasers with $I \geq 10^{20}$ W/cm^2 makes us expect that their interaction with nuclei may result in Coulomb excitation of nuclear states and, if the threshold energies could be exceeded, in electronuclear reactions. The second possibility is connected with bremsstrahlung gamma quanta with energies of about several megaelectronvolts induced in a plasma by those electrons. Such quanta can excite nuclei and induce photonuclear reactions.

The simplest possibility of excitation of electro- and photo-fission of uranium-238 under strong laser field was considered in [149, 150]. Energy thresholds of such reactions are about 10 MeV (corresponding cross sections of electro-fission and photo-fission are, $\cong 10^{-27}$ cm^2 and 10^{-25} cm^2, respectively). If such high energies of electrons will be achieved, then, as was mentioned in [149], the action of a 100 fs pulse of KrF laser with intensity 10^{21} W/cm^2 on a uranium target would result in 10^4 electro-fission events and in two orders of magnitude greater number of photo-fission events, this being well sufficient for experimental detection. We think, however, that the energies of electrons must be estimated with great care. Electron energy may be taken equal to that of electron oscillations in a vacuum laser field only for a very rarefied medium. In the case of a condensed uranium target the rate of heating and final energies of electrons will be determined by the balance between energy absorption and losses in the skin-layer. Hence, the relationship between laser intensity and mean electron energy will be more complicated than was taken in [149, 150].

The estimation of average energy ε_e from the theory of the anomalous skin-effect with regard for the limitations of thermal conductivity (3.9) and (3.11) yields ε_e to be about 1 MeV at a pulse duration of 100 fs and intensity 10^{20} W/cm^2. That is, more precise estimations result in higher values of laser intensity needed to obtain laser-induced fission reactions. Note that the reactions in question would be useful as a means to detect relativistic electrons and gamma quanta produced in plasmas.

However, even at nonrelativistic electron energies, collisional excitation of nuclei and some other processes of inelastic scattering of electrons by nuclei are possible. For example, uranium-235 possesses a nuclear octupole transition with very low energy (close to 75 eV) [4, 151]. The possible experiment consists in electron (or laser) excitation of such atom with consequent transfer of energy to the nucleus. It is not excluded that by choosing properly the target composition and the excitation conditions one could create a medium with inverted population of nuclear levels, just as the medium for X-ray recombination laser is produced in cold plasma.

Rather long ago it was suggested [152] that a strong laser field can affect the processes of beta-decay of nuclei. This possibility is based on the fact that the final state of the reaction (free electron) may be strongly perturbed by an electromagnetic field at intensities above the relativistic values $I \geq 10^{19}$ W/cm^2. Hence, the rate of beta-decay was predicted to change in the presence of a strong laser field. However, these results now seem to be doubtful [153].

Also we should mention the proposal from the Laurence Livermore National Laboratory (USA) on direct initiation of fusion reaction [4]. If a powerful ultrashort pulse irradiates of gas target of deuterium and tritium then fast electrons leaving the focal volume accelerate ions to energies of several tens of kiloelectronvolts. Such ions fuse with cold nuclei. Thus, an ultrashort source of neutrons with energies 14.1 MeV with very high brightness can be obtained. Such a source can be used for diagnostics in experiments on controlled fusion and plasma physics.

4.2. Effects of Nonlinear Quantum Electrodynamics Arising in Colliding Powerful Laser and Relativistic Electron Beams

An external electric field affects the states and transformations of microparticles when its amplitude exceeds a certain critical value E_∞. The value can be determined from the condition that the work done by this field on the scale of the Compton electron wavelength $\lambda_c = \hbar/m_e c \approx 10^{-10}$cm equals the electron rest mass $m_e c^2$. Then, $E_\infty = m_e^2 c^3/e\hbar \approx 10^{16}$ V/cm and the corresponding intensity is $I_\infty \approx 10^{30}$ W/cm^2. It is clear that this level of intensity cannot be achieved by lasers,

at least in the predictable future. One of the processes which can occur in this field is the decay of a photon into an electron-positron pair ("breakdown" of physical vacuum).

Several years ago, a proposal was made [14] to realize a field of the order of E_∞ (or photons of corresponding energies) by colliding a laser beam with intensity $I > 10^{19}$ W/cm^2 with a relativistic electron beam with energy of electrons about 50 GeV. Back-scattered photons, whose initial energy is about 1 eV, will receive energy of the order of that of the electrons (in fact, smaller than that due to nonlinear effects). A slightly different idea about this process can be obtained by calculating the electric field in the frame where the electron rests. According to special relativity theory, the field in the electron frame differs from that in the laboratory frame by a factor γ ($\gamma = \varepsilon_e / m_e c^2$ is the relativistic factor of the ratio of electron's energy to its rest energy). Hence, when a laser beam with $I \approx 10^{19}$ W/cm^2 ($E \approx 10^{11}$ V/cm) collides with an electron beam with $\varepsilon_e = 50$ GeV ($\gamma = 10^5$) the field strength in the electron frame amounts to $E \approx 10^{16}$ V/cm. This experiment, including the construction schedule of the installation and a program of researches was proposed [14]. The scientific program of future experiments involves investigations into a series of effects which were theoretically considered during the last four decades [13]. Similar experiments are also planned in the USSR (at Lebedev Physics Institute in Moscow).

Note that at least two types of experiments are possible here, namely, scattering of laser photons by electrons and interaction of scattered photons with electrons and laser photons. We should specify some effects expected to occur in the sequence they would arise with increasing laser intensity and electron beam energy.

Nonlinear Thomson scattering might be observed at electron energies above 50 MeV. In this case, the maximum of the scattering spectrum would be shifted to higher frequencies and the shift would depend on the laser intensity. Just as in linear Thomson scattering, the energies of incident and scattered photons are supposed to be small compared to the electron rest energy and the recoil momentum can be neglected (in contrast to the Compton effect).

The scattering process in nonlinear Compton scattering can involve two or more photons. The energy of a scattered photon is comparable with or greater than the electron rest energy and depends on both the energy of incident photons and their intensity.

Production of electron-positron pairs would be observed in the interaction of several laser photons with one high-energy scattered photon. Similar experiments can result in the observation of "light-by-light" scattering. However, in this case the initial and final states must be two-photonic. The other effects to be mentioned are polarization of vacuum and a decrease of electron rest mass in a strong field. The nonlinear effects of quantum electrodynamics in strong fields are considered in detail elsewhere [13].

4.3. Unruh Effect Induced by Ultra-Short Laser Pulses

Here we consider one more nonlinear effect of quantum electrodynamics, the so-called Unruh effect, namely, the generation of electromagnetic radiation by a neutral body moving with acceleration. This effect is also proposed to be studied in experiments involving the collision of beams as discussed in the previous Section. However, the necessary intensities were estimated in [14] to be up to 10^{23} W/cm^2. Here we will touch upon the other proposal made in [154] to detect the Unruh effect using accelerated motion of ionization waves with velocities in excess of light speed produced in matter by subpicosecond laser pulses.

On the basis of general relativity theory it was concluded in [155, 156] that an observer moving with acceleration g must emit electromagnetic waves with characteristic frequencies $\omega_u \cong g/c$ (or with temperature $T_u \cong \hbar g/c$). For conditions on Earth ω_u is only 10^{-10} s^{-1} and can never be observed. Hence, in [154] it was proposed to use the methods of nonlinear optics to achieve values of acceleration about $g \cong 10^{23}$ cm/s^2. Then the Unruh frequency shifts into the range of microwaves and observations can be attempted.

The idea of [154] is to produce an accelerated ionization wave using ultrashort laser pulses (see Fig. 18). In order to do this, a laser pulse is focused on a thin semiconducting foil whose thickness is of the order of that of the skin-layer and length is of the order of $\lambda_u = 2\pi c / \omega_u$. The shape of the wave front is to be concave so that the front travels along the target with the required acceleration. The laser beam power must be high enough to provide a high rate of ionization over the entire target length. The ionization wave appearing at the front will be a source of Unruh radiation. Note that the ionization wave in this scheme travels with velocity, exceeding the speed of light hence the time of its passage through the target is much shorter than the period of Unruh radiation. This would hinder its detection.

CONCLUSION

To conclude this review we should point out the results obtained just recently on both the technology of high-power ultra-short laser pulses generation and their interaction with matter outline the perspectives and possible applications.

Lasers. Table 1 lists the parameters of some laser systems which have achieved record performance. The power level of subpicosecond lasers is now well above the terawatt level and the intensities on targets are very close to relativistic values ($I\lambda^2 \cong 10^{19}$ W/cm^2). Some laser installations possess rather good contrast and high intensity, hence interesting results on their interaction with solid targets are expected in the near future. To the present time, experiments with femtosecond pulses (10 to 20 fs) having intensity 10^{14} - 10^{15} W/cm^2 have been carried out. Higher intensities will seemingly be achieved soon. Some laboratories plan to obtain

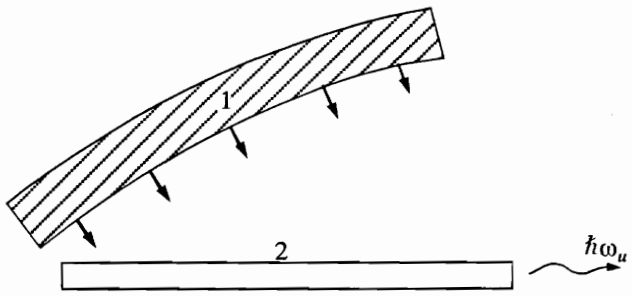

Fig. 18. *Scheme of the proposed experiment for detection of Unruh radiation [154]: 1 – laser pulse; 2 – semiconductor plate.*

intensities of 10^{20} W/cm^2 in the next year and 10^{21} - 10^{23} W/cm^2 in 2 to 3 years.

Nonlinear Optics. Since the thresholds for ionization (and, therefore, for breakdown of dielectrics) increase as the laser pulses shorten up to 2×10^{13} W/cm^2 at 50 fs, the intensities characteristic for studies of nonlinear effects in transparent media are now significantly higher. We can expect that in the near future intensities up to 10^{14} W/cm^2 will be available for investigations into the processes of self-action of laser pulses in their propagation through dense gases and optical media. Of great interest for applications are the effects of changes of frequency and duration of laser pulses in strongly nonlinear media.

Multiple Ionization of Atoms. One of the present-day achievements is the production of highly stripped ions (Xe^{+9}; U^{+10}) in collisionless plasmas by ionization in a strong field. At higher intensities it is possible to produce ions with any required charge and excitation states. In addition to the fundamental importance of those results for atomic physics, they are promising from the view point of media for short wavelength (X-ray) lasers. It is worth noting that the plasma thereby produced is very unusual, namely, it is collisionless non-equilibrium plasma with ions and electrons in rest whose mean energy can be controlled by varying the polarization and duration of the laser pulses.

Acceleration of Electrons. The very strong electric fields of ultrashort laser pulses allow such lasers to be used for the acceleration of electrons. Depending on the acceleration scheme, lasers with pulse durations from several tens of picoseconds to less than one picosecond are to be used. It is expected that at intensities of about 10^{19} W/cm^2 in rarefied gas, electrons could be accelerated to several hundreds of megaelectronvolts.

Generation of Short Wavelength Radiation. Under ultrashort laser pulses, dense targets (gases or solids) become sources of hard radiation with pulse duration about that of the incident laser radiation. Different mechanisms of such radiation are possible. The first is bremsstrahlung and recombination X-ray radiation, and fluorescence during relaxation of excited states. Second, harmonics of incident radiation are generated due to both nonlinear interaction with individual atoms and collective nonlinear processes in plasmas which are connected with rapid ionization by the laser field. At present, high harmonics (up to the thirtieth) were detected when illuminating noble gases (Kr, Xe, Ar) by lasers with wavelengths from 248 to 1064 nm. The efficiency of power transformation into X-rays is expected to reach 10^{-5}, i.e. it can compete with X-ray lasers. Hence, a subpicosecond source of coherent radiation with wavelengths about 10 nm or shorter and with intensity $\leq 10^{14}$ W/cm^2 can be thereby produced. Such sources are unique instruments with high temporal resolution for diagnostics in plasma physics, biology, chemistry, and other sciences.

At intensities above 10^{19} W/cm^2, generation of harmonics in the interaction of laser pulses with ultrarelativistic electrons can be expected. Theory predicts that coherent radiation of harmonics with wavelengths shorter than one nanometer will appear. This shortening of the wavelength is directly connected with the excess of laser intensity over the relativistic value I_r.

There is one more possibility for generation of higher harmonics by irradiating solid targets with subpicosecond pulses with relativistic intensities and extremely high contrast ratio ($> 10^{10}$). In this case the generation mechanism is connected with a force acting on electrons crossing a sharp boundary between plasma and vacuum. The maximum harmonics number is determined by the ration of electron plasma frequency to laser frequency; it can be as high as several tens for targets with high atomic numbers.

Interaction with Solids. Experiments in this field are of interest since they can yield superdense plasmas (as dense as solid) with highly stripped ions staying at rest during the subpicosecond pulse and with hot electrons (up to ultrarelativistic energies). In experiments carried out until now, electrons have been heated to several hundreds of electronvolts and very steep gradients of plasma at power density of 10^{17} W/cm^2 (the scale being less than one tenth of a micron) were detected at relatively low contrast ratio using rather long pulses. Since laser technology continues to develop, we can expect experiments with high contrast ratio ($> 10^{10}$), short pulses (about 100 fs) and intensity above the relativistic value to become possible in the near future. Then, superdense plasmas with very highly stripped ions (perhaps, hydrogen-like uranium) would probably be obtained by combined ionization by the field and by electron collisions. If megaelectronvolts electrons will be generated, then the relativistic plasma thereby produced will emit bremsstrahlung gamma quanta with energies of about 1 MeV and higher. Note that such plasmas will yield extremely high pressures (above 10^3 Mbar), i.e., it will be a valuable laboratory object to study substances under extreme conditions and to simulate astrophysical processes.

Nuclear Reactions. Electrons and gamma quanta with megaelectronvolt energies may excite high nuclear states and, provided the corresponding

thresholds are exceeded, induce electro- and photonuclear reactions, in particular, fission. Though strong direct effects of laser fields on the state of nuclei (except for excitation of high levels) can hardly be expected at intensities 10^{19} - 10^{20} W/cm^2, investigation of these nuclear states would help in looking for new approaches to the development of gamma-lasers.

Quantum Electrodynamics. No direct influence of powerful electric fields produced by lasers (intensity about 10^{30} W/cm^2) on processes involving elementary particles will be observed in the predictable future. However, the proposed experiments on colliding laser beams (intensity 10^{19} W/cm^2) with ultrarelativistic electron beams (energies of about 50 GeV) would allow one to study many effects of nonlinear quantum electrodynamics which were predicted theoretically but are not available to experiment, in particular, nonlinear Thomson scattering, nonlinear Compton effect, production of electron-positron pairs, light-on-light scattering, Unruh effect, etc. Such experiments are now planned, and corresponding results could be expected in the next few years.

Summarizing this review we should point out that development and improvement of a new compact laboratory instrument – high-power subpicosecond lasers – have given rise to new questions about the interaction of strong electromagnetic fields on matter in many branches of science: Nonlinear optics, plasma physics, solid state physics, nuclear physics, and nonlinear quantum electrodynamics. The first results are already obtained. Extensive studies are now in progress and we believe that many proposals considered herein will soon be realized.

REFERENCES

1. *European High Performance Laser Facility* (Scientific and Technical Working Group Report), 1990.
2. Taylor, A.J., Tallman, C.R., Roberts, J.P. *et al.*, 1990, *Opt. Lett.*, **15**, 39.
3. Eberly, J.H., Maine, P., Strickland, D., and Mourou, G., 1987, *Laser Focus*, **23**, 84.
4. Perry, M.D., Campbell, E.M., Hunt, J.T. *et al.*, 1987, *Ultra-High Brightness (> 10^{21} W/cm^2) Laser Facility*, LLNL Report.
5. Yamakawa, K., Berty, C.P.J., Shiraga, H. *et al.*, 1991, Paper presented to IAEA Technical Committee Meeting on Drivers for Inertial Confinement Fusion, 1991, April 15-19, Osaka, Japan.
6. Schoenlein, R.W., Bigot, J.-Y., Portella, M.T., and Shank, C.V., Paper presented to IAEA Technical Committee Meeting on Drivers for Inertial Confinement Fusion, 1991, April 15 - 19, Osaka, Japan.
7. Andre, M., Sauteret, C., Husson, D. *et al.*, Paper presented to IAEA Technical Committee Meeting on Drivers for Inertial Confinement Fusion, Osaka, Japan, April 15 - 19, 1991.
8. Watanabe, S., Endoh, A., Watanabe, M. *et al.*, 1989, *J. Opt. Soc. Amer. B*, **6**, 1870.
9. Watanabe, M., Hata, K., Adachi, T. *et al.*, 1990, *Opt. Lett.*, **15**, 845.
10. Akhmanov, S.A., Vysloukh, V.A., and Chirkin, A.S., 1988, *Optics of Femtosecond Laser Pulses* (Moscow: Nauka) (in Russian).
11. Gamaly, E.G., Dragila, R., and Tikhonchuk, V.T., 1990, *Priroda*, no. 12, 15.
12. Delone, N.B. and Fedorov, M.V., 1989, *Usp. Fiz. Nauk*, **158**, 215.
13. Ritus, V.I., *1979, Trudy FIAN*, **111** (Moscow: Nauka); Nikishov, A.I. and Ritus, V.I., 1988, *Zh. Eksp. Teor. Fiz.*, **94**, 31; 1990, **98**, 1138.
14. Fernow, R.C., Kirk, H.G., Bigio, I.J. *et al.*, 1986, Proposal for Experimental Studies of Nonlinear Quantum Electrodynamics, DOE/ER/3072-38, USA, July 30, 1986.
15. Basov, N.G., Zakharenkov, Yu.A., Zorev, N.N. *et al.*, 1982, *Heating and Compression of Fusion Targets by Laser Beams* (Moscow: VINITI) (in Russian).
16. Li, X.F., L'Huillier, A., Ferray, M. *et al.*, 1989, *Phys. Rev. A*, **39**, 5751.
17. Hora, H., 1981, *Physics of Laser Driven Plasmas* (New York: Wiley).
18. Gamaly, E. and Dragila, R., 1990, *Phys. Rev. A*, **42**, 929.
19. Baldwin, K.G.H. and Boreham, B.W., 1981, *J. Appl. Phys.*, **52**, 2627; Augst, S., Strickland, D., Meyerhofer, D.D. *et al.*, 1989, *Phys. Rev. Lett.*, **63**, 2212.
20. Dewar, R.L., 1974, *Phys. Rev. A*, **10**, 2107.
21. Ding, Y.J. and Kaplan, A.E., 1989, *Phys. Rev. Lett.*, **63**, 2725.
22. Barr, J.R.M., Everall, N.J., Hooker, C.J. *et al.*, 1988, *Opt. Commun.*, **66**, 127; Watanabe, S., Endoh, A., Watanabe, A., and Sarukura, N., 1988, Short Wavelength Lasers and their Applications, *Springer Proc. in Physics*, **30**, ed. by Yamanaka, C. (Berlin: Springer-Verlag).
23. Corkum, P.B., 1983, *Opt. Lett.*, **8**, 514.
24. Fisher, R.A. and Bischel, W.K., 1974, *Appl. Phys. Lett.*, **24**, 468; Lemberg, R.H. and McMahon, J.M., 1976, *Appl. Phys. Lett.*, **28**, 205; Natansuka, H. and Grischkowsky, D., 1981, *Opt. Lett.*, **6**, 13; Strickland, D. and Mourou, G., 1985, *Opt. Commun.*, **56**, 219; Maine, P., Strickland, D., Bado, P., Pessot, M., and Mourou, G., 1988, *IEEE J. of Quant. Electron.*, **QE-24**, 398.
25. Ferray, M., Lompre, L.A., Gobert, O. *et al.*, 1990, *Opt. Commun.*, **75**, 278; Perry, M.D., Patterson, F.G., and Weston, J., 1990, *Opt. Lett.*, **15**, 381.
26. Treacy, E.B., 1969, *IEEE J. of Quant. Electron.*, **QE-5**, 454.
27. Kashyap, R. and Blow, K., 1988, *Electronics Lett.*, **24**, 47; Hand, D.P. and Russel, P.St.J., 1988, *Opt. Lett.*, **13**, 767.
28. Tomlinson, W., Stolen, R.H., and Shank, C.V., 1984, *J. Opt. Soc. Amer. B*, **1**, 139.
29. Chuang, Y.-H. and Meyerhofer, D.D., 1990, 20-th Annual Anomalous Absorption Conference, Traverse City, 1990.
30. Nikolaus, B., Grischkowsky, D., and Balant, A.C., 1983, *Opt. Lett.*, **8**, 189; Stolen, R.H., Botineau, J., and Ashkin, A., 1982, *Opt. Lett.*, **7**, 512.
31. Wang, Y. and Dragila, R., 1990, *Phys. Rev. A*, **41**, 5645.
32. Szabo, G. and Bor, Z., 1990, *Appl. Phys. B*, **50**, 51.
33. Hunt, J.T., Renard, P.A., and Simmons, W.W., 1977, *Appl. Optics*, **16**, 779; Hunt, J.T., Glaze, J.A., Simmons, W.W, and Renard, P.A., 1978, *Appl. Optics*, **17**, 2053.

34. Key, M.H., Shaw, M.J., Ross, I.N. *et al.*, 1989, Rutherford-Appleton Laboratory Report, RAL-89-133.
35. Harvey, E.C., Hooker, C.J., and Lister, J.M.D, 1990, Rutherford-Appleton Laboratory Report, RAL-90-026.
36. Harris, D.B., 1991, Overview LANL ICF Program, Report presented at FPA Annual Meeting, Princeton, June 25 - 26, 1991.
37. Owadano, Y., Okuda, I., Matsumoto, Y. *et al.*, 1991, Paper Presented at IAEA Technical Committee Meeting on Drivers for ICF, Osaka, Japan, April 15, 1991.
38. Key, M.H., Barnett, K., Baily-Salins, R. *et al.*, 1991, Paper Presented at IAEA Technical Committee Meeting on Drivers for ICF, Osaka, Japan, April 15, 1991.
39. Keldysh, L.V., 1964, *Zh. Eksp. Teor. Fiz.*, **47**, 1945.
40. Agostini, P., Fabre, F., Mainfray, G., and Petite, G., 1979, *Phys. Rev. Lett.*, **42**, 1127.
41. Reiss, H.R., 1980, *Phys. Rev. A*, **22**, 1786.
42. Reiss, H.R., 1987, *J. Opt. Soc. Amer. B*, **4**, 726.
43. Reiss, H.R., 1990, *Phys. Rev. A*, **42**, 1476.
44. McIlrath, T.J., Bucksbaum, P.H., Freeman, R.R., and Bashkansky, M., 1987, *Phys. Rev. A*, **35**, 4611.
45. Muller, H.G., van Linden van den Heuvell, H.B., Agostini, P. *et al.*, 1988, *Phys. Rev. Lett.*, **60**, 565.
46. Freeman, R.R., Bucksbaum, P.H., Milchberg, H. *et al.*, 1987, *Phys. Rev. Lett.*, **59**, 1092.
47. Eberly, J.H., Su, Q., and Javanainen, J., 1989, *Phys. Rev. Lett.*, **62**, 881.
48. Javanainen, J., Su,Q., Eberly, J.H., 1988, *Phys. Rev. A*, **38**, 3430.
49. Mainfray, G. and Lompre, L.-A., 1989, Conference on Super-Intense Laser-Atom Physics, Univ. of Rochester, N.Y., USA, June 28-30, 1989.
50. Lompre, L.-A., L'Huillier, A., and Mainfray, G., 1990, ICOMPV Abstracts, Sept. 24-28, 1990, Paris, France.
51. Chin, S.L., Rolland, C., Corcum, P.B., and Kelley, P., 1988, *Phys. Rev. Lett*, **61**, 153.
52. Corcum, P.B. and Rolland, C., 1989, *The Supercontinuum Laser Source*, ed. by Alfano, R.R. (Berlin: Springer-Verlag), 318.
53. Perry, M.D., Szoke, A., Landen, O.L., and Campbell, E.M., 1988, *Phys. Rev. Lett*, **60**, 1270.
54. Luk, T.S., Johan, V., Egger H. *et al.*, 1985, *Phys. Rev. A*, **32**, 214.
55. L'Huillier, A., Lompre, L.A., Mainfray, G., and Manus, C., 1982, *Phys. Rev. Lett*, **48**, 1814; 1983, *J. Phys. B: At. Mol. Phys.*, **16**, 1363.
56. McPherson, A., Gibson, G., Jara, H. *et al.*, 1987, *J. Opt. Soc. Amer. B*, **4**, 595.
57. L'Huillier, A., Lompre, L.A., Mainfray, G., and Manus, C., 1983, *Phys. Rev. A*, **27**, 2503.
58. Boyer, K. and Rhodes, C.K., 1985, *Phys. Rev. Lett.*, **54**, 1490.
59. Szoke, A. and Rhodes, C.K., 1985, *Phys. Rev. Lett.*, **56**, 720.
60. Lee, P.H.Y., Casperson, D.E., Schappert, G.T., and Olson, G.L., 1989, Conference on Super-Intense Laser-Atom Physics, Unit. of Rochester, N.Y., June 28-30, 1989.
61. Lodling, K., Frasinski, L.J., Hatherly, P., and Barr, J.R.M., 1987, *J. Phys. B: At. Mol. Phys.*, **20**, 525.
62. Chin, S.L., Yergeau, F., and Lavigne, P., 1985, *J. Phys. B*, **18**, 213; Chin, S.L., Xiong, W., Lavigne, P., 1987, *J. Opt. Soc. Amer. B*, **4**, 853.
63. Augst, S., Strickland, D., Chin, S.L. *et al.*, 1989, Conference on Super-Intense Laser-Atom Physics, Unit. of Rochester, N.Y., June 28 - 30, 1989.
64. Ammosov, M.V., Delone, N.B., and Krainov, V.P., 1989, *Zh. Eksp. Teor. Fiz.*, **91**, 2008.
65. Corkum, P.B., Burnett, N.M., and Brunel, F., 1989, *Phys. Rev. Lett.*, **62**, 1259.
66. Burnett, N.M., Corkum, P.B., 1989, *J. Opt. Soc. Amer. B*, **6**, 1195.
67. Landau, L.D. and Lifshits, E.M., 1963, *Quantum Mechanics: Non-Relativistic Theory* (Moscow: GIFML), 328 (in Russian).
68. Perelomov, A.M., Popov, V.S., and Terentiev, M.V., 1966, *Zh. Eksp. Teor. Fiz.*, **51**, 617.
69. Xiong, W. and Chin, S.L., 1991, *Zh. Eksp. Teor. Fiz.*, **99**, 481.
70. Askar'yan, G.A., 1962, *Zh. Eksp. Teor. Fiz.*, **42**, 1360.
71. Auston, D.H. and Nuss, M.C., 1988, *IEEE J. of Quant. Electron.*, **QE-24**, 184.
72. Wood, W., Foght, G., and Downer, M.C., 1988, *Opt. Lett.*, **13**, 984.
73. Bloembergen, N., 1973, *Opt. Commun.*, **8**, 285.
74. Wilks, S.C., Dawson, J.M., and Mori, W.B., 1988, *Phys. Rev. Lett.*, **61**, 337.
75. Gildenburg, V.B., Krupnov, V.A., and Semenov, V.E., 1988, *Pis'ma Zh. Tekh. Fiz.*, **14**, 1695.
76. Gildenburg, V.B., Kim, A.V., and Sergeev, A.M., 1990, *Pis'ma Zh. Eksp. Teor. Fiz.*, **51**, 91.
77. Kim, A.V., Lirin, S.F., Sergeev, A.M. *et al.*, 1990, *Phys. Rev. A*, **42**, 2493.
78. Downer, M.C., Wood, W.M., Banyai, W.M., and Trisnadi, J., 1989, Summaries of Papers "High Energy Density Physics with Subpicosecond Laser Pulses Topical Meeting", Snowbird, Utah, USA, Sept. 11 - 13, 1989.
79. Yablonovich, E., 1974, *Phys. Rev. Lett.*, **32**, 1101; 1974, *Phys. Rev. A*, **10**, 1988.
80. Szoke, A., 1988, NATO ASI Series Physics B, ed. by Bandrauk, A. (New York: Plenum), **171**, 207.
81. Ferray, M., L'Huillier, A., Li, X.F. *et al.*, 1988, *J. Phys. B: At. Mol. Opt. Phys.*, **21**, 31.
82. Bokor, J., Bucksbaum, P.H., and Freeman, R.R., 1983, *Opt. Lett.*, **8**, 217.
83. McPherson, A., Gibson, G., Jara, H. *et al.*, 1987, *J. Opt. Soc. Amer. B*, **4**, 595.
84. Kulander, H.C. and Shore, B.W., 1989, *Phys. Rev. Lett.*, **62**, 524.
85. Eberly, J.H., Su, Q., and Javanainen, J., 1989, *Phys. Rev. Lett.*, **62**, 881.
86. Lompre, L.A., L'Huillier, A., and Mainfray, G., 1989, Abstract of Conference on Super-Intense Laser-Atom Physics, Univ. of Rochester, N.Y., USA, June 28 - 30, 1989, p. 6.
87. Shore, B.W. and Kulander, K.C., 1989, Abstract of Conference on Super-Intense Laser-Atom Physics, Univ. of Rochester, N.Y., USA, June 28 - 30, 1989, p. 8.
88. Brunel, F., Abstract of Conference on Super-Intense Laser-Atom Physics, Univ. of Rochester, N.Y., USA, June 28 - 30, 1989, p. 83.
89. Gladkov, S.M. and Koroteev, N.I., 1990, *Usp. Fiz. Nauk.*, **160**, 105.

90. Sarachik, E.S. and Schappert, G.T., 1970, *Phys. Rev. D*, **1**, 2738.
91. Rinker, G.A., Biedenharn, L.C., and Solem, J.C., 1989, Conference on Super-Intense Laser-Atom Physics, Univ. of Rochester, N.Y., USA, June 28 - 30, 1989.
92. Bardsley, J.N., 1989, Summaries of Papers "High Energy Density Physics with Subpicosecond Laser Pulses Topical Meeting", Snowbird, Utah, USA, Sept. 11 - 13, 1989.
93. Penetrante, B.M. and Bardsley, J.N., 1991, *Phys. Rev. A*, **43**, 3100.
94. Sarukura, N., Hata, K., Adachi, T., Nodomi, R., and Watanabe, M., 1991, *Phys. Rev. A*, **43**, 1669.
95. Joshi, C., Mori, W.B., Katsouleas, T. *et al.*, 1984, *Nature*, **311**, 525; Gorbunov, L.M., 1989, *Priroda*, no. 5, 15; Dawson, J.M., 1990, *V Mire Nauki*, no. 5, 24; Lowson, J.D., 1989, *Usp. Fiz. Nauk*, **158**, 304.
96. Tajima, T. and Dawson, J.M., 1979, *Phys. Rev. Lett.*, **43**, 267.
97. Rosenbluth, M.N. and Liu, C.S., 1972, *Phys. Rev. Lett.*, **29**, 701.
98. Sugihara, R. and Midzuno, Y., 1979, *J. Phys. Soc. Japan*, **47**, 1290; Katsouleas, T. and Dawson, J.M., 1983, *Phys. Rev. Lett.*, **51**, 392.
99. Chen, P., Dawson, J.M., Huff, R.W., and Katsouleas, T., 1985, *Phys. Rev. Lett.*, **54**, 693.
100. Gorbunov, L.M. and Kirsanov, V.I., 1987, *Zh. Eksp. Teor. Fiz.*, **93**, 509; Bulanov, S.V., Kirsanov, V.I., and Sakharov, A.S., 1989, *Pis'ma Zh. Eksp. Teor. Fiz.*, **50**, 176.
101. Sprangle, P., Esray, E., Ting, A., and Joyce, G., 1988, *Appl. Phys. Lett.*, **53**, 2146.
102. Clayton, C.E., Joshi, C., Darrow, C., and Umstadter, D., 1985, *Phys. Rev. Lett.*, **54**, 2343; Ebrahim, N.A., Lavigne, L., and Aithal, S., 1985, *IEEE Trans. Nuclear Science*, **47**, 2291.
103. Raizer, Yu.P., 1974, *Laser Spark and Propagation of Discharges* (Moscow: Nauka) (in Russian).
104. Gamaly, E.G. and Tikhonchuk, V.T., 1988, *Pis'ma Zh. Eksp. Teor. Fiz.*, **48**, 413.
105. Landau, L.D. and Lifshits, E.M., 1982, *Electrodynamics of Continuous Media* (Moscow: Nauka) (in Russian).
106. Ginzburg, V.L., 1967, *Propagation of Electromagnetic Waves in Plasmas* (Moscow: Nauka) (in Russian).
107. Brunel, F., 1987, *Phys. Rev. Lett.*, **59**, 52.
108. Brunel, F., 1988, *Phys. Fluids*, **31**, 2714.
109. Cauble, R. and Rozmus,W., 1987, *Plasma Physics*, **37**, 405.
110. Lifshits, E.M. and Pitaevskii, L.P., 1979, *Physical Kinetics* (Moscow: Nauka) (in Russian).
111. Rozmus, W. and Tikhonchuk, V.T., 1990, *Phys. Rev. A*, **42**, 7401.
112. Silin, V.P., 1973, *Effect of Laser Radiation on Plasmas* (Moscow: Nauka) (in Russian); 1985, *Usp. Fiz. Nauk*, **145**, 225.
113. Zel'dovich, Ya.B. and Raizer, Yu.P., 1966, *Physics of Shock Waves and High-Temperature Hydrodynamic Phenomena* (Moscow: Nauka) (in Russian).
114. Fedosejevs, R., Ottmann, R., Sigel, R. *et al.*, 1990, *Phys. Rev. Lett.*, **64**, 1250.
115. Murnane, M.M., Kapteyn, H.C., and Falcone, R.W., 1989, *Phys. Rev. Lett.*, **62**, 15.
116. Keiffer, J.C., Audebert, P., Chaker, M. *et al.*, 1989, *Phys. Rev. Lett.*, **62**, 760.
117. Milchberg, H.M. and Freeman, R.R., 1990, *Phys. Fluids B*, **2**, 1395.
118. Rosen, M.D., 1989, *Preprint LLNL-89*, Livermore.
119. Gamaly, E.G., Kiselev, A.E., and Tikhonchuk, V.T., 1990, *J. Sov. Laser Res.*, **11**, 277.
120. Aleksandrov, A.F., Bogdankevich, L.S., and Rukhadze, A.A., 1988, *Principles of Plasma Electrodynamics* (Moscow: Vysshaya Shkola) (in Russian).
121. Dragila, R. and Gamaly, E.G., 1991, Submitted to Phys. Rev. A.
122. Aliev, Yu.M., Vukovich, S., Gradov, O.M. *et al.*, 1977, *Pis'ma Zh. Eksp. Teor. Fiz.*, **25**, 351.
123. Afanas'ev, Yu.V., Basov, N.G., Krokhin, O.N. *et al.*, 1978, Interaction of Strong Laser Radiation with Plasmas, In: *Advances in Science and Technology, Ser. Radiotechniques* (Moscow: VINITI), **17**.
124. Nuckolls, J.A., 1982, *Physics Today*, no. 9, 24.
125. Landen, O.L., Stearns, D.G., and Campbell, E.M., 1989, *Phys. Rev. Lett.*, **63**, 1475.
126. Nam, C.H., Tighe, W., Suckewer, S. *et al.*, 1987, *Phys. Rev. Lett.*, **59**, 2427.
127. Chaker, M., Kieffer, J.C., Matte, J.P. *et al.*, 1991, *Phys. Fluids B*, **3**, 167.
128. Milchberg, H.M. and Freeman, R.R., 1990, *J. Opt. Soc. Amer. B*, **6**, 1351.
129. Fedosejevs, R., Ottmann, R., Sigel, R. *et al.*, 1990, *Appl. Phys. B*, **50**, 79.
130. Harris, S.E. and Kmetec, J.D., 1988, *Phys. Rev. Lett.*, **61**, 62.
131. Matthews, D.L., Haggelstein, P.L., Rosen, M.D. *et al.*, 1985, *Phys. Rev. Lett.*, **54**, 110.
132. Seely, J.F., Brown, C.M., Feldman, U. *et al.*, 1985, *Opt. Commun.*, **54**, 289.
133. Suckewer, S., Skinner, C.H., Milchberg, H. *et al.*, 1985, *Phys. Rev. Lett.*, **55**, 1753.
134. Steyer, M., Schafer, F.P., Szatmari, S., and Kuhnle, G., 1990, *Appl. Phys.* B, **50**, 265.
135. Burnett, N.M. and Corkum, P.B., 1989, *J. Opt. Soc. Amer. B*, **6**, 1195.
136. Corkum, P.B., Burnett, N.M., and Brunel, F., 1989, *Phys. Rev. Lett.*, **62**, 1259.
137. Bezzerides, B., Jones, R.D., and Forslund, D.W., 1982, *Phys. Rev. Lett.*, **49**, 202.
138. Grebogi, C., Tripathi, V.K., and Chen, H.-H., 1983, *Phys. Fluids*, **26**, 1904.
139. Carman, R.L., Forslund, D.W., and Kindel, J.M., 1981, *Phys. Rev. Lett.*, **46**, 29.
140. Carman, R.L., Rhodes, C.K., and Benjamin, R.F., 1981, *Phys. Rev. A*, **24**, 2649.
141. Milchberg, H.M. and Freeman, R.R., 1988, *Phys. Rev. Lett.*, **61**, 2364.
142. Nam, C.H., Tighe, W., Valeo, E., and Suckewer, S., 1990, *Appl. Phys. B*, **50**, 275.
143. Stamper, J.A., Papadopoulos, R., Sudan, R.N. *et al.*, 1971, *Phys. Rev. Lett.*, **26**, 1012.
144. Weibel, E.W., 1959, *Phys. Rev. Lett.*, **2**, 83.

145. Morse, R.L. and Nielson, C.W., 1971, *Phys. Fluids*, **14**, 830; Davidson, R.C., Hammer, D.A., Haber, I., and Wagner, C.P., 1972, *Phys. Fluids*, **15**, 917.
146. Steiger, A.D. and Woods, C.H., 1972, *Phys. Rev. A*, **5**, 1467; Abdullaev, A.Sh. and Frolov, A.A., 1981, *Zh. Eksp. Teor. Fiz.*, **81**, 927; Abdullaev, A.Sh., 1988, *Fizika Plasmy*, **14**, 365.
147. Mulser, P., Pfalzner, S., and Cornolti, F., 1989, *Proc. 19 ECLIM*, Madrid (Singapore: World Sci. Publ.); Mulser, P. and Cornolti, F., Abstracts 20 ECLIM, Schlirsee, 1990.
148. Rae, S.C. and Burnett, K., 1990, *Phys. Fluids B*, **2**, 1015.
149. Boyer, K., Luk, T.S., and Rhodes, C.K., 1988, *Phys. Rev. Lett.*, **60**, 557.
150. Askar'yan, G.A., 1988, *Pis'ma Zh. Eksp. Teor. Fiz.*, **48**, 179.
151. Weiss, M.S., 1989, Paper M2 presented at "High Energy Density Physics with Subpicosecond Laser Pulses Topical Meeting", Snowbird, Utah, USA, Sept. 11-13, 1989.
152. Becker, W., Louisell, W.H., McCullen, J.D., and Sculley, M.D., 1981, *Phys. Rev. Lett.*, **47**, 1262.
153. Ritus, V.I., Private communication.
154. Yablonovitch, E., 1989, *Phys. Rev. Lett.*, **62**, 1742.
155. Unruh, W.G., 1976, *Phys. Rev. D*, **14**, 870.
156. Davies, P.C.W., 1975, *J. Phys. A*, **8**, 609.
157. Baldwin, K.G.H. and Boreham, 1951, B.W., *J. Appl. Phys.*, 52, 2627.

VLADIMIR T. TIKHONCHUK received the Ph. D. degree in Physics and Mathematics from Moscow Engineering Physics Institute in 1974 and Doctor of Science degree from Lebedev Physics Institute in 1987. He currently holds the position of Leading Research Fellow at Lebedev Institute and also holds the position of Professor of Physics at Physics Department of Moscow State Pedagogical Institute (part-time).
He is author and coauthor of more than 150 scientific papers on plasma physics, laser-plasma interactions and nonlinear optics.His current research interests are in high power short laser pulses interactions with plasmas, emission of electromagnetic waves from plasmas and nonlinear optics of photorefractive crystals.

EUGENE G. GAMALY received the Ph. D. and Doctor of Science (all in Physics and Mathematics) from Lebedev Physics Institute in 1970 and 1980, respectively. He currently holds the position of Leading Research Fellow at Lebedev Institute and also holds the position of Professor of Physics at Physics Department of Moscow Aviation Institute (part of time).
He is author and coauthor of more than 130 scientific papers on laser plasma interactions, high-temperature hydrodynamics and inertial fusion. His current research interests are in high power ultrashort laser pulses interactions with matter and its applications.

BARRY LUTHER-DAVIES is the head of the Laser Physics Centre in the Research School of Physical Sciences and Engineering at the Australian National University. His main research interests are the physics of laser produced plasmas, high power laser development, and non-linear optics. He has published eighty papers on these topics.

YANJIE WANG is PhD student within the Laser Physics Centre at the Australian National University engaged in the study of group velocity mismatched frequency doubling of picosecond Nd laser pulses as part of a project to develop a 10 TW/0.25 ps laser source.

ANDREY RODE is Research Fellow within the Laser Physics Centre at the Australian National University. His research interests are the laser-plasma interaction, plasma X-ray radiation, X-ray optics, and laser thermo-nuclear fusion. He has published forty two papers on these topics.